Mémoire

Auteur : Tribolet, Augustin
Promoteur(s) : 23983; Cudell, Jean-René
Faculté : Faculté des Sciences
Diplôme : Master en sciences spatiales, à finalité approfondie
Année académique : 2023-2024
URI/URL : http://hdl.handle.net/2268.2/19935

University of Liège
Faculty of sciences

Master in Space Sciences, Research Focus

Modified Gravity Theories and the Amplification of Inflationary Perturbations

Supervisor: Alessandro Tronconi
Co-supervisor: Jean-René Cudell

Augustin Tribolet
Academic year 2023-2024

Abstract

The superpotential technique allows the reconstruction of inflationary models. Assuming that the Hubble parameter is a function of the scalar field, we can reconstruct the scalar field potential. In this thesis, we are interested in using this technique to find the conditions on the reconstructed potential leading to the formation of Primordial Black Holes in the early universe. It has indeed been shown that PBHs can form if a growing mode of the Mukhanov-Sasaki equation is present, or if the scalar perturbation spectrum is blue-tilted. These two conditions place different constraints on the inflationary model. In particular, we applied the superpotential technique to a series of inflationary models. Compared to other reconstruction methods, this technique has been found to be very powerful in such a context. It leads to quite general predictions for the shape of the inflaton potential needed for the amplification. The case of inflation in the context of General Relativity was first investigated. Exploiting the conformal mapping and the Jordan-Einstein frame transformation, the analysis was extended to non-minimally coupled inflaton. The case of $f(R)$ theories was also studied in detail.

Contents

Introduction

Many fundamental questions arise in the context of classical cosmology, preventing us from understanding the evolution of the universe in its entirety. One of its most challenging issues is that the initial conditions of the primordial universe appear highly fine-tuned. To address these challenges, the model of inflation has been introduced as an extension to the classical framework. Inflation is defined as a period of rapid exponential expansion in the early universe driven by a new scalar field, called the inflaton field. It properly sets the initial conditions for the subsequent hot Big Bang model of classical cosmology. But more remarkably, inflation provides a mechanism for the generation of primordial density fluctuations. These fluctuations are believed to be the seeds for the formation of the anisotropies observed in the Cosmic Microwave Background (CMB) and for the formation of the Large-Scale Structures (LSS) in the universe. In the early universe, the presence of such energy density perturbations has also led to the conclusion that highly dense objects could have been formed through gravitational collapse. These objects are called Primordial Black Holes (PBHs). Depending on their mass, PBHs have a variety of possible cosmological implications. The most promising and studied is their contribution to the dark matter content of the universe.

Several observations indicate that most of the mass of the universe remains invisible. One of the invisible and not yet understood components constitutes the so-called dark matter problem. In the late universe, dark matter could explain the observations of galaxy rotation and the evolution of galaxy clusters, both showing missing gravitational attraction. In the early universe, the formation of the LSS also requires additional matter for the CMB overdensities to form the first galaxies. The measurements of the baryon-to-photon ratio from the Big Bang Nucleosynthesis (BBN) [1] and the CMB [2] indicate the same evidence of a missing constituent, see [3], [4] for more details. Consequently, dark matter (DM) must be present in both the late universe and the early universe. This invisible matter is referred to as non-baryonic matter due to its exotic physical behaviour. There are no particles within the Standard Model (SM) of particle physics that exhibit these properties. However, instead of a new particle, the missing matter could be in the form of compact objects spread throughout the entire universe. While the so-called MACHOs [5], or Massive Compact Halo Objects, in our galaxy have been ruled out by gravitational lensing observations, PBHs have a much wider possible range of masses, which still makes them a potential DM candidate [6]. Recently, PBHs have regained huge interest within the community with the discoveries of gravitational wave observations. Indeed, with the high number of detections of black hole mergers observed by LIGO and Virgo, the question about a primordial origin comes back into light.

The formation of PBHs in the early universe requires some specific features in the inflationary dynamics. At small scales, the perturbations remain unconstrained by observation. If their amplitudes are amplified compared to those observed at larger scales, they could form PBHs through gravitational collapse. It has been shown that such amplification can occur if a growing mode of the Mukhanov-Sasaki equation is present, or if the power spectrum of the perturbations shows an excess at small scales. Such conditions can be obtained if a particular phase is introduced in the potential during which the inflaton field evolves towards a de Sitter attractor. The core of the thesis is to study the potential in the vicinity of such a de Sitter attractor. To do so, we use the superpotential technique

to reconstruct the inflationary potential. Imposing the conditions for the amplification of the perturbations, specific constraints on the form of the potential and consequently on the inflationary dynamics are obtained. In this thesis, we are interested in applying this procedure to General Relativity (GR) and modified gravity theories which can be connected to GR by a redefinition of the inflaton field and a conformal transformation of the metric.

This thesis is organised as follows. In the first Chapter 1, we start by briefly presenting the formalism and achievements of classical cosmology. We introduce the limitations of this theory in Section 1.2 with the flatness and the homogeneity problems. Inflation is then formally presented in Section 1.3. Once we combine General Relativity and quantum mechanics to describe inflation, we end up with a natural explanation of the formation of density fluctuations. In Chapter 2, we introduce the quantum description of inflation with the theory of perturbations in cosmology. We use this formalism to describe the evolution of the perturbations. In Chapter 3, we review the physics behind the possibility of forming PBHs in the early universe. The two mechanisms to produce amplified perturbations are described in Section 3.3. In Chapter 4, we introduce the superpotential method, with the new idea of reconstructing inflationary potentials leading to the amplification of perturbations. This new approach is first applied in the context of GR in Section 4.2. The last two chapters detail its application to modified gravity theories. In Chapter 5, we investigate non-minimally coupled scalar fields, while in Chapter 6, we study $f(R)$ gravity theories.

In this work, natural units with $\hbar = c = 1$ have been used for simplicity and convenience. We also work with the reduced Planck mass, denoted as $\mathrm{M_P^2} = (8\pi G)^{-1}$. The notation over-dot and prime refer to the derivative with respect to (w.r.t.) cosmic time and conformal time, respectively.

1 Homogeneous cosmology

1.1 Friedman-Lemaître-Roberson-Walker model

In the 1950s, the expansion of the universe was discovered, which led to the idea of an evolving universe. More particularly, the universe could be understood as a thermal evolution driven by the expansion of the universe. In this Section, we review this classical description of the evolution of the universe, mostly basing our approach on the following references [7]–[10].

In classical cosmology, the universe is described as homogeneous and isotropic on large scales. It means that the universe appears the same in all directions, and at all locations in the universe. It can be described by the Friedman-Lemaître-Roberson-Walker (FLRW) metric:

$$ds^2 = dt^2 - a^2(t)\left[\frac{dr^2}{1-Kr^2} + r^2(d\theta^2 + sin^2\theta d\phi^2)\right],$$

where t is the cosmic time and K is the space curvature: $K = 0$ for a flat universe, $K > 0$ for a spatially closed universe and $K < 0$ for a spatially open universe. The scale factor $a(t)$ describes the relative size of the universe as it evolves over time.

By defining the coordinate $\chi \equiv dr/\sqrt{1-Kr^2}$, it is possible to write the metric in a more convenient way:

$$ds^2 = dt^2 - a^2(t)\left(d\chi^2 + f\left(\chi^2\right)\left(d\theta^2 + \sin^2\theta\, d\phi^2\right)\right), \tag{1}$$

where

$$f\left(\chi^2\right) \equiv \begin{cases} \sinh^2\chi & K=-1 \\ \chi^2 & K=0 \\ \sin^2\chi & K=+1 \end{cases}.$$

Note that the coordinates (t, r, θ, ϕ) or (t, χ, θ, ϕ) are comoving coordinates, which means that they are moving along with the expansion of the universe. Comoving quantities are related to physical ones by the scale factor:

$$r(t) = a(t)x,$$

where the physical distance $r(t)$ evolves proportionally to the expansion, while the comoving distance x remains constant.

The dynamics of the expansion is contained in the scale factor $a(t)$. The Friedmann equations describe its evolution as a function of the matter content in the universe. They are obtained from the Einstein equations:

$$R_{\mu\nu} - \frac{1}{2}Rg_{\mu\nu} \equiv G_{\mu\nu} = 8\pi G T_{\mu\nu} - \Lambda g_{\mu\nu}, \tag{2}$$

where Λ is the cosmological constant which can describe dark energy. The Ricci tensor $R_{\mu\nu}$ and the Ricci scalar R are defined as:

$$R_{\mu\nu} = \Gamma^{\alpha}_{\mu\nu,\alpha} - \Gamma^{\alpha}_{\mu\alpha,\nu} + \Gamma^{\alpha}_{\beta\alpha}\Gamma^{\beta}_{\mu\nu} - \Gamma^{\alpha}_{\beta\nu}\Gamma^{\beta}_{\mu\alpha}, \quad R \equiv g^{\mu\nu}R_{\mu\nu},$$

with the Christoffel symbols defined as: $\Gamma^{\mu}_{\alpha\beta} \equiv \frac{g^{\mu\nu}}{2}\left[g_{\alpha\nu,\beta} + g_{\beta\nu,\alpha} - g_{\alpha\beta,\nu}\right]$. For the FLRW metric case, the non-zero components of the Ricci tensor and the Ricci scalar are given by:

$$\begin{cases} R_{00} &= -3\frac{\ddot{a}}{a}, \\ R_{ij} &= \left(\frac{\ddot{a}}{a} + 2\frac{\dot{a}^2}{a^2} + \frac{2K}{a^2}\right) g_{ij}, \\ R &= 6\left(\frac{\ddot{a}}{a} + \frac{\dot{a}^2}{a^2} + \frac{K}{a^2}\right). \end{cases} \tag{3}$$

The stress-energy tensor $T_{\mu\nu}$ contains all the energy content of the universe. Homogeneity and isotropy imply the stress-energy tensor to be diagonal with identical spatial components. Assuming a perfect fluid of energy density $\rho(t)$ and pressure $p(t)$, the stress-energy tensor for a free-falling observer takes the following form:

$$T_{\mu\nu} = (\rho - p)u_\mu u_\nu + p g_{\mu\nu} = \mathrm{diag}(\rho, -p, -p, -p), \tag{4}$$

where we have introduced the time-like velocity 4-vector $u_\mu = (1, 0, 0, 0)$, in a comoving frame with the fluid.

Using these results, the first Friedmann equation is obtained from the 00-component of the Einstein equations:

$$H^2 = \frac{1}{3\mathrm{M}_\mathrm{P}^2}\rho - \frac{K}{a^2} + \frac{\Lambda}{3}, \tag{5}$$

where H is the Hubble parameter:

$$H \equiv \frac{\dot{a}}{a}. \tag{6}$$

It describes the rate of expansion of the universe. The second Friedmann equation is obtained from the ii-components of the Einstein equation, where the Hubble parameter is simplified using the first Friedmann equation (5). It describes the acceleration of the scale factor:

$$\frac{\ddot{a}}{a} = -\frac{1}{6\mathrm{M}_\mathrm{P}^2}(\rho + 3p) + \frac{\Lambda}{3}. \tag{7}$$

An additional equation can be obtained from the conservation of the total stress-energy tensor, $\nabla_\mu T^{\mu\nu} = 0$. The 0-component of this equation leads to the conservation equation:

$$\dot{\rho} + 3H(p + \rho) = 0. \tag{8}$$

The equations of state of the fluids in the universe can be described by a linear relation:

$$p = w\rho. \tag{9}$$

Despite not being the most general form, it can be used to describe most of the evolution of the universe. Non-relativistic particles (dust) are described by $w = 0$, while relativistic particles have $w = 1/3$. The cosmological constant Λ, possibly leading to an accelerated expansion, has a negative fluid pressure corresponding to $w = -1$.

Using Eq. (9), the conservation equation (8) takes the following form:

$$\frac{\dot{\rho}}{\rho} = -3(1 + w)\frac{\dot{a}}{a},$$

which has as solution:

$$\rho \propto a^{-3(1+\omega)}. \tag{10}$$

In Table 1, we can find the evolution of the different fluid densities. Except for the cosmological constant, they reflect the fact that the expansion of the universe dilutes the different kinds of constituents. The scale factor a describes the expansion in each spatial direction. As a consequence, the evolution of matter density is diluted in the three dimensions of space. For the radiation density, the additional power of the scale factor comes from the redshift.

	w	$\rho(a)$	$a(t)$
MD	0	a^{-3}	$t^{2/3}$
RD	$\frac{1}{3}$	a^{-4}	$t^{1/2}$
Λ	-1	a^0	e^{Ht}

Table 1: Evolution of the energy densities and scale factor of the constituents of the universe. MD, RD state for matter domination and radiation domination respectively.

We can also use the result (10) in the first Friedmann equation (5), to extract the time dependence of the scale factor:

$$\frac{\dot{a}}{a} = \frac{1}{\sqrt{3}\mathrm{M_P}}\sqrt{\rho} \;\Rightarrow\; \frac{da}{a} \propto a^{-\frac{3}{2}(1+w)}dt,$$

where we have assumed a spatially flat expanding universe and neglected the cosmological constant. The general solution of this equation is given by:

$$t \propto a^{\frac{3}{2}(1+w)}. \tag{11}$$

In Table 1, we have specified the individual cases. In Figure 1, we can see the different evolution of the three types of composition.

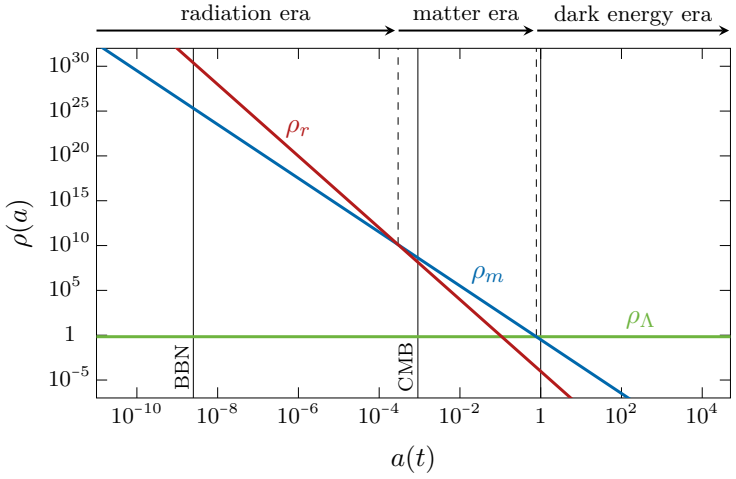

Figure 1: Evolution of the energy density for non-relativistic particles (matter), relativistic particles (radiation) and dark energy density as a function of time. Pict. taken from [11].

Classical cosmology, based on the FLRW model, allows us to draw several important conclusions about the origin and evolution of the universe. First, classical cosmology demonstrates that the universe is not static but expanding. The FLRW model allows us

to trace the evolution of the universe's expansion rate over time. In the past, the universe was dominated by radiation. Due to the expansion of the universe, the universe passed from a radiation-dominated universe (RDU) to a matter-dominated universe (MDU). The transition happened at the matter-radiation equality level, see Figure 1. By continuing to expand, the universe is currently in a period dominated by the cosmological constant Λ. In the same way, a transition has occurred at the matter-Λ equality level.

The expansion of the universe predicts a thermal history of the universe. In the course of its expansion, the universe has cooled. The effective interactions at high temperature are governed by the rate of expansion: interactions decouple as soon as their reaction rate becomes lower than the expansion rate. In particular, the universe emerges from a state where high-temperature matter is ionised and in thermodynamic equilibrium. Once the background temperature was sufficiently low to allow the binding of electrons with nuclei, photons were able to propagate freely through the universe. This period is called recombination, and the last scattering of photons with electrons defines the last scattering surface. Today, we observe these free photons with a redshifted wavelength in the Cosmic Microwave Background, see Figure 2, which is the relic of this ionised state in the past. Before the formation of the CMB, small density inhomogeneities caused the formation of acoustic oscillations in the plasma. It led to small temperature fluctuations imprinted in the CMB. The angular momentum spectrum of the CMB matches the theoretical prediction, see [12].

It also agrees with the Big Bang Nucleosynthesis. BBN is the period of the universe during which almost all the basic nuclei were formed [2]. This has only been possible for a specific range of temperatures. Indeed, the temperature needed to be low enough for the nuclei to stay in bound state ($T \lesssim 1$ MeV) and high enough to allow the Coulomb potential to be crossed for the nuclear reactions. The abundance of these elements matches the theoretical predictions described by the Boltzmann equation, see [12], [13].

1.2 FLRW model's problems

Despite the great success of the FLRW cosmology, a number of inconsistencies remain unexplained in the context of classical cosmology. The most important of these are the horizon problem and the flatness problem: the universe seems to have very specific and fine-tuned initial conditions in the primordial universe. In this Section, we review briefly these problems[1] and their resolution with the introduction of an inflationary period of the universe, before the RDU described by classical cosmology. This Section is mainly based on the references [9], [11], [15]–[17].

1.2.1 The flatness problem

The flatness problem can be easily understood from the expression of the Friedmann equation (5). Indeed, one can see that the curvature term decreases with the scale factor as $1/a^2$. Comparing with the evolutions in Table 1, the matter density ρ_m decreases as $1/a^3$ and the radiation density ρ_r as $1/a^4$. This means that the ordinary constituents of the universe decrease much faster with the scale factor. As suggested by observation, the

[1] See the original article of Alan H. Guth [14].

only explanation for the fact that the curvature does not dominate today is to assume an extremely small initial value for it. Within classical cosmology, there is no mechanism that can explain such a tiny curvature, and this leads to the flatness problem of the FLRW model. To express it more rigorously, let us rewrite the Friedmann equation (5) as follows, neglecting the cosmological constant:

$$1 = \Omega_{tot}(t) - \frac{K}{(aH)^2},$$

where we have defined $\Omega_{tot} = \sum_i \Omega_i$ and $\Omega_i = \frac{1}{3\mathrm{M}_\mathrm{P}^2}\frac{\rho_i}{H^2}$. Using this equation, one can define the time-dependent curvature parameter:

$$\Omega_K(t) \equiv -\frac{K}{(aH)^2} = 1 - \Omega_{tot}(t). \tag{12}$$

Using Eq. (11), we can find the evolution of this quantity for a MDU and a RDU. Using Table 1, we find for both cases $H \propto t^{-1}$. Therefore, for RD, we have $\Omega_K \propto t \propto a^2$, while for MD, we find $\Omega_K \propto t^{2/3} \propto a$. For a time t_i deep in the early universe, during the RD, and a time t_0 defined as the present time, in the MD, we can then express the following ratio:

$$\frac{\Omega_K(t_0)}{\Omega_K(t_i)} = \frac{a_0/a_{eq}}{(a_i/a_{eq})^2} \;\Rightarrow\; \Omega_K(t_0) = \Omega_K(t_i)\frac{a_{eq}}{a_0}\left(\frac{a_0}{a_i}\right)^2,$$

where we have defined a_{eq} as the scale factor at the moment of matter-radiation equality. Using the relation for redshift $\frac{a_{eq}}{a_0} = (1+z_{eq})^{-1} \approx \frac{1}{3500}$ [15] and the evolution in RD $\rho_r \propto \frac{1}{a^4}$, we finally find:

$$\Omega_K(t_0) \approx \frac{\Omega_k(t_i)}{3500}\left(\frac{\rho_{r,i}}{\rho_{r,0}}\right)^{1/2}.$$

The time t_i in the RDU can be taken as the Planck time for which $\rho_{r,i}^{1/4} \sim \mathrm{M_P}$. The radiation density today is given by $\rho_{r,0} \approx 7.8042 \times 10^{-34}$ g/cm^3 [8], which can be converted into electron-Volts (eV): $\rho_{r,0}^{1/4} \approx 2.41 \times 10^{-4}$ eV. These results lead to the condition $\Omega_K(t_0) = 10^{60}\Omega_K(t_i)$. The last measurement from the Planck experiment measurements of the CMB anisotropies gives $|\Omega_K(t_0)| < 0.005$ at the present time [12]. Consequently, we must have the extremely small fine-tuned initial condition: $|\Omega_K(t_i)| < 10^{-62}$ at the Planck time.

1.2.2 The horizon problem

Observations of the CMB show that the universe was highly homogeneous and isotropic on a large scale in the past, see Figure 2. Temperature anisotropies are indeed extremely small and universal:

$$\frac{\delta T}{T_0} \sim \left.\frac{\delta\rho}{\rho}\right|_{\mathrm{CMB}} \sim 10^{-5}, \tag{13}$$

where T_0 is the CMB temperature today ($T_0 \sim 2.73$ K). As we shall see, this observation is surprising as the CMB appears to be causally disconnected. There is no physical mechanism to explain why the universe appears so homogeneous.

The maximum distance between two regions that are causally connected is determined by the maximum distance that light can travel. To express it, we introduce the conformal time η via the relation:

$$d\eta = \frac{dt}{a}, \tag{14}$$

where t is the cosmic time. This allows us to rewrite the FLRW metric, in Eq. (1), as conformal to Minkowski. For a radial photon (θ and ϕ constants), we have that the line element is reduced to:

$$ds^2 = a^2(\eta)(d\eta^2 - d\chi^2) = 0.$$

This equation gives the greatest comoving distance that a photon can travel between an initial time t_i and a subsequent time t. We then define the so-called comoving particle horizon:

$$\Delta\chi_{max}(t) = \eta(t) - \eta(t_i) = \int_{t_i}^{t} \frac{dt'}{a(t')}. \tag{15}$$

We can now use the result in Eq. (11) to express $dt/a \propto a^{\frac{3}{2}(1+w)-2}$, and we find the following expression for the comoving horizon:

$$\Delta\chi_{max}(t) = \eta(t) - \eta(t_i) \propto \frac{2}{(1+3w)}\left(a^{\frac{1}{2}(1+3w)} - a_i^{\frac{1}{2}(1+3w)}\right), \tag{16}$$

For all ordinary matter, $w > -1/3$, the comoving particle horizon is growing and dominated by late time, $a \gg a_i$. Therefore, it is finite and there exist regions in the CMB that were not in causal contact in the past. Since the CMB is highly homogeneous, the horizon problem stands for the fact that it is not possible to explain why two regions of the CMB have the same average temperature while being causally disconnected.

To be more explicit, let us consider a flat universe composed of matter and radiation, neglecting the contribution of the cosmological constant. The derivative w.r.t. cosmic time can be expressed in the following way:

$$\frac{d}{dt} = \frac{da}{\dot{a}} = H\frac{d}{d\ln a}. \tag{17}$$

Therefore, we can rewrite the expression of the comoving particle horizon, in Eq. (15), as follows:

$$\Delta\chi_{max}(t) = \int_{a_i}^{a} \frac{da}{a^2 H} = \int_{\ln a_i}^{\ln a} (aH)^{-1} d\ln a. \tag{18}$$

The first Friedmann equation (29) is often written in terms of the critical energy density. The critical energy density is: $\rho_{crit,0} = 3\mathrm{M_P}H_0^2$. The first Friedmann equation becomes:

$$H^2 = H_0^2\left(\frac{\rho_{m,0}}{\rho_{crit,0}}a^{-3} + \frac{\rho_{r,0}}{\rho_{crit,0}}a^{-4}\right) = H_0^2\frac{\rho_{m,0}}{\rho_{crit,0}}\left(a + a_{eq}\right)a^{-4}$$

where we used, in the last equality, $\rho_{r,0} = a_{eq}\rho_{m,0}$. Using this result, we find:

$$a^2 H = H_0\sqrt{\frac{\rho_{m,0}}{\rho_{crit,0}}}\sqrt{a + a_{eq}}.$$

We can therefore express the distance travelled by light between the conformal time η_1 and η_2 as:

$$\eta_2 - \eta_1 = \int_{a_1}^{a_2} \frac{da}{a^2 H} = \frac{2}{\sqrt{\Omega_{m,0}}} H_0^{-1} \left(\sqrt{a_2 + a_{\rm eq}} - \sqrt{a_1 + a_{\rm eq}} \right).$$

Two points of the last scattering surface separated by more than two comoving horizons were not in causal contact. The comoving distance from the observer today and the surface of last scattering is given in a flat universe by $d_A(\eta_{\rm rec}) = \eta_0 - \eta_{\rm rec}$. Therefore, the angular separation corresponding to a causal region at recombination is given by:

$$\theta_h \approx \frac{2\Delta\chi_{max}(\eta_{\rm rec})}{d_A(\eta_{\rm rec})} = \frac{2(\eta_{\rm rec} - \eta_i)}{\eta_0 - \eta_{\rm rec}} = 0.036\,{\rm rad} \approx 2.1^\circ.$$

where we used $a_0 = 1$ for the scale factor today, $a_{eq} = 3500^{-1}$ at the matter-radiation equality, $a_{\rm rec} = 1100^{-1}$ at recombination, and $a_i \to 0$ deep in the early universe [11]. The number of causally disconnected regions of the last scattering surface is then approximated by $\frac{4\pi}{0.036^2} \approx 10^4$. As a result, there must exist a mechanism to make these 10^4 patches causally connected in order for the last scattering surface to be very homogeneous as observed today.

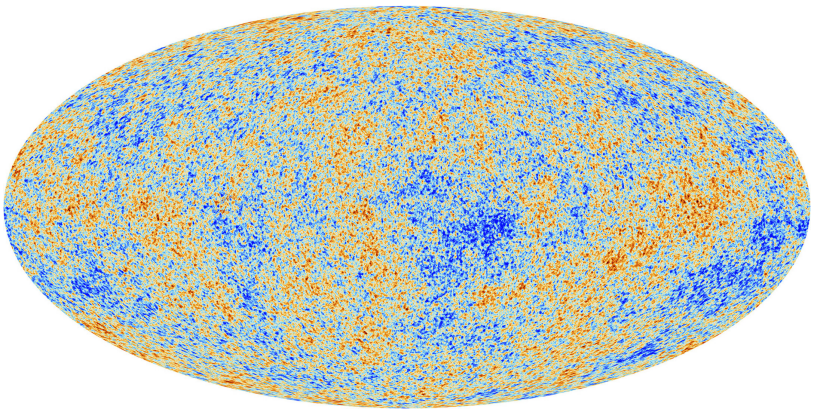

Figure 2: CMB anisotropies measured by PLANCK. The universe appears homogeneous at large scales. At smaller scales, small inhomogeneities of the order 10^{-5} are present. Credit ESA.

1.2.3 Introduction of an inflationary phase

The origin of the problems is linked to the fact that the RDU and MDU have a decelerating expansion. This can be seen using the dynamical equation (7) with either MD or RD, neglecting Λ and K:

$$\frac{\ddot{a}}{a} = -\frac{4\pi G}{3}(1 + 3w)\rho. \tag{19}$$

It shows that for ordinary matter, for which both pressure and energy density are positive, one has $\rho + 3p > 0$ giving $\frac{\ddot{a}}{a} < 0$. This condition is known as the Strong Energy Condition (SEC). It reflects the fact that gravity is attractive, which implies the universe to decelerate during RD and MD.

Since $a^2H^2 = \dot{a}^2$ is decreasing, the curvature density, defined in Eq. (12), is increasing with time. It is exactly the reason why the initial condition of the curvature density needs to be so small. The idea behind inflation is to assume the existence of an accelerated phase of expansion before the RDU and MDU. It is equivalent to say that the SEC must be violated, see Eq. (19). In this way, Ω_K is decreasing during the whole duration of this period. It is then possible to generate dynamically a very small initial value of the curvature density, without having to assume a fine-tuned initial condition for K. Using the evolution of the scale factor, in Eq. (11), we can express the evolution of the Hubble parameter and the condition leading to the violation of the SEC:

$$H = \frac{\dot{a}}{a} = \frac{2}{3(1+w)}\frac{1}{t} \;\Rightarrow\; aH \propto t^{\frac{2}{3(1+w)}-1} = a^{-\frac{1}{2}(1+3w)}. \tag{20}$$

The SEC, $\rho + 3p > 0$, effectively leads to a decelerating expansion. The only way to have $\dot{a}$ increasing is to violate the SEC: $1+3w < 0 \Leftrightarrow w < -1/3$. Such a condition requires the existence of a negative pressure fluid. Now let us check the horizon problem. By imposing the violation of the SEC, we now obtain a really large comoving particle horizon due to the contribution from early times, see Eq. (16) using $a_i \to 0$ and $w < -1/3$[2]. Therefore, inflation gives an early phase where the universe was causally connected long before the conventional hot Big Bang, thereby also solving the horizon problem.

Let us make a comment on the comoving particle horizon, defined in Eq. (18). In Section 2.1, we are going to introduce the comoving Hubble radius as $(aH)^{-1}$. In contrast to the comoving particle horizon, the comoving Hubble radius is defined as the comoving distance that light can travel during one Hubble time. In other words, particles whose distance is greater than one comoving Hubble radius cannot be in causal contact. So the comoving particle horizon is linked to the comoving Hubble radius, but they are intrinsically different. In fact, the comoving particle horizon is calculated by the time integration of the Hubble radius. In the standard Big Bang cosmology, the comoving Hubble radius is increasing, since aH is decreasing. We have found that the comoving particle horizon was really small in the past, leading to the horizon problem, see Eq. (15). The particle horizon is then dominated by the value of the comoving Hubble radius at late times. For this reason, the particle horizon and the Hubble radius are often used to refer to the same concept. However, one should keep in mind that when we introduce inflation, the Hubble radius is decreasing, which means that the comoving particle horizon is dominated by the value of the Hubble radius at early times. Consequently, inflation makes the comoving particle horizon much larger than the actual Hubble radius.

In the context of inflation, it will be useful to introduce the number of e-folds to parameterise time evolution. Such a number represents the logarithmic growth of the scale factor between two times t_1 and t_2:

$$N(t_1, t_2) = \int_{t_1}^{t_2} dt H(t) = \ln\left(\frac{a(t_2)}{a(t_1)}\right). \tag{21}$$

It is particularly useful during inflation because of the extremely fast-growing scale factor. It can be shown that the minimum number of e-folds required for inflation to solve the

[2]Note that using the inverse of Eq. (20) in Eq. (18), one can check that we find our previous result in Eq. (16).

flatness and horizon problems is of the order $N(t_{end}, t_i)_{min} \sim 60$, see [15] for instance.

Another useful trick is that the derivative w.r.t. conformal time, see Eq. (14), is related to the derivative w.r.t. cosmic time:

$$Q' = a\dot{Q}.$$

The conformal Hubble parameter $\mathcal{H}$ can be defined using this definition. It is related to the Hubble parameter in the following way:

$$H = \frac{\dot{a}}{a} = \frac{a'}{a^2} \;\Rightarrow\; \mathcal{H} \equiv \frac{a'}{a} = aH. \tag{22}$$

1.3 Single-field inflation

As we just saw in the previous Section, solving the flatness and the horizon problems is possible by introducing a period of rapid and exponential expansion in the early universe, before the hot Big Bang. In this Section, we study how it is possible to generate such an inflationary period by introducing a new scalar field in the energy content of the universe. We call it the inflaton field. This inflationary paradigm has become the most common extension of modern cosmology and is supported by some observations. This Section has the same general references as the previous Section 1.2.

1.3.1 Slow-roll inflation

Inflation requires the violation of the SEC, $w < -1/3$, see Section 1.2.3. The cosmological constant or vacuum energy, $w = -1$, is an important example satisfying the SEC violation. It gives the so-called de Sitter universe for which the evolution of the scale factor takes the form $a(t) = e^{Ht}$ with a constant rate of expansion $H = \text{cst.}$, see Table 1. However, if a cosmological constant is at the origin of inflation, the expansion phase would last forever. One needs to introduce a mechanism that stops inflation. A way to produce an accelerated expansion, but with a natural end towards classical cosmology, is to introduce a new scalar field dominating the matter content in the early universe. In this scenario, inflation is driven by this field, called the inflaton field. We present in this Section the simplest models, considering the minimal coupling between the scalar field and gravity.

Let us consider a homogeneous scalar field $\phi(t, \vec{x}) = \phi(t)$ dominating the energy content of the early universe. In this context, the matter-gravity action takes the following form:

$$S = S_E + S_\phi = \frac{\mathrm{M_P^2}}{2} \int d^4x\sqrt{-g}R + \int d^4x\sqrt{-g}\left[-\frac{1}{2}g^{\mu\nu}\partial_\mu\phi\partial_\nu\phi - V(\phi)\right], \tag{23}$$

where S_E is the Einstein-Hilbert action and S_ϕ is the inflaton action, with the general Lagrangian for a scalar field. We define $V(\phi)$ as the potential of the inflaton field and R is the Ricci scalar, defined in Eq. (3). Taking the approximation of a flat universe $K = 0$, the spatial metric reduces to δ_{ij} which implies that the metric determinant is given by: $\sqrt{-g} = a^3$. Varying this new action, w.r.t. the inflaton field $\frac{\delta S}{\delta \phi} = 0$, we get the

Klein-Gordon equation[3]:

$$\ddot{\phi} + 3H\dot{\phi} + \frac{dV}{d\phi} = 0 \tag{24}$$

The energy-momentum tensor for the scalar field is given by[4]:

$$T_{\mu\nu} \equiv -\frac{2}{\sqrt{-g}}\frac{\partial S_\phi}{\partial g^{\mu\nu}} = \partial_\mu\phi\partial_\nu\phi + g_{\mu\nu}\left[-\frac{1}{2}g^{\alpha\beta}\partial_\alpha\phi\partial_\beta\phi - V(\phi)\right]. \tag{25}$$

Using the energy-momentum tensor of a perfect fluid, see Eq. (4) and the energy-momentum tensor for the inflaton field, Eq. (25), we find the pressure and energy densities:

$$\rho = \frac{1}{2}\dot{\phi}^2 + V(\phi), \tag{26}$$

$$p = \frac{1}{2}\dot{\phi}^2 - V(\phi). \tag{27}$$

Consequently, the scalar field behaves like a fluid with an equation of state given by:

$$w = \frac{p}{\rho} = \frac{\frac{1}{2}\dot{\phi}^2 - V(\phi)}{\frac{1}{2}\dot{\phi}^2 + V(\phi)} < -1/3, \tag{28}$$

where $w < -1/3$ must be dynamically verified during inflation. We see that the SEC violation is achieved when the potential energy is much greater than the kinetic energy: $\frac{1}{2}\dot{\phi}^2 \ll V(\phi)$. In other words, when the inflaton field is slowly rolling into its potential. The dynamic induced by this condition is called "slow-roll" inflation. In the limit $\dot{\phi} \to 0$, the scalar field is fixed and we recover the de Sitter universe evolution, with $w = -1$. However, now inflation ends naturally when the SR parameters $\epsilon_i \approx 1$. This occurs when the inflaton has reached its minimum and starts oscillating[5]. Inflation is for this reason referred to as a quasi-de Sitter evolution. It means that the universe underwent an almost constant rate of expansion[6].

The first Friedmann equation (5) can be obtained using Eq. (26). The second Friedmann equation is obtained by deriving the first one w.r.t. cosmic time, and substituting the Klein-Gordon equation (24):

$$H^2 = \frac{1}{3\mathrm{M_P^2}}\rho = \frac{1}{3\mathrm{M_P^2}}\left(\frac{1}{2}\dot{\phi}^2 + V(\phi)\right), \tag{29}$$

$$\dot{H} = -\frac{1}{2\mathrm{M_P^2}}\dot{\phi}^2. \tag{30}$$

To parameterise the expansion, we can introduce the first slow-roll parameter, ϵ_1. In order to have an accelerated expansion, we need to impose the Hubble constant to vary slowly:

$$\epsilon_1 \equiv -\frac{d\ln H}{dN} = -\frac{d\ln H}{dt}\frac{dt}{dN} = -\frac{\dot{H}}{H^2} \ll 1, \tag{31}$$

[3]One needs to use the following relation $\dot{\phi}\delta(\dot{\phi}) = \dot{\phi}\frac{d}{dt}(\delta\phi)$ and perform an integration by parts.

[4]We used the relation $\frac{\delta\sqrt{-g}}{\delta g^{\mu\nu}} = -\frac{1}{2}\sqrt{-g}g_{\mu\nu}$ in the second equality, to write $T_{\mu\nu} = -2\frac{\partial\mathcal{L}_\phi}{\partial g^{\mu\nu}} + g_{\mu\nu}\mathcal{L}_\phi$.

[5]This period is called "reheating". To generate the RDU which begins the classical picture of the hot Big Bang cosmology, the universe needs indeed to reheat after inflation. It is during this period that the inflaton field decays into the matter content of the classical cosmology, see [11], [18] for instance.

[6]As mentioned earlier, a de Sitter universe never stops growing: $ds^2 = -dt^2 + e^{2Ht}d\vec{x}^2$.

where N is the number of e-folds, defined in (21), t is the cosmic time, and H the Hubble parameter. This is the first slow-roll condition and it is equivalent to the accelerated expansion conditions for inflation: $-\frac{\dot{H}}{H^2} = -\frac{\ddot{a}a}{\dot{a}^2} + 1 \ll 1 \;\Rightarrow\; \ddot{a} > 0$, where the scale factor $a > 0$. In order to solve the classical cosmological problems, the fast expansion driven by the inflaton field must last long enough. Indeed, the first slow-roll condition needs to last over an extended period of at least 60 e-folds, see annex 1.2. Therefore, we need the variation of the first SR parameter to be slow, $\epsilon_1 \ll 1$, which can be expressed with the second slow-roll condition:

$$\epsilon_2 \equiv \frac{d\ln\epsilon_1}{dN} = \frac{d\ln\epsilon_1}{dt}\frac{dt}{dN} = \frac{\dot{\epsilon_1}}{H\epsilon_1} \ll 1. \tag{32}$$

In fact, a set of slow-roll parameters can be introduced with the same idea. Slow-roll parameters are introduced as a way to replace the degrees of freedom: the inflation field and the Hubble parameter. These parameters are used to describe the behaviour of the scalar field driving inflation and the expansion rate of the universe. The idea is that during a period of SR inflation, these parameters are smaller than unity, so that their time derivatives are even smaller. This hierarchy is established through a recursive definition of the SR parameters and proves to be useful to simplify the inflationary dynamics. Different hierarchies exist, each of them related to the evolution of distinct (homogeneous) degrees of freedom. In this work, we use two different slow-roll hierarchies. Depending on the model considered, one hierarchy may be more useful to describe the dynamics of the system. The first hierarchy introduced so far is that of the Hubble flow functions. The Hubble flow functions are defined recursively as follows:

$$\begin{aligned} \epsilon_0 &= \frac{H_0}{H}, \\ \epsilon_{i+1} &= \frac{\dot{\epsilon_i}}{H\epsilon_i}. \end{aligned} \tag{33}$$

A second hierarchy commonly used is that of the scalar field flow function[7]. The scalar field flow functions are defined as:

$$\begin{aligned} \delta_0 &= \frac{\phi}{\phi_0}, \\ \delta_{i+1} &= \frac{\dot{\delta_i}}{H\delta_i}. \end{aligned} \tag{34}$$

From the two Friedmann equations, we understand that the SR condition $\frac{1}{2}\dot{\phi}^2 \ll V(\phi)$, is equivalent to the condition of a slow-varying Hubble parameter. From Eq. (30), we can write the second SR parameter in Eq. (32) as $\epsilon_2 = 2\epsilon_1 + \frac{2\ddot{\phi}}{H\dot{\phi}}$. We conclude that the second SR condition is satisfied provided that the acceleration of the inflaton is small:

$$\ddot{\phi} \ll H\dot{\phi}. \tag{35}$$

There exists a wide variety of inflation models that have been developed. In [19], a comprehensive review of the different inflation models is presented. In this thesis, we will focus on single-field inflation, where the expansion of the universe during inflation is

[7] In general, the ϵ_i and the δ_i can be related through the homogeneous Friedmann and Klein-Gordon equations.

driven by a unique scalar field known as the inflaton field[8].

Let us end this Section by expressing the SR parameters in conformal time. This will be useful in the study of the evolution of the perturbations with the Mukhanov-Sasaki equation, see Section 2.3. Let's recall that the number of e-folds is defined as $dN = d\ln a = Hdt = \mathcal{H}d\eta$, see Eq. (21). Then, the Hubble flow functions, see Eqs. (33), can be expressed as:

$$\epsilon_1 = -\frac{d\ln H}{dN} = -\frac{d\ln \mathcal{H}/a}{dN} = 1 - \frac{\mathcal{H}'}{\mathcal{H}^2}, \tag{36}$$

$$\epsilon_i = \frac{1}{\epsilon_{i-1}}\frac{d\epsilon_{i-1}}{dN} = \frac{\epsilon'_{i-1}}{\mathcal{H}\epsilon_{i-1}}. \tag{37}$$

The scalar field flow function, see Eqs. (34), can also be defined in terms of the conformal time:

$$\delta_1 = \frac{\sigma'}{\sigma\mathcal{H}}, \tag{38}$$

$$\delta_i = \frac{\delta'_{i-1}}{\mathcal{H}\delta_{i-1}}. \tag{39}$$

1.3.2 Attractor solution

Let us now introduce the concept of attractor, following the references [8], [11], [18]. To illustrate the principle, let us choose a potential of the form $V(\phi) = \frac{1}{2}m\phi^2$. Starting from the KG equation (24) and using $\ddot{\phi} = \dot{\phi}\frac{d\dot{\phi}}{d\phi}$, we obtain the following differential equation:

$$\frac{d\dot{\phi}}{d\phi} = -\frac{\sqrt{\frac{3}{2}}\frac{1}{\mathrm{M_P}}\left(\dot{\phi}^2 + m^2\phi^2\right)^{1/2}\dot{\phi} + m^2\phi}{\dot{\phi}}. \tag{40}$$

This differential equation can be translated into a phase space diagram, see Figure 3. Whatever the initial conditions, the scalar field evolves towards a unique solution, called the attractor solution. This solution is SR inflation. Noting that SR inflation can be characterised by $\ddot{\phi} \ll H\dot{\phi}$, we can neglect $d\dot{\phi}/d\phi$. The first SR condition $\frac{1}{2}\dot{\phi}^2 \ll \frac{1}{2}m^2\phi^2$ is satisfied for $|\phi|$ large. Using these SR conditions in Eq. (40), we find:

$$\dot{\phi}_{att} \approx -\sqrt{\frac{2}{3}}m\mathrm{M_P}.$$

The SR attractor solution is almost constant for large values of the field, i.e. slowly varying. When this is no longer the case, the SR condition is no longer satisfied and we recover the oscillating behaviour of the scalar field in its potential around the minimum, see Figure 3. To find this result, we start from Eq. (29), $\dot{\phi}^2 + m^2\phi^2 = 6\mathrm{M_P^2}H^2$, and make the following change of variable:

$$\begin{aligned} \dot{\phi} &= \sqrt{6}\mathrm{M_P}H\sin\theta, \\ m\phi &= \sqrt{6}\mathrm{M_P}H\cos\theta. \end{aligned} \tag{41}$$

[8] In contrast, multi-field inflation proposes an inflationary phase driven by several distinct scalar fields.

By deriving the second expression w.r.t. time, we find the expressions of $\dot{\theta}$ and $\dot{H}$: $\dot{H} = -3H^2 \sin^2\theta$ and $\dot{\theta} = -m - \frac{3}{2}H \sin 2\theta$. Therefore, H is a decreasing function of time, and $\theta \simeq -mt + \alpha$ with α a constant phase which can be set to zero. Going back in Eqs. (41), we find an oscillating inflaton field and a spiral attractor in the phase space, see Figure 3.

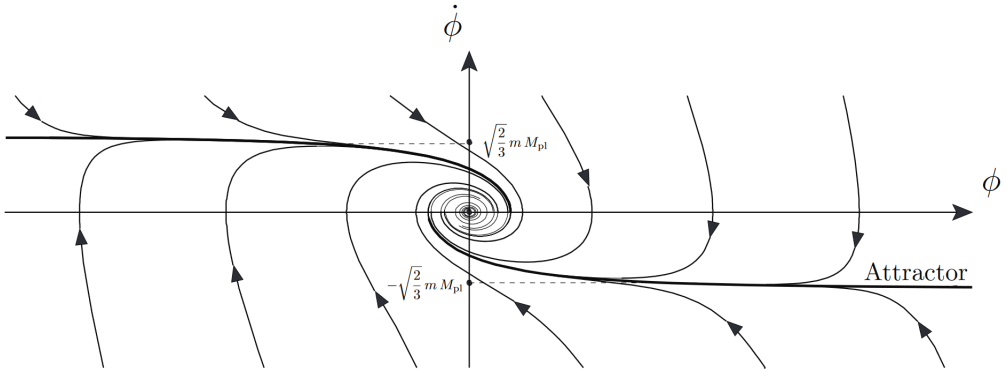

Figure 3: Phase space diagram describing the inflaton field in a potential $V(\phi) = \frac{1}{2}m^2\phi^2$. The attraction towards the SR solution is illustrated. Pict. taken from [9].

In the literature, it is usually assumed that the inflaton field evolves towards a de Sitter attractor. As we will see, SR inflation is indeed compatible with the CMB observations, see Section 2.3.3. In Section 3.3.2, we are going to introduce another type of attractor solution in order to produce PBHs. This is done by a proper inflaton potential which leads to the so-called ultra-slow-roll (USR) inflation, or constant-roll (CR) inflation. In the study of inflationary dynamics and its implications for the formation of PBHs, it is necessary to check the stability of the scalar field close to its attractor. This analysis corresponds to studying how small perturbations around the attractor evolve in time. If the fluctuations in the scalar field remain small and oscillate around the attractor, the solution is said to be stable. On the other hand, if they are growing, potentially leading to a departure from the attractor solution, it indicates instability. By assessing stability close to the USR or CR attractor, we will be able to find the conditions for the production of PBHs during such a phase, see Section 4.2 for the whole discussion in the context of GR.

1.3.3 Constant-roll inflation

In SR inflation, the inflaton field slowly rolls down its potential. As we saw before, this SR condition is mathematically equivalent to $\ddot{\phi}/H\dot{\phi} \ll 1$, see Eq. (35). It can be used to simplify the Klein-Gordon equation in Eq. (24):

$$V_{,\phi} \approx -3H\dot{\phi} \Leftrightarrow \frac{\ddot{\phi}}{H\dot{\phi}} \approx 0.$$

The CR inflation [20]–[22] is a general case, interpolating between standard SR and USR approximations. In this case, the inflationary model is defined by a constant rate of roll with a constant parameter $\alpha \equiv V_{,\phi}/H\dot{\phi}$. The Klein-Gordon equation (24) is given by:

$$\ddot{\phi} + (3+\alpha)H\dot{\phi} = 0 \Leftrightarrow \frac{\ddot{\phi}}{H\dot{\phi}} = -(3+\alpha) = \text{cst.}. \tag{42}$$

The first Friedmann equation (30) can be used to express the second derivative of the inflaton as $\ddot{\phi} = -\frac{M_P^2 \ddot{H}}{\dot{\phi}}$. Using this result in Eq. (42), we find the equivalent Klein-Gordon equation expressed as follows:

$$\ddot{H} + 2(3+\alpha) H \dot{H} = 0. \tag{43}$$

As we saw earlier, we can use the SR parameters to replace the degrees of freedom and their derivatives. Using the definitions (33) and (34), we can express the second SR parameters as:

$$\epsilon_2 = \frac{\ddot{H}}{\dot{H} H} + 2\epsilon_1,$$
$$\delta_2 = \frac{\ddot{\phi}}{\dot{\phi}\phi} - \delta_1 + \epsilon_1.$$

Using these results in Eqs. (42) and (43) respectively, we find:

$$2\epsilon_1^2 - \epsilon_1\epsilon_2 - 2(3+\alpha)\epsilon_1 = 0 \xrightarrow{\epsilon_1 \neq 0} 2\epsilon_1 - \epsilon_2 + 2(3+\alpha) = 0, \tag{44}$$
$$\delta_1(\delta_2 + \delta_1 - \epsilon_1) + (3+\alpha)\delta_1 = 0 \xrightarrow{\delta_1 \neq 0} \delta_2 + \delta_1 - \epsilon_1 + (3+\alpha) = 0,$$

where the solution ϵ_1 is a constant de Sitter solution. By differentiating twice Eq. (44) w.r.t. cosmic time, we find the following conditions:

$$2\epsilon_1 - \epsilon_3 = 0 \;\Rightarrow\; 2\epsilon_1 = \epsilon_3,$$
$$2\epsilon_1\epsilon_2 - \epsilon_3\epsilon_4 = 0 \;\Rightarrow\; \epsilon_2 = \epsilon_4$$

More generally, we have that $\epsilon_{2i+1} = 2\epsilon_1$ and $\epsilon_{2i} = \epsilon_2$ with i a natural integer. In addition, it has been shown that CR admits solutions describing the evolution to a de Sitter attractor, see [20], [23] for more details. Using such a limit $\epsilon_1 \to 0$ in Eq. (44), the odd SR parameters can take a zero value and the even ones a constant and different from zero value. Therefore, in the limit $N \gg 1$, we can have a hierarchy with zero odd parameters and constant even parameters. Note that we have the same pattern for the scalar flow functions. In the following, we are going to use these asymptotic values to generate PBHs.

The particular case of USR inflation [24], [25] is defined by $\alpha = 0$[9]. In other words, the variation of the potential $V_{,\phi} \approx V_{,\phi\phi} \approx 0$ is negligible, while $\ddot{\phi}$ becomes significant for the dynamics. In the Klein-Gordon equation (24), it basically means neglecting the slope of the potential:

$$\ddot{\phi} \approx -3H\dot{\phi} \;\Rightarrow\; \frac{\ddot{\phi}}{H\dot{\phi}} \approx -3. \tag{45}$$

Solving this equation for $\dot{\phi}$ using Eq. (6), we find:

$$\dot{\phi} \propto a^{-3} \propto e^{-3N}, \tag{46}$$

where in the last equality, we used the result from Table 1 for $w = -1$ and the definition of N, see Eq. (21). Therefore, we find that the velocity of the field is decreasing very

[9]The case $\alpha \approx -3$ gives back SR. Any other value corresponds to a different constant rate of roll.

rapidly. This explains the denomination "ultra-slow-roll" inflation, the slow-varying behaviour of the field is enforced during the USR regime. The scalar field is almost fixed for the duration of the USR phase and the field variation becomes more and more negligible. The universe is then dominated by the potential energy, which gives rise to the eternal de Sitter expansion. Thus, USR is even closer to de Sitter inflation evolution, in which $H = \text{cst.}$ and $w = -1$, than SR. In SR inflation, we had $w < -1/3$, while in USR we have $w \to -1$ as it can be seen from Eq. (28) taking $\dot{\phi}^2 \ll V(\phi)$. As the derivative of the potential vanishes during USR, one can add an inflection point in the overall potential of the inflaton to include a phase of USR. However, one usually assumes USR phases with a duration of a small number of e-folds to avoid eternal inflation.

Let us continue the analysis of the difference between the SR and USR regimes. The first slow-roll parameter, defined in Eq. (31), can be expressed using the second Friedmann equation (30):

$$\epsilon_1 = \frac{\dot{\phi}^2}{2\mathrm{M}_\mathrm{P}^2 H^2}. \tag{47}$$

Using this expression, we can express the second SR parameter defined in Eq. (32) as:

$$\epsilon_2 = \frac{2\ddot{\phi}}{H\dot{\phi}} + 2\epsilon_1. \tag{48}$$

Using Eq. (46) into Eq. (47), we find that the first SR parameter is evolving very rapidly $\epsilon_1 \propto e^{-6N}$ during USR. It gives extremely smaller and smaller values of $\epsilon_1 \ll 1$ as the universe expands compared to SR in which $\epsilon_1 \ll 1$ but is usually nearly constant. Using Eq. (45) into (48), we find that the second parameter is also varying very rapidly but it evolves towards a constant value $\epsilon_2 \approx -6$. This is completely different from the SR case $\epsilon_2 \ll 1$.

2 Quantum fluctuations during inflation

Inflation can explain the flatness and the horizon problems of classical cosmology. However, what makes its great success is the fact that the inflaton field can produce small density perturbations. They give a possible origin of the formation of the anisotropies in the Cosmic Microwave Background[10], see Figure 2. In addition, the universe is observed to be structured in a very particular way: galaxies are grouped in clusters of galaxies, which eventually are grouped in superclusters. These particular features on large scales are called the Large Scale Structures [26]. We currently understand these structures as sharing the same origin as the anisotropies imprinted in the CMB. These small seeds were the starting point of a long gravitational collapse to the large structures observed today[11]. As a result, the introduction of inflation gives a natural explanation to the origin of these seeds.

In the last Section, the inflaton field was considered as a function of time (homogeneous field), which drives the dynamics of the universe. Then, by using the Friedmann equations (29) and (30), one can calculate the end of inflation with the rupture of the SR condition (31). The expectation value of the inflaton field can therefore be used to parameterise the time evolution. Due to the uncertainty principle, we expect the inflaton field to have spatial fluctuations. In other words, this means that all the regions of the universe do not end inflation at the exact same time. Inflation leaves regions with greater or lower density, depending on when inflation ended. It is precisely these spatial perturbations which could be at the origin of the initial seeds of the perturbations that later evolved into the structures we observe today.

We now want to describe more generally the dynamics of such perturbations, introducing spatial and time dependencies of the scalar field. To do so, we introduce the spatial perturbation of the inflaton field $\delta\phi$ around its background value $\bar{\phi}$:

$$\phi(t) \to \phi(\vec{x}, t) = \bar{\phi}(t) + \delta\phi(\vec{x}, t), \tag{49}$$

where the condition $\delta\phi \ll \bar{\phi}$ must be satisfied to keep the accelerated expansion (generated by the background value, $\bar{\phi}$).

Since during inflation, the energy content was dominated by the inflaton field, any perturbation of the inflaton field produced fluctuations in the stress-energy tensor $T_{\mu\nu}$:

$$\delta\phi \;\Rightarrow\; \delta T_{\mu\nu}.$$

Einstein's equations describe how the energy content in the universe influences the curvature of spacetime, see Eq. (2). Gravity is coupled to any kind of component in the universe, including the inflaton field. Consequently, any perturbations of the inflaton field induced fluctuations in the spacetime itself, and hence in the spacetime curvature:

$$\delta T_{\mu\nu} \;\Rightarrow\; \delta R_{\mu\nu} - \frac{1}{2}\delta\left(g_{\mu\nu}R\right) = 8\pi G\delta T_{\mu\nu} \;\Rightarrow\; \delta g_{\mu\nu}. \tag{50}$$

[10] As briefly discussed in Section 1.1, the CMB reflects the decoupling of the photon from the hot plasma constituting the early universe. It brings us information about the state of the universe 380,000 years after the Big Bang.

[11] This accretion process took place during matter-domination. It is described by the Jeans instabilities which capture gravitational instabilities, see for example [8].

In addition, the Klein-Gordon equation describes the evolution of the field and is obtained by varying the inflaton action. Since the action (23) contains the metric perturbations, they also induce a back-reaction on the scalar field perturbations [27]:

$$\delta g_{\mu\nu} \;\Rightarrow\; \delta S \;\Rightarrow\; \delta\phi.$$

All in all, we end up with an intimate coupling between the scalar field and the metric perturbations:

$$\delta\phi \Leftrightarrow \delta g_{u\nu}.$$

As a consequence, we need to study both of them simultaneously to understand the evolution and the consequences of the (quantum) perturbations of the inflaton field. The small induced curvature perturbations have affected the dynamics of the matter content of the universe when inflation ends, explaining the particular feature of the matter distribution in both the CMB and the LSS.

We are going to illustrate how we describe the formation and evolution of these perturbations. In Section 2.1, we will first discuss the perturbations' evolution depending on their relation with the Hubble horizon. Then, we will briefly outline the description of the metric perturbations with the so-called perturbed Einstein equations and the related gauge invariance, see Section 2.2. Finally, we will see how we can describe the evolution of these perturbations from their production to the late universe in Section 2.3. These general references [11], [18], [27], [28] have been used throughout the Chapter.

2.1 Super-horizon and sub-horizon Perturbations

We will see later on that cosmology is often studied with the statistical properties of the primordial density perturbations. To do so, perturbations are decomposed in terms of the power spectrum in Fourier space. In this context, a cosmological perturbation is characterised by its comoving wavenumber $k \sim 1/(\text{comoving length})$, or its comoving wavelength λ. The wavelength and the inverse of the wavenumber can be considered as the physical scale of the perturbation.

The expansion rate is characterised by the Hubble parameter, see Eq. (6). The Hubble-Lemaître law describe the recession of galaxies from each other:

$$v = HD, \tag{51}$$

where v is the recession velocity, H is the Hubble parameter expressed at a given time, and D is the separation distance. Each point in the universe moves away from each other with a speed proportional to their separation. The inverse of the Hubble parameter H^{-1} has a time unit (or length unit in natural units), it gives an estimate of the age of the universe. The distance $D_H = c/H$ ($1/H$ in natural units) corresponds approximately to the distance that light can travel in one Hubble time. It is called the Hubble distance or Hubble radius. The Hubble radius can be used to define a scale of causal interactions: it defines the distance over which particles are causally connected within one Hubble time[12].

[12]Note that taking back the Hubble-Lemaître law in Eq. (51), objects moving at a speed greater than the speed of light are not in causal contact with the observation point. It corresponds to objects behind the Hubble radius:

$$c = HD_H = \frac{D_H}{1/H}.$$

In comoving coordinates, we can further define the comoving Hubble distance or radius as $R_H = (aH)^{-1}$. The comoving Hubble radius represents the comoving distance that light can travel during one Hubble time. In contrast to the fixed perturbation wavelength when working in comoving coordinates, the comoving Hubble radius is evolving with the expansion:

$$\frac{d}{dt}\left(\frac{1}{aH}\right) = -\frac{\ddot{a}}{a^2H^2}.$$

During inflation, the accelerated expansion of the universe $\ddot{a} > 0$, makes the comoving Hubble radius decrease. Using Eq. (20), we have that R_H decreases as a^{-1} during inflation, which can also be deduced from the fact that the Hubble radius is nearly constant. In contrast, it increased as a and $a^{1/2}$ for the RDU and MDU respectively, see Table 1. Currently, the universe is dominated by the cosmological constant Λ, so that the comoving radius is again decreasing as a^{-1}. When studying the evolution of the fluctuations produced in the early universe, we can compare their comoving wavelengths with the size of the Hubble radius. This comparison provides us with two sets of perturbations: super-Hubble and sub-Hubble modes[13]. We call the super-Hubble regime, the regime where fluctuations have wavelengths longer than the comoving Hubble radius: $k^{-1} > (aH)^{-1}$. In contrast, the period during which the perturbation wavelengths are inside the comoving Hubble radius is called the sub-Hubble regime: $k^{-1} < (aH)^{-1}$. Physically, it means that within one Hubble time, the whole perturbation scale is in causal contact.

Figure 4 represents the evolution of a given perturbation during the early universe. When a perturbation mode is produced, it begins evolving inside the Hubble radius. Indeed, as the Hubble radius is extremely large during inflation, all the perturbations start their evolution in the sub-Hubble regime. As the universe expanded, the Hubble radius decreased. At some time, the mode crossed the Hubble horizon, becoming a super-horizon mode when $k = aH$. When inflation ended, the standard picture of the hot Big Bang emerges[14]. During this period, the Hubble radius is growing, so that the mode could potentially re-enter the horizon again when $k = aH$. The time of re-entry depends on the scale k^{-1} of the perturbation. Indeed, small-scale modes exit the horizon later during inflation and re-enter the horizon earlier in the post-inflationary era. These modes are often associated with the formation of smaller structures, such as galaxies and other cosmic objects. Large-scale modes have the exact opposite behaviour. These perturbation modes are associated with LSS in the universe, such as the distribution of galaxies.

Horizon re-entry is an important concept to understand the formation of PBHs in the early universe. It defines the time at which light can traverse the comoving scale of the perturbation $1/k$ within one Hubble time, i.e. $1/k \sim 1/(aH)$. We will use this concept in Section 3.

[13]In the literature, we also use the term super-horizon and sub-horizon, due to the fact that in classical cosmology, the comoving horizon is dominated by the Hubble radius in the late universe, see the discussion on Eq. (18).

[14]Reheating is the phase just following the end of inflation. It marks the beginning of the classical Hot Big Bang cosmology. It is the quantum fluctuation of the inflaton field, in its minimum, that generated the actual particle content of the universe.

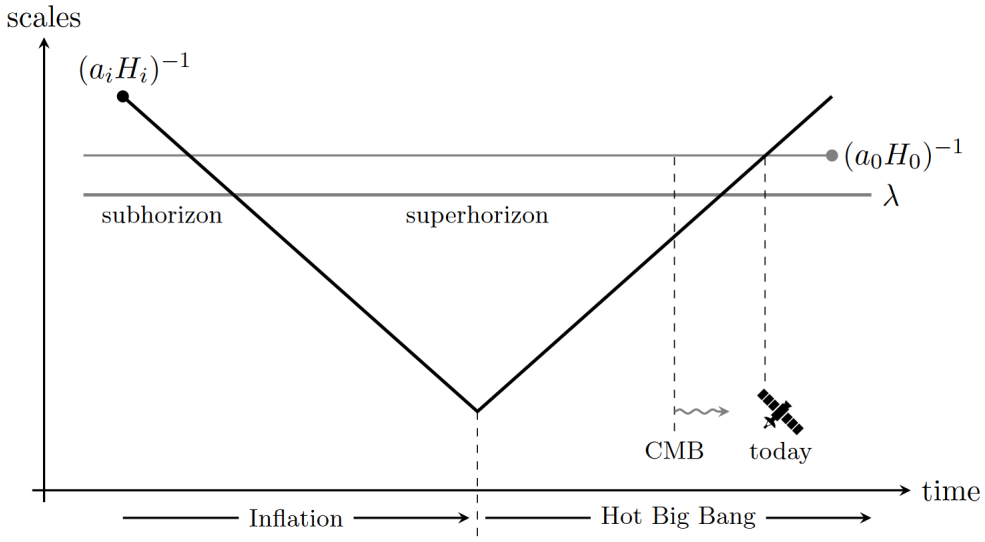

Figure 4: Evolution of perturbations during the inflation and the Hot Big Bang. Each mode enters the super-horizon regime because of inflation. During this phase, perturbations are causally connected. Pict. taken from [11].

2.2 Cosmological perturbation theory

We have seen that the perturbations of the inflaton field, in Eq. (49), induce perturbations in the metric, see Eq. (50). In this Section, we introduce the description of the metric perturbations and present the corresponding perturbed Einstein equations. Note that a complete derivation can be found in [27].

We start by perturbing the FLRW metric to first-order, since we are interested in the evolution of the perturbations at linear order. We write the metric as the sum of the flat FLRW metric, described by the background metric $\bar{g}_{\alpha\beta}$, and its small perturbation $\delta g_{\alpha\beta}$:

$$ds^2 = \left[\bar{g}_{\alpha\beta} + \delta g_{\alpha\beta}\left(x^\gamma\right)\right] dx^\alpha dx^\beta,$$

with $|\delta g_{\alpha\beta}| \ll |\bar{g}_{\alpha\beta}|$. The background metric can be expressed in conformal time as $\bar{g}_{\alpha\beta} dx^\alpha dx^\beta = a^2(\eta)\left(d\eta^2 - \delta_{ij} dx^i dx^j\right)$.

We can write this perturbed metric by introducing the perturbed quantities in the spatial and time components:

$$ds^2 = a^2(\eta)\left[-(1+2A)d\eta^2 + 2B_i dx^i d\eta + \left(\delta_{ij} + 2E_{ij}\right) dx^i dx^j\right], \tag{52}$$

where all the functions A, B_i, and E_{ij} depend on space and time. Note that the factors 2 are introduced for convenience in the derivation of the quantity of interest. It is possible to classify all the perturbed metric components B_i and E_{ij} into scalar-vector-tensor (SVT) ones, thanks to the so-called SVT decomposition. Indeed, the SVT decomposition allows us to write any three-vector into a divergenceless vector, and the gradient of a scalar:

$$B_i = \underbrace{\partial_i B}_{\text{scalar}} + \underbrace{\hat{B}_i}_{\text{vector}},$$

where we have $\partial^i \hat{B}_i = 0$. Moreover, the SVT decomposition applied to rank-2 symmetric

tensor gives:

$$E_{ij} = \underbrace{C\delta_{ij} + \left(\partial_i\partial_j - \frac{1}{3}\delta_{ij}\nabla^2\right)E}_{\text{scalar}} + \underbrace{\frac{1}{2}\left(\partial_i\hat{E}_j + \partial_j\hat{E}_i\right)}_{\text{vector}} + \underbrace{\hat{E}_{ij}}_{\text{tensor}},$$

where C and E are scalars, $\hat{E}i$ a transverse vector, and $\hat{E}ij$ a traceless tensor.

One can verify that the Einstein equations to linear order do not couple the different SVT types. Thanks to this decomposition, we can therefore study scalar, vector, and tensor perturbations separately: each of them evolves independently. Scalar perturbations are associated with variations in the spatial curvature or the gravitational potential. Thus, they are responsible for the variations in the density perturbations observed in the CMB. On the other hand, vector perturbations do not affect the spatial curvature of the universe. These modes arise when a cosmological fluid has a rotational velocity. They are negligible during inflation. Finally, tensor perturbations describe gravitational waves [29]. They are important in the study of the polarisation of the CMB but do not affect the scalar sector at linear order. As a result, scalar perturbations have the most significant impact on the formation of the LSS and the CMB anisotropies. As we will see, these fluctuations may also be crucial in the formation of PBHs. We therefore restrict our analysis to scalar perturbations. We are left with the four scalar quantities to describe the scalar metric perturbation: A, B, C, and E.

2.2.1 Gauge freedom

Before going any further in deriving the evolution of perturbations, we need to introduce the problem of gauge redundancy. Indeed, general relativity is a gauge theory in which all coordinate transformations, from a local frame to another, define gauge transformations. When we considered the classical FLRW description of the universe, it was natural to express the dynamics by choosing the coordinate system respecting the symmetries, i.e. those of the homogeneous and isotropic universe. However, there is no evident preferable coordinate system to analyse perturbations. We therefore need to study this aspect in more detail. Mathematically, we can define the coordinate transformation at the same physical point q as follows:

$$x^\mu(q) \mapsto \tilde{x}^\mu(q) = x^\mu(q) + \xi^\mu(q), \tag{53}$$

where ξ^μ is an infinitesimal 4-vector which can be decomposed as:

$$\begin{aligned}\xi^0 &\equiv T,\\ \xi^i &\equiv L^i = \partial^i L + \hat{L}^i.\end{aligned}$$

This gauge freedom can cause fictitious perturbations to appear in addition to, or even instead of, physical ones. Fictitious perturbations reflect the gauge nature of general relativity and the particular coordinate system considered.

To illustrate this point, let us follow the approach in [18]. We first consider the homogeneous and isotropic FLRW universe. The energy density is unperturbed, and we have a homogeneous energy distribution $\rho(\mathbf{x}, t) = \rho(t)$. This mathematically means that we have a constant energy over the hypersurfaces $t = \text{cst}$, see Figure 5. Because of gauge

freedom, we can change the coordinate system. We can choose a different time coordinate, $\tilde{t}$, related to the old homogeneous frame, in the following way:

$$t \to \tilde{t} = t + \delta t(\mathbf{x}, t),$$

where $\delta t \ll t$. Since the energy density is a scalar, it has the same value at a given physical point in both the old and the new frames: $\tilde{\rho}(\tilde{t}, \mathbf{x}) \equiv \rho(t(\tilde{t}, \mathbf{x}))$. However, the energy density on the hypersurfaces $\tilde{t} = \text{cst.}$ now depends on the spatial coordinates $\mathbf{x}$, see Figure 5. We therefore no longer have a homogeneous universe in the new coordinate system:

$$\tilde{\rho}(\tilde{t}, \mathbf{x}) \equiv \rho(t(\tilde{t}, \mathbf{x})) = \rho(\tilde{t} - \delta t(\mathbf{x}, t)) \simeq \rho(\tilde{t}) - \frac{\partial \rho}{\partial t}\delta t \equiv \rho(\tilde{t}) + \delta\rho(\mathbf{x}, \tilde{t}).$$

So, in the new frame, we end up with a background energy $\rho(\tilde{t})$, with spatial fluctuations $\delta\rho(\mathbf{x}, \tilde{t})$. These perturbations are related to the change of coordinates and are therefore non-physical. This illustrates the essence of the gauge problem.

Coming back to the perturbation evolution problem, we now know that the perturbed quantities of interest, $\delta\phi$ and $\delta g_{\mu\nu}$, depend on the specific gauge choice. For the metric perturbations, we first conclude that the degrees of freedom used to describe scalar perturbations of the metric (A, B, C, and E) are not all physical. It can be shown that only two are physical [27]. The transformation of the metric perturbations, in Eq. (54), can be found using the transformation of the metric tensor $g_{\mu\nu}(x) = \frac{\partial \tilde{x}^\alpha}{\partial x^\mu}\frac{\partial \tilde{x}^\beta}{\partial x^\nu}\tilde{g}_{\alpha\beta}(\tilde{x})$. Considering the change of coordinates in Eq. (53) and perturbing to linear order, we find:

$$\begin{aligned} &A \mapsto A - T' - \mathcal{H}T, && \\ &B \mapsto B + T - L', && \hat{B}_i \mapsto \hat{B}_i - \hat{L}_i', \\ &C \mapsto C - \mathcal{H}T - \tfrac{1}{3}\nabla^2 L, && \\ &E \mapsto E - L, && \hat{E}_i \mapsto \hat{E}_i - \hat{L}_i, \quad \hat{E}_{ij} \mapsto \hat{E}_{ij}. \end{aligned} \tag{54}$$

The transformation of the perturbation of the field is found similarly using Eq. (49) with the gauge transformation described in Eq. (53). Expanding to linear order, we find the following transformation:

$$\delta\phi \mapsto \delta\phi - \bar{\phi}' T. \tag{55}$$

There are two different approaches to solve the gauge problem: we can either find the evolution of the gauge-invariant variables by rewriting the Einstein equation in terms of these gauge-invariant quantities, or we can choose a specific gauge and perform the computation in the gauge chosen. In this thesis, we will fix the gauge using $C = E = 0$. Using this condition, we see that the scalar part of the perturbed metric, in Eq. (52), has no spatial perturbations, or equivalently $\delta g_{ij} = 0$. This gauge is called the spatially flat gauge (SF).

As an example of gauge-invariant quantities, we can report the following Bardeen variables as follows:

$$\begin{aligned} \Psi &\equiv A + \mathcal{H}\left(B - E'\right) + \left(B - E'\right)', \\ \Phi &\equiv -C + \frac{1}{3}\nabla^2 E - \mathcal{H}\left(B - E'\right). \end{aligned}$$

In addition, we introduce the comoving curvature perturbation, being a gauge-invariant quantity composed of the gravitational potential and the inflaton perturbation:

$$\mathcal{R} = -C + \frac{1}{3}\nabla^2 E + H\frac{\delta\phi}{\dot{\phi}} \overset{\text{SF}}{=} H\frac{\delta\phi}{\dot{\phi}}, \tag{56}$$

where in the last equality, we used the spatially flat gauge $C = E = 0$. The gauge invariance of all these quantities can be verified using the transformations in Eqs. (55) and (54). Note that in the following, we will remove the bar notation for the background quantities.

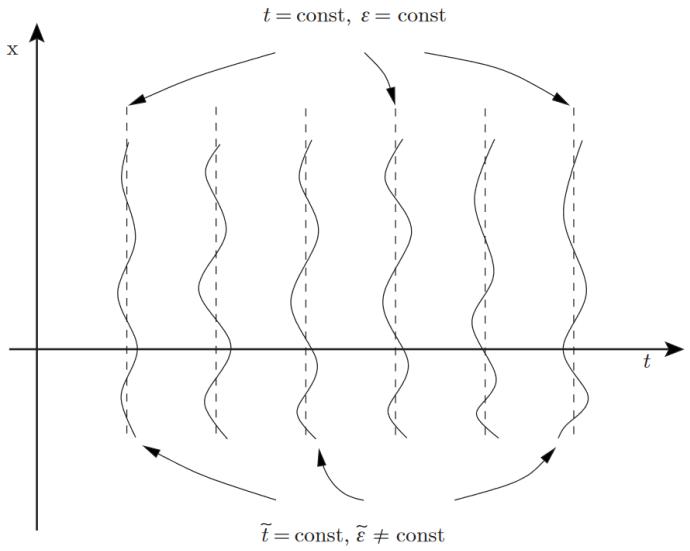

Figure 5: Gauge problem arising from the relativistic description of the universe. The quantity $\epsilon \equiv \rho$ is the energy density. Pict. taken from [18].

2.2.2 Perturbed Einstein equations

In the SF gauge, the perturbed metric in Eq. (52) takes the following form:

$$g_{\mu\nu} \overset{\text{SF}}{=} a^2 \begin{pmatrix} -(1+2A) & \partial_i B \\ \partial_i B & \delta_{ij} \end{pmatrix} \Rightarrow g^{\mu\nu} \overset{\text{SF}}{=} \frac{1}{a^2}\begin{pmatrix} -(1-2A) & \partial^i B \\ \partial^i B & \delta^{ij} \end{pmatrix},$$

where in the last equality, we wrote the inverse of this metric expressed at linear order.

This metric leads to the perturbed Einstein equations:

$$\delta G_{\mu\nu} = \delta R_{\mu\nu} - \frac{1}{2}\delta g_{\mu\nu} R - \frac{1}{2} g_{\mu\nu}\delta R = \delta T_{\mu\nu}$$

It turns out that it is easier to work with higher and lower indices mixed together:

$$\delta G^{\mu}_{\nu} = \delta\left(g^{\mu\alpha} G_{\alpha\nu}\right) = \delta g^{\mu\alpha} G_{\alpha\nu} + g^{\mu\alpha}\delta G_{\alpha\nu} = \delta T^{\mu}_{\nu}$$

It can be shown, see [27], that the perturbed Einstein tensor in the SF gauge is given by:

$$\delta G_0^0 \overset{\text{SF}}{=} \frac{1}{a^2}\left(6\mathcal{H}^2 A + 2\mathcal{H}\nabla^2 B\right), \tag{57}$$

$$\delta G_i^0 \overset{\text{SF}}{=} \frac{1}{a^2}\left(-2\mathcal{H}\partial_i \Phi\right), \tag{58}$$

$$\begin{aligned}\delta G_j^i \overset{\text{SF}}{=} \frac{1}{a^2}\Bigg[&\left(2\mathcal{H}A' + 4\frac{a''}{a}A - 2\mathcal{H}^2 A + \partial_i\partial^i A + 2\mathcal{H}\partial_i\partial^i B + \partial_i\partial^i B'\right)\delta_j^i \\ &-\partial^i\partial_j A - 2\mathcal{H}\partial^i\partial_j B - \partial^i\partial_j B'\Bigg].\end{aligned}$$

where the prime denotes the derivative w.r.t. conformal time (see the definition in Eq. (14)).

In the case of inflation, the energy content of the universe is dominated by the inflaton field. Using the energy-momentum tensor in Eq. (25), we can now write its perturbed version in the following way:

$$\begin{aligned}\delta T_\nu^\mu =&\partial^\mu\delta\phi\partial_\nu\phi + \partial^\mu\phi\partial_\nu\delta\phi - \delta g_\nu^\mu\left(\frac{1}{2}g^{\alpha\beta}\partial_\alpha\phi\partial_\beta\phi + V(\phi)\right) \\ &- g_\nu^\mu\left(\frac{1}{2}\delta g^{\alpha\beta}\partial_\alpha\phi\partial_\beta\phi + g^{\alpha\beta}\partial_\alpha\delta\phi\partial_\beta\phi + \frac{\partial V}{\partial\phi}\delta\phi + \frac{\partial V}{\partial\phi}\delta\phi\right).\end{aligned}$$

Using the conformal time for the background quantities, in Eqs. (27) and (26):

$$T_0^0 = \frac{1}{2}\phi'^2 + V(\phi)a^2, \quad T_i^0 = 0, \quad T_j^i = \left(\frac{1}{2}\phi'^2 - V(\phi)a^2\right)\delta_j^i,$$

one can show that the energy-momentum tensor perturbations are given by [27]:

$$\begin{aligned}\delta T_0^0 &\overset{\text{SF}}{=} A\phi'^2 - \delta\phi'\phi' - \delta\phi\frac{\partial V}{\partial\phi}a^2, \\ \delta T_i^0 &\overset{\text{SF}}{=} -\partial^i\delta\phi\phi', \\ \delta T_j^i &\overset{\text{SF}}{=} \left(-A\phi'^2 + \delta\phi'\phi' - \delta\phi\frac{\partial V}{\partial\phi}a^2\right)\delta_j^i.\end{aligned}$$

To conclude, perturbations of the metric generalise the Einstein equations into perturbed Einstein equations. The field perturbation describes perturbations in the energy content of the universe. We obtain a set of equations coupling the scalar field and the metric perturbations.

2.3 Evolution of scalar perturbations

To study the evolution of the scalar perturbations at linear order, we need to write the perturbed Klein-Gordon equation. It describes the equation of motion of the perturbation $\delta\phi$. The Klein-Gordon equation is given by:

$$\frac{1}{\sqrt{-g}}\partial_\nu\left(\sqrt{-g}g^{\mu\nu}\partial_\nu\phi\right) = \frac{\partial V}{\partial\phi}.$$

To leading order, it gives the usual homogeneous Klein-Gordon equation (24). Using the perturbed metric in (52) and the perturbed field in Eq. (49), it gives the perturbed Klein-Gordon equation [27]:

$$\delta\phi'' + 2\mathcal{H}\delta\phi' - \nabla^2\delta\phi - A'\phi' - \nabla^2 B\phi' \overset{\text{SF}}{=} -\delta\phi\frac{\partial^2 V}{\partial\phi^2}a^2 - 2A\frac{\partial V}{\partial\phi}.$$

We can suppress the perturbed quantities A and $\nabla^2 B$ using the perturbed Einstein equations (57) and (58). Performing the change of variable $v = a\delta\phi$, one can finally show that the perturbed Klein-Gordon equation reduces to:

$$v_k'' + \left(k^2 - \frac{z''}{z}\right)v_k = 0, \tag{59}$$

where v_k is the Fourier transform of $v(\eta, \mathbf{x})$. We have defined the variable z in conformal time as:

$$z \equiv \frac{a\phi'}{\mathcal{H}}. \tag{60}$$

The Hubble parameter in conformal time $\mathcal{H}$ is defined in Eq. (22). Eq. (59) is called the Mukhanov-Sasaki equation. It describes the way in which metric and matter fluctuations influence each other: the evolution of density fluctuations is influenced by the kinetic energy k^2 and the dynamics of the inflationary model z. It connects the behaviour of the scalar field perturbation to the expansion of the universe, providing the temporal evolution of the perturbations.

The function z is a time-dependent function and depends on the inflationary model considered. Eq. (60) is valid for general relativity. In this work, we are also interested in modified theories of gravity. The generalisation of the derivation of the Mukhanov-Sasaki equation in these frameworks can be found in [30]–[32]. The variable z of Eq. (60) then takes the following form:

$$z \equiv \frac{a\phi'}{\mathcal{H}}\sqrt{Z} = \frac{a\dot{\phi}}{H}\sqrt{Z}. \tag{61}$$

The change of variable suppressing the friction term proportional to $\delta\phi'$, is generalised to: $v = a\sqrt{Z}\delta\phi$. We will define the function Z later when studying the particular cases individually. With this specific definition of z, we can write the third term of the Mukhanov-Sasaki equation in the general form:

$$\frac{z''}{z} \equiv a^2 H^2 f_{\text{MS}}. \tag{62}$$

The function f_{MS} can be expressed through the SR parameters. In the case of general relativity, the function z given by Eq. (60) can be expressed as follows:

$$\epsilon_1 = -\frac{\dot{H}}{H^2} = \frac{1}{2\text{M}_\text{P}^2}\frac{(\phi')^2}{\mathcal{H}^2} \;\Rightarrow\; z = \sqrt{2}\text{M}_\text{P} a\sqrt{\epsilon_1}. \tag{63}$$

where we used the definition of the first SR parameter with Eq. (30) expressed in conformal time. The corresponding function f_{MS} is expressed in Eq. (264), see annex A.1 for the derivation.

We are interested in studying the consequences of the scalar perturbation on the evolution of the universe. To do so, we need to calculate the evolution of the comoving curvature perturbation, defined in Eq. (56). We can express it in terms of the variable v and the function z:

$$\mathcal{R} \overset{\text{SF}}{=} \mathcal{H}\frac{\delta\phi}{\phi'} = \frac{v}{z}. \tag{64}$$

The resolution of the Mukhanov equation therefore gives the evolution of the comoving curvature perturbation. Before proceeding in this direction, we need to quantise the inflaton field perturbations, which are a quantum field.

2.3.1 Quantising inflationary perturbations

To describe the quantum fluctuation of the scalar field, we need to use quantum field theory on curved spacetime. In this Section, we review the main steps and refer to the reference [17] for complete details. To perform this description, we follow the canonical quantisation procedure. First, we promote the field $v(\eta, \mathbf{x})$ and its conjugate momentum $\pi(\eta, \mathbf{x})$ into quantum operators $\hat{v}(\eta, \mathbf{x})$ and $\hat{\pi}(\eta, \mathbf{x}) = dv(\eta, \mathbf{x})/d\eta$. Then, we impose the equal-time commutation relation:

$$[\hat{v}(\eta, \mathbf{x}), \hat{\pi}\,(\eta, \mathbf{x}')] = i\delta^{(3)}\,(\mathbf{x} - \mathbf{x}')\,, \tag{65}$$

where $\delta^{(3)}$ is the 3-dimensional Dirac delta function. This essentially means that modes at different spatial coordinates are independent and commute. This is the definition of locality, see [33]. The field $\hat{v}$ and its conjugate momentum can then be expanded in Fourier modes:

$$\begin{aligned}\hat{v}(\eta, \mathbf{x}) &= \int \frac{d^3k}{(2\pi)^3}\hat{v}_{\mathbf{k}}(\eta)e^{i\mathbf{k}\cdot\mathbf{x}},\\ \hat{\pi}(\eta, \mathbf{x}) &= \int \frac{d^3k}{(2\pi)^3}\hat{\pi}_{\mathbf{k}}(\eta)e^{i\mathbf{k}\cdot\mathbf{x}}.\end{aligned} \tag{66}$$

The commutation relation (65) becomes:

$$\begin{aligned}[\hat{v}_{\mathbf{k}}(\eta), \hat{\pi}_{\mathbf{k}'}(\eta)] &= \int d^3x \int d^3x' \,[\hat{v}(\eta, \mathbf{x}), \hat{\pi}\,(\eta, \mathbf{x}')]\, e^{-i\mathbf{k}\cdot\mathbf{x}}e^{-i\mathbf{k}'\cdot\mathbf{x}'}\\ &= i(2\pi)^3\delta^{(3)}\,(\mathbf{k} + \mathbf{k}')\,,\end{aligned} \tag{67}$$

The operators $\hat{v}_k(\eta)$ satisfy the Mukhanov-Sasaki equation. The general solution of such an equation can be expressed through a linear combination of the complex mode functions v_k and their complex conjugates as [17]:

$$\hat{v}_{\mathbf{k}}(\eta) = v_k(\eta)\hat{a}_{\mathbf{k}} + v_k^*(\eta)\hat{a}^\dagger_{-\mathbf{k}},$$

where $\hat{a}_{-\mathbf{k}}$ and $\hat{a}^\dagger_{-\mathbf{k}}$ are time-independent creation-annihilation operators and $\hat{v}_{-\mathbf{k}} = \hat{v}^\dagger_{\mathbf{k}}$. Inserting this expression in the Fourier expansion (66), we find the following mode expansion of the field operator $\hat{v}$:

$$\hat{v}(\eta, \mathbf{x}) = \int \frac{d^3k}{(2\pi)^3}\left[\hat{a}_{\mathbf{k}}v_k(\eta)e^{i\mathbf{k}\cdot\mathbf{x}} + \hat{a}^\dagger_{\mathbf{k}}v_k^*(\eta)e^{-i\mathbf{k}\cdot\mathbf{x}}\right]. \tag{68}$$

Using the mode expansion of the fields (68) and Eq. (67), the commutation relation (65) becomes the usual commutation relation for creation and annihilation operators:

$$[\hat{a}_{\mathbf{k}}, \hat{a}^{\dagger}_{\mathbf{k}'}] = (2\pi)^3 \delta^{(3)} (\mathbf{k} + \mathbf{k}') \,, \tag{69}$$

provided that the mode functions v_k and v_k* are properly normalised, i.e. the Wronksian $W[v_k, v_k^*]$ is given by:

$$W[v_k, v_k^*] \equiv v_k v_k'^* - v_k' v_k^* = i. \tag{70}$$

Let us note that the mode function v_k defining the mode expansion is not unique. One can indeed use a Bogoliubov transformation and define new mode functions (using linear combinations of the mode functions and their complex conjugates). Different mode functions give a different particle interpretation. Therefore, we are left with an ambiguity to define the physical vacuum state:

$$\hat{a}_{\mathbf{k}} (\eta_i) |0\rangle = 0.$$

The vacuum state can be defined as the ground state of the Hamiltonian, which is time-dependent. A way to solve the ambiguity is thus to choose a particular moment in time and find the corresponding lowest energy eigenstate of the Hamiltonian. In the context of quantum fields in de Sitter spacetime, the Bunch-Davies vacuum state is a natural choice. It is defined as the minimum energy eigenstate in the early universe, at $\eta \to -\infty$. As we will see in the next Section, the Mukhanov-Sasaki equation then reduces to the equation of a harmonic oscillator with a fixed frequency $\omega_k^2 = k^2$. Therefore for each Fourier mode, we take the vacuum state of the harmonic oscillator at $\eta \to -\infty$. The corresponding mode function for this vacuum is of the form, see [11]:

$$\lim_{k\eta \to -\infty} v_k(\eta) = \frac{1}{\sqrt{2k}} e^{-ik\eta}, \tag{71}$$

This condition defines the Bunch-Davies initial condition. The mode function $v_k(\eta)$ satisfying the limit (71) as initial condition is called the Bunch-Davies mode function.

2.3.2 Sub-Hubble and super-Hubble regimes

To have a first idea of the evolution of v_k, we will split the evolution into sub-Hubble and super-Hubble regimes [20], defined in Section 2.1. Let us consider the formation of quantum field perturbations at early times, during inflation. At this time, we have a quasi-constant expansion with a slow-varying scalar field: $\phi'/\mathcal{H} \sim$ cst.. Then, using Eq. (63), we find: $\frac{z''}{z} \approx \frac{a''}{a} = \frac{(a^2 H)'}{a} \approx 2R_H^{-2}$. As mentioned earlier, the Hubble radius during inflation is large. All the perturbations we observe today in the CMB and the LSS are in the sub-Hubble regime and we have $k^2 \gg z''/z$. The Mukhanov-Sasaki equation becomes the equation of a harmonic oscillator of fixed frequency $\omega_k^2 = k^2$:

$$v_k'' + k^2 v_k = 0.$$

The general solution of this differential equation is a superposition of a progressive and regressive plane waves: $v_k = C_+ e^{-ik\eta} + C_- e^{ik\eta}$. The integration constants are fixed by imposing as initial condition, the Bunch-Davies condition (71):

$$\lim_{k\eta \to -\infty} C_+ e^{-ik\eta} + C_- e^{ik\eta} = \frac{1}{\sqrt{2k}} e^{-ik\eta} \;\Rightarrow\; C_+ = \frac{1}{\sqrt{2k}} \text{ and } C_- = 0. \tag{72}$$

Thus, the perturbations have an oscillatory behaviour when they are still inside the Hubble radius. The comoving curvature perturbation R_k, defined in Eq. (64), is therefore also oscillating.

As the expansion evolves, the Hubble radius decreases. At some point, the mode can eventually enter the super-Hubble regime in which we have $k^2 \ll z''/z$:

$$v_k'' - \frac{z''}{z} v_k = 0.$$

By multiplying by z and adding the null term $zv_k' - z'v_k$, we can write this equation as $\frac{d}{d\eta}(zv_k' - z'v_k) = 0$. After integration and division by z^2, we can again make appear a conformal time derivative: $\frac{d}{d\eta}\frac{v_k}{z} = \frac{B_k}{z^2}$, and finally obtain the general super-Hubble solution:

$$R_k = \frac{v_k}{z} = A_k + B_k \int \frac{d\eta}{z^2} = A_k + C_k \int \frac{dt}{a^3 \epsilon_1}, \tag{73}$$

where A_k, B_k, and C_k are integration constants, and we used Eq. (63) in the last equality. Consequently, the curvature perturbation is a linear combination of two solutions: a constant solution given by A_k and a growing or decreasing solution depending on the form of z. In the standard SR inflation, ϵ_1 is approximately constant. Therefore, the function which multiplies C_k is decreasing as $a^{-3} \to 0$. In this case, the constant solution is going to dominate for a large. We say that the comoving curvature perturbation on large scales is frozen. It will remain frozen until horizon re-entry. In Section 3.3, we are going to see that PBHs can be produced if a growing solution is instead present.

2.3.3 Power spectrum

In the early universe, the sub-horizon perturbations oscillate. Since the inflaton is a quantum field, the amplitude of these oscillations has a quantum mechanical behaviour. By definition, the mean value of the density perturbations vanishes for the vacuum, $\langle \hat{v}(\eta, \mathbf{x}) \rangle \equiv \langle 0 | \hat{v} | 0 \rangle = 0$. To describe statistically the fluctuations, one must calculate the vacuum expectation value of the square of $\hat{v}(\eta, x)$. It has non-zero quantum fluctuations:

$$\begin{aligned} \langle \hat{v}^2(\eta, x) \rangle &= \int \frac{d^3k}{(2\pi)^3} \int \frac{d^3k'}{(2\pi)^3} v_k(\eta) v_{k'}^*(\eta) \langle 0 | [\hat{a}_{+\mathbf{k}}, \hat{a}^\dagger_{-\mathbf{k}'}] | 0 \rangle \\ &= \int \frac{d^3k}{(2\pi)^3} |v_k(\eta)|^2 = \int d\ln k \frac{k^3}{2\pi^2} |v_k(\eta)|^2 . \end{aligned} \tag{74}$$

where $|0\rangle$ is the Bunch-Davies vacuum state and we used Eq. (69) in the second equality. This relation expresses the vacuum fluctuations of the Mukhanov-Sasaki field. We can now define the dimensionless power spectrum of the scalar perturbation as the statistical distribution of these fluctuations, using Eq. (64) into (74):

$$\mathcal{P}_\mathcal{R}(k, \eta) \equiv \frac{k^3}{2\pi^2} |\mathcal{R}_k(\eta)|^2 = \frac{k^3}{2\pi^2} \frac{|v_k(\eta)|^2}{z^2(\eta)}. \tag{75}$$

In order to compare the theoretical predictions of a model of inflation with observation, one needs to compute the power spectrum and compare it with the observed one (which

can be inferred by CMB anisotropies). It describes how the amplitude of the perturbations varies as a function of the scale k^{-1}.

The spectral index is often introduced to describe the slope of the power spectrum:

$$n_s - 1 = \frac{d \ln \mathcal{P}_{\mathcal{R}}(k, \eta)}{d \ln k} \tag{76}$$

The spectral index is said to be red-tilted when $n_s - 1 < 0$. It means that for decreasing wavelengths or increasing wavenumbers k, the power spectrum decreases. In contrast, the power spectrum is blue-tilted when $n_s - 1 > 0$. In such cases, the power spectrum increases for increasing wavenumbers k. When the spectral index is null, the spectrum is flat or "scale-invariant". This means that the amplitude of the power spectrum is independent of k. Flatness is a consequence of a constant Hubble parameter H. A red-tilted spectrum, in contrast, usually indicates a slowly decreasing $H(t)$.

Let us now calculate explicitly the primordial power spectrum generated by a SR inflationary phase [11], [34], [35]. To do so, the Mukhanov-Sasaki equation (59) needs to be solved for the mode functions v_k. In GR, the function z is defined in Eq. (63). In Annex A.1, the first and second derivatives have been calculated:

$$\frac{z'}{z} = \mathcal{H}\left[1 + \frac{1}{2}\epsilon_2\right], \tag{77}$$

$$\frac{z''}{z} \approx \mathcal{H}^2\left[2 - \epsilon_1 + \frac{3}{2}\epsilon_2\right]. \tag{78}$$

The first expression is exact, while the second is approximated to first order in the SR parameters. We now want to express the conformal Hubble parameter $\mathcal{H}$, defined in Eq. (22), in the same approximate SR expansion.

Let us first calculate the expression of the conformal time, defined in Eq. (14), in terms of the SR parameters:

$$\begin{aligned}\eta &= \int \frac{dt}{a} = \int \frac{da}{a^2 H} = -\frac{1}{aH} + \int \frac{1}{a}\frac{dH^{-1}}{da} da = -\frac{1}{aH} + \int \frac{\epsilon_1}{a^2 H} da, \\ &= -\frac{1}{aH} - \frac{\epsilon_1}{aH} + \int \frac{1}{a}\frac{d\left(\epsilon_1 H^{-1}\right)}{da} da = -\frac{1}{aH} - \frac{\epsilon_1}{aH} + \int \frac{\epsilon_1 \epsilon_2}{a^2 H} - \frac{\epsilon_1^2}{a^2 H} da,\end{aligned} \tag{79}$$

where we have integrated by parts twice using $da = aH dt$ and used the relations:

$$\begin{aligned}\frac{1}{a}\frac{dH^{-1}}{da} &= -\frac{1}{aH^2}\frac{dH}{da} = \frac{\epsilon_1}{a^2 H}, \\ \frac{1}{a}\frac{d\left(\epsilon_1 H^{-1}\right)}{da} &= \frac{1}{aH}\frac{d\epsilon_1}{da} + \frac{\epsilon_1}{a}\frac{dH^{-1}}{da} = \frac{\epsilon_1 \epsilon_2}{a^2 H} - \frac{\epsilon_1^2}{a^2 H}.\end{aligned}$$

From Eq. (79), we can express the conformal Hubble parameter up to linear order as:

$$\mathcal{H} = aH \approx -\frac{1}{\eta}(1 + \epsilon_1). \tag{80}$$

By inserting Eq. (80) into Eq. (78), we find to linear order:

$$\frac{z''}{z} = \frac{1}{\eta^2}\left[2 + 3\left(\epsilon_1 + \frac{1}{2}\epsilon_2\right)\right].$$

Therefore, we can write the Mukhanov-Sasaki equation (59) as follows:

$$v_k'' + \left(k^2 - \frac{\nu^2 - 1/4}{\eta^2}\right) v_k = 0, \quad \text{where} \quad \nu \equiv \frac{3}{2} + \epsilon_1 + \frac{1}{2}\epsilon_2, \tag{81}$$

and ν can be considered constant to such an approximation order. Defining the changes of variables $v_k \to \eta^{1/2}\tilde{v}_k$ and $k\eta \to s$, Eq. (81) can be recast in the form of a Bessel equation:

$$s^2 \frac{d^2\tilde{v}_k}{ds^2} + s\frac{d\tilde{v}_k}{ds} + \left(s^2 - \nu^2\right)\tilde{v}_k = 0.$$

This equation has its general solution expressed through the Bessel functions $J_\nu(s)$ and $Y_\nu(s)$:

$$\tilde{v}_k(s) = AJ_\nu(s) + BY_\nu(s).$$

Imposing the Wronskian condition (70) together with the Bunch-Davies initial condition (71), it is possible to find the expression of A and B [17] and write the Bunch-Davies vacuum mode function as:

$$\tilde{v}_k(\eta) = \frac{\sqrt{\pi}}{2}\sqrt{-\eta}H_\nu^{(1)}(-k\eta) \tag{82}$$

where $H_\nu^{(1)}(-k\eta) = J_\nu(k\eta) - iY_\nu(k\eta)$ is the Hankel function of the first kind.

To compute the power spectrum of $\mathcal{R} = v/z$, we need the expression of $z(\eta)$. Using Eq. (80) in Eq. (77), and integrating over η, we get:

$$z(\eta) = z_*\left(\eta/\eta_*\right)^{\frac{1}{2}-\nu}, \tag{83}$$

where η_* is a reference time, coming from the integration. A convenient choice for η_* will be $\eta_* = -k_*^{-1}$, which is the time of horizon crossing of the mode with wavenumber k_*. Indeed, we saw that after horizon exit, the modes are frozen. It is therefore not necessary to follow the evolution of the mode after horizon exit. Inserting Eqs. (82) and (83) into the definition of the power spectrum of the scalar perturbation (75), we find:

$$\mathcal{P}_\mathcal{R}(k) = \frac{k^3}{2\pi^2}\frac{1}{2\epsilon_1^* M_{\rm Pl}^2 a_*^2}\left(-k_*\eta\right)^{2\nu-1}\frac{\pi}{4}(-\eta)\left|H_\nu^{(1)}(-k\eta)\right|^2. \tag{84}$$

The Hankel function can be approximated using the late-time limit $k\eta \to 0^-$ as follows:

$$\lim_{k\eta\to 0^-}\left|H_\nu^{(1)}(-k\eta)\right|^2 = \frac{2^{2\nu}\Gamma(\nu)^2}{\pi^2}(-k\eta)^{-2\nu} \approx \frac{2}{\pi}(-k\eta)^{-2\nu},$$

Using this limit and $a_* = k_*/H_*$ in Eq. (84), we finally obtain:

$$\mathcal{P}_\mathcal{R}(k) = \frac{1}{8\pi^2\epsilon_1^*}\frac{H_*^2}{M_{\rm Pl}^2}\left(\frac{k}{k_*}\right)^{3-2\nu}, \tag{85}$$

where all the quantities with a star $_*$ are evaluated at the time of horizon exit t_* of the mode with wavenumber k_*. We see that the whole dynamics of inflation is contained into ϵ_1 and ν. Extracting the scale dependence of the power spectrum, see Eq. (76), we get the spectral index:

$$n_s - 1 \equiv 3 - 2\nu = -2\epsilon_1 - \epsilon_2. \tag{86}$$

The current constraints on the spectral index are set by CMB measurements of the PLANCK mission to $n_s = 0.965 \pm 0.004$ [36]. Thus, the latest measurement of the power spectrum indicates a time-dependent inflationary phase. This is in agreement with SR inflation, in which the power spectrum turns out to be slightly red-tilted due to the smallness of the SR parameters, see Eq. (86). As a result, SR inflation predicts the correct nearly flat power spectrum due to the approximate time translation invariant dynamics (ϵ_i small). The time-dependence allows inflation to end, leaving the universe with density fluctuations, responsible for the formation of the CMB anisotropies and the LSS [37]. In the next Section, we will see how they can also be responsible for the generation of the PBHs.

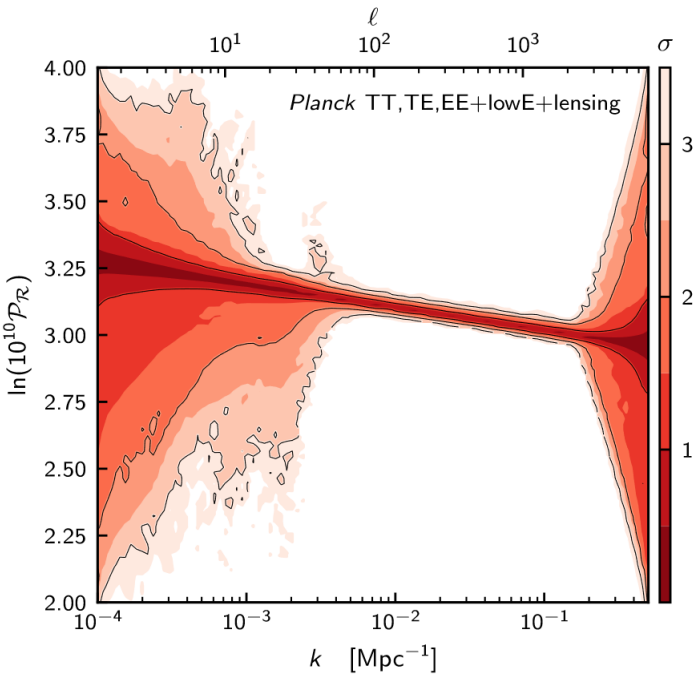

Figure 6: Reconstruction of the primordial power spectrum from the PLANCK data analysis 2015. The left and right parts are not well constrained due to the lack of resolution. Pict. taken from [36].

3 Primordial Black Holes

A black hole (BH) is defined as a stellar object characterised by a huge gravitational field. Mathematically, general relativity predicts that a black hole forms when its mass M collapses into the corresponding Schwarzschild radius:

$$R_S = \frac{2GM_{\rm BH}}{c^2}, \tag{87}$$

where G is the gravitational constant, M is the mass of the black hole, and c is the speed of light. So it relates the mass of a black hole to the size of its event horizon[15]. We can then classify them according to their radius [6]. Stellar-mass BHs are produced by the astrophysical evolution of stellar objects. Their mass is typically several times the solar mass ($M_\odot$). Higher in the mass range, intermediate-mass BHs are thought to form from the gravitational collapse of the first primordial stars, with masses greater than $100M_\odot$. Finally, supermassive BHs are found at the centres of galaxies with masses between 10^6 and $10^{10}M_\odot$.

BHs formed by stellar evolution come from stellar objects with mass greater than the Chandrasekhar mass, $1.4M_\odot$. However, density perturbations in the early universe can also form BHs [38]. These black holes are called Primordial Black Holes, in the sense that they originate from the density fluctuations of the early universe and not from the conventional collapse of massive stars [39]. PBHs can have a wide range of possible masses. As a result, they are interesting for several explanations of open cosmological questions. They may, for instance, be the seeds for the formation of supermassive BHs. Much lower in mass, there is a small mass window allowing PBHs to explain the whole DM content. The mass of a BH is expressed by its Schwarzschild radius in Eq. (87). PBHs, covering the entire DM content, have a tiny size between 0.1 and 1 angstrom [39], i.e. the size of the smallest atoms.

In Section 3.1, we are going to review the physics behind the formation of PBHs. In Section 3.2, we will see the different constraints on the mass window allowed for PBHs. In contrast to other dark matter candidates, PBHs do not require new physics or new particles, but a particular inflationary phase must be introduced. In the context of inflation, the usual SR condition needs to be modified. Studying the formation of PBHs therefore means studying the inflation dynamics. In Section 3.3, we will review the various possibilities of achieving this. This Chapter is based on [3], [28], [40] as main references.

3.1 Formation mechanism

Inflation provides a natural mechanism for the production of PBHs. To understand the formation of PBHs from an initial overdensity, it is essential to remember that gravitational information travels at the speed of light. Therefore, an initial density perturbation of scale k^{-1} can start to collapse provided that its content is in causal contact. It means that the matter content within a given perturbation will feel the whole gravitational

[15]The event horizon is defined as the maximal distance at which events can still be influenced. Note the difference with the particle horizon, which is defined as the maximal distance past events could affect us.

attraction once the light signal has travelled a distance comparable to k^{-1}. Just after inflation, we enter RD in which the scale factor evolves as $a \propto t^{1/2}$, see Table 1. Therefore, since $H = \frac{\dot{a}}{a} = \frac{1}{2t} \sim t^{-1}$, the Hubble time H^{-1} is a good estimator for the age of the universe just after inflation. As we saw before, the comoving distance that a light signal can travel in one Hubble time is the Hubble radius $R_H = (aH)^{-1}$. Therefore, in one Hubble time after inflation, a given perturbation will be in causal contact if $k^{-1} \sim (aH)^{-1}$. It is the definition of horizon re-entry introduced previously in Section 2.1. In other words, in the sub-Hubble regime, comoving curvature perturbations may collapse and can potentially form PBHs.

Following this picture, we conclude that PBHs are formed with a mass similar to the horizon mass M_H, which is the mass enclosed within the Hubble horizon [41]:

$$M_{\rm PBH} \sim M_H, \tag{88}$$

In this work, we shall consider perturbations re-entering the Hubble horizon during the RD universe. During MD, the horizon mass would be huge: the horizon mass at matter-radiation equality is already of the order $M_H^{(eq)} \sim 10^{17} M_\odot$ [42]. However, during RD, radiation pressure is extremely large, see Eq. (9): $p = \frac{1}{3}\rho$. The condition for accretion is determined by the competition between the curvature perturbation collapsing due to gravity and the radiation pressure, see Figure 7. Therefore, in addition to horizon re-entry,

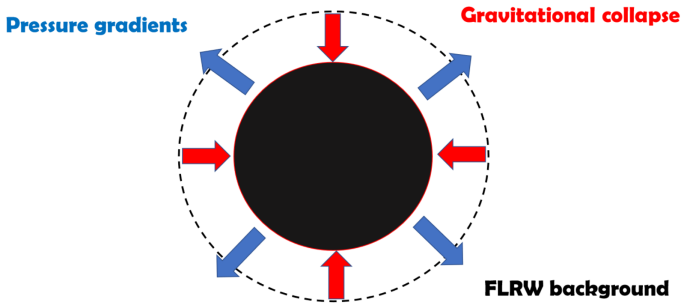

Figure 7: Gravitational collapse against radiation dilution of a perturbation on a FLRW background. Pict. taken from [43].

perturbations also need a large amplitude to undergo sufficient gravitational collapse and form PBHs. More precisely, the density perturbations need to be amplified w.r.t the ones responsible for the generation of the anisotropies in the CMB. These last ones have an amplitude constrained by the CMB observations [36]:

$$\delta = \frac{\delta\rho}{\rho} \sim \mathcal{P}_\mathcal{R}\left(k_{\rm CMB}\right)^{1/2} \sim \frac{\delta T}{T_0} \sim 5 \times 10^{-5}.$$

where we used the relation (13). The quantity δ is called the density contrast. We saw earlier that the power spectrum is slightly red-tilted at CMB scales. However, at smaller scales, the power spectrum is not well constrained and it is therefore possible for the perturbations to be larger, see Figure 6. Thus, we are interested in a mechanism producing amplified perturbations at small scales: $k_{\rm PBH}^{-1} \ll k_{\rm CMB}^{-1}$. This corresponds to requiring an amplified power spectrum: $P_\mathcal{R}(k_{\rm PBH}) \gg P_\mathcal{R}(k_{\rm CMB}) \sim 10^{-9}$ [36]. If the overdensities exceed in some region a certain threshold δ_c at re-entry:

$$\delta \equiv \left.\frac{\delta\rho}{\rho}\right|_{k=aH} \sim \mathcal{P}_\mathcal{R}\left(k_{\rm PBH}\right)^{1/2} > \delta_c, \tag{89}$$

these regions begin to collapse, eventually forming PBHs. In [44], Carr estimated the threshold using Newtonian gravity and introducing the sound speed of the density perturbations c_s:

$$\delta > \delta_c \simeq c_s^2,$$

The sound speed gives the speed of propagation of the pressure wave generated by the over-density. A smaller sound speed corresponds to a lower pressure and a faster collapse. The sound speed is related to the equation of state (9): $p = w\rho = c_s^2\rho$. During RD, this estimation gives $\delta_c \simeq c_s^2 = 1/3$[16]. More recently, refined estimates have given $\delta_c = 0.45$ [43].

The amount of PBHs formed in the early universe can be related to the amplitude $\mathcal{P}_\mathcal{R}(k_{\rm PBH})$, see Eq. (89). Let us introduce the fraction of DM consisting in PBHs today:

$$f_{\rm PBH} \equiv \left.\frac{\rho_{\rm PBH}}{\rho_{\rm DM}}\right|_{t_0},$$

The case $f_{\rm PBH} = 1$ corresponds to the situation where PBHs constitute the whole dark matter content. It might be possible as well that PBHs do not constitute the whole dark matter content: $0 < f_{PBH} < 1$. We can also introduce the PBHs collapse fraction defined at the time of formation:

$$\beta = \left.\frac{\rho_{\rm PBH}}{\rho_{\rm tot}}\right|_{\rm form}$$

During the RDU, when PBHs are assumed to be formed, the total energy density evolves as: $\rho_{\rm tot} = \rho_{\rm r} \propto a^{-4}$. On the other hand, once PBHs are formed, their density is that of pressureless matter (dust): $\rho_{\rm PBH} = \rho_{\rm m} \propto a^{-3}$. Therefore, during RDU and until matter-radiation equality, the collapse fraction evolves as the scale factor $\rho_{\rm PBH}/\rho_{\rm tot} \propto a$:

$$\beta \sim \frac{a_{\rm form}}{a_{\rm eq}} \left.\frac{\rho_{\rm PBH}}{\rho_{\rm tot}}\right|_{\rm eq}.$$

Since $\rho_{\rm PBH}/\rho_{\rm tot}$ does not change a lot between matter-equality and today, we can approximately relate the two PBH fractions at the time of formation and today as follows[17]:

$$f_{\rm PBH} \simeq \frac{a_{\rm eq}}{a_{\rm form}}\beta. \tag{90}$$

Since $a_{\rm form} \ll a_{\rm eq}$, a significant fraction of the DM component in the form of PBHs today only requires a really small fraction of the total energy component in the form of PBHs at the time of formation. Note that this conclusion is general for all dark matter candidates.

Finally, let us remember that small-scale perturbations re-entered the horizon earlier than larger scales, see Figure 4. The horizon re-entry of the amplified perturbations at very small scales (k_{PBH}^{-1}) occurred during the RD universe. This is well consistent with the previous consideration on the horizon mass.

[16]Note that one could deduce that everything collapses when $c_s \to 0$, in MDU. However, this relation is only valid when the initial overdensity can be assumed spherically symmetric. The lack of pressure and the longer collapse time for smaller perturbations δ induce non-sphericity effects.

[17]Note that this description is only an approximation. We refer to [28] for the complete details.

3.1.1 PBH masses

Let us now estimate the PBH masses, in Eq. (88). The initial overdensities at the origin of galaxy formation are of the order $\delta \sim 10^{-4}$, and it took billions of years to form them [45]. In contrast, the initial overdensities must be extremely large for PBH formation, see Eq. (89). Once the horizon scale has been reached, it required only 10 Hubble times $1/H_{k=aH}$ to form the corresponding PBH [40]. In a RDU, the scale factor evolves as $a \propto t^{1/2}$. The time of formation expressed in number of e-folds is then given by:

$$\Delta N_{\rm form} = \ln\left(\frac{10}{H_{k=aH}}\right)^{1/2} - \ln\left(\frac{10}{H_{k=aH}}\right) \approx 1.$$

Therefore, the collapse of an initial overdensity into a PBH just after horizon re-entry is extremely fast, approximately one e-fold. The time of PBH formation can be approximated as the time of the horizon re-entry of the corresponding mode, i.e., we assume an immediate formation when $k = aH$.

This approximation enforces the first intuition about the PBH masses in Eq. (88), and the radius of the horizon mass is exactly defined by the Hubble distance:

$$M_{\rm PBH} \sim M_H(k) = \rho V|_{k=aH} = \frac{4\pi}{3}\rho\left(\frac{1}{H}\right)^3,$$

where ρ is the energy density. Note that as the mass is a physical quantity, we have considered the physical length, instead of the comoving one. The physical quantity corresponding to the Hubble radius $R_H = 1/(aH)$ is the Hubble distance $D_H = 1/H$, see Section 2.1. The first Friedmann equation in RDU gives $H^2 \propto \rho \propto a^{-4} \propto t^{-2}$. Using these last results, we can express the PBH mass as a function of the time of horizon re-entry i.e. $M_{\rm PBH} \propto \rho^{-1/2} \propto a^2 \propto t$, which is often written in the form:

$$M_{\rm PBH}(a) = \left(\frac{a_{\rm form}}{a_{\rm eq}}\right)^2 M_H^{\rm (eq)} \simeq \left(\frac{a_{\rm form}}{a_{\rm eq}}\right)^2 10^{17} M_\odot, \tag{91}$$

$$M_{\rm PBH}(t) \sim 10^{15}\frac{t}{10^{-23}\ {\rm s}}\ {\rm g}. \tag{92}$$

Due to Hawking radiation, PBHs of mass 10^{15} g would be completely evaporated today. It is for this reason that the PBH mass is often expressed with this mass reference in the last expression. Depending on the time of mode re-entry, a very wide range of masses can be produced, and PBHs represent the only black holes potentially smaller than one solar mass. If PBHs are formed during the Planck time (10^{-43} s), they would have a Planck mass, $\rm M_P \sim 10^{-5}$ g, and $10^5 M_\odot$ if they formed around $t \sim 1$ s. Let us now consider the PBH mass corresponding to one solar mass. In this case, the PBHs formed during the QCD epoch $t \sim 10^{-6}$ s, using Eq. (92). This phase began when quarks were no longer asymptotically free and bound into hadrons, when the energy dropped below 200 MeV [46]. Using Eq. (91), it corresponds to $a_{\rm form} \sim 10^{-9} a_{\rm eq}$. Assuming that the whole DM content is in the form of PBHs, $f_{\rm PBH} = 1$, one finds $\beta \sim 10^{-8}$ using Eq. (90). In other words, solar-mass PBHs at the time of formation represent only 10 parts per billion of the whole universe.

3.1.2 Collapse fraction

As we saw earlier, overdensities exceeding the collapse threshold δ_c can form PBHs. Therefore, the PBH abundance at the time of formation β is directly related to such overdensities at horizon re-entry. To estimate the collapse fraction β, it is possible to use the Press-Schechter model of gravitational collapse [47]. This method is used in the context of large-scale structure formation. Since we are identically dealing with perturbations at different length scales, one can apply it for PBH formations. Let us introduce the probability density function (PDF) of initial overdensities $P(\delta)$. It describes the likelihood to find an overdensity δ and it can be used to find the collapse fraction:

$$\beta \equiv \left.\frac{\rho_{\rm PBH}}{\rho}\right|_{\rm form} = \int_{\delta_{\rm c}}^{\infty} P(\delta) d\delta, \tag{93}$$

In the following, we assume a Gaussian distribution for the perturbations δ:

$$P_G(\delta) = \frac{1}{\sqrt{2\pi}\sigma} e^{-(\delta-\mu)^2/2\sigma^2}, \tag{94}$$

where μ is the mean and σ^2 is the variance of the distribution. The variance is an important quantity, as the larger it is, the more the probability density will spread around the mean. Consequently, more overdensities will exceed the threshold δ_c and lead to a larger β. By choosing a zero mean $\mu = 0$ for the overdensity distribution, we can integrate Eq. (93):

$$\beta = \int_{\delta_{\rm c}}^{\infty} \frac{d\delta}{\sqrt{2\pi}\sigma} \exp\left(-\frac{\delta^2}{2\sigma^2}\right) = \frac{1}{2}\,{\rm Erfc}\left(\frac{\delta_{\rm c}}{\sqrt{2}\sigma}\right) \simeq \frac{\sigma}{\sqrt{2\pi}\delta_{\rm c}} \exp\left(-\frac{\delta_{\rm c}^2}{2\sigma^2}\right), \tag{95}$$

where the function ${\rm Erfc} = 1 - {\rm Erf}$ is the complementary error function. Using the limit $\delta_c/\sigma \ll 1$, an asymptotic expansion has been performed in the last equality, ${\rm Erfc}(x) \sim 1 - \frac{2}{\sqrt{\pi}}x$.

3.1.3 Primordial scalar fluctuation

We now want to relate this result to the amplitude of the scalar perturbation generated during inflation. To do so, the density contrast δ can be Taylor expanded at linear order in the curvature perturbation $\mathcal{R}$ as follows [48]:

$$\delta(\vec{x}, t) \simeq \frac{2(1+w)}{(5+3w)} \frac{\nabla^2 \mathcal{R}(\vec{x})}{(aH)^2} + \mathcal{O}(\mathcal{R}^2) \;\Rightarrow\; \delta_k \simeq -\frac{4}{9}\left(\frac{k}{aH}\right)^2 \mathcal{R}_k,$$

where the second equality is written in Fourier space, in the RDU with $w = 1/3$. Therefore, using the definition of the power spectrum in Eq. (75), we can finally write:

$$\mathcal{P}_\delta(k) \simeq \frac{16}{81}\left(\frac{k}{aH}\right)^4 \mathcal{P}_\mathcal{R}(k). \tag{96}$$

Since we chose a Gaussian distribution for δ, see Eq. (94), the variance can be related to the primordial power spectrum $\mathcal{P}_\delta$. The density contrast δ represents the fluctuation in density w.r.t. to the average density of the universe. Since PBH formation is sensitive to specific scales where the density exceeds the critical threshold δ_c, it is necessary to smooth

the density contrast. This is done by using a window function $\mathcal{W}$ on a scale relevant to PBH formation, i.e. the scale corresponding to the horizon re-entry $B \sim k^{-1} = (aH)^{-1}$. This eliminates fluctuations on small scales while highlighting larger scales. In other words, it makes it easier to identify regions where the density is sufficiently high for the formation of PBHs. Doing so, it can be shown that the variance of the Gaussian distribution can be expressed as [49]:

$$\sigma^2(B) \equiv \left\langle \delta^2 \right\rangle = \int_0^\infty d\ln k \; \mathcal{W}^2(k, B)\mathcal{P}_\delta(k),$$

Common choices for the window function are the volume-normalised Gaussian or top hat functions, which have their Fourier transform respectively given by:

$$\mathcal{W}(k, B) = \exp\left(-\frac{k^2B^2}{2}\right), \quad \mathcal{W}(k, B) = \frac{3\sin(kB) - 3kB\cos(kB)}{(kB)^3}.$$

These window functions suppress high-frequency modes in Fourier space. In the case where the curvature power spectrum $\mathcal{P}_\delta$ is characterised by a narrow peak around the wave-number $k_{\rm PBH}$, the integral over Fourier modes can be approximated by evaluating the power spectrum at horizon re-entry:

$$\sigma^2 \sim \mathcal{P}_\delta\left(k_{\rm pbh}\right) \;\Rightarrow\; \mathcal{P}_\mathcal{R}\left(k_{\rm pbh}\right) \sim \frac{81}{16}\mathcal{P}_\delta\left(k_{\rm pbh}\right) \sim 5\sigma^2, \tag{97}$$

where in the second part, we used Eq. (96) evaluated at horizon re-entry $k = aH$. Using Eq. (95), one can do a rough estimate for the initial scalar perturbation required for the formation of PBH:

$$\mathcal{P}_\mathcal{R} \sim \frac{5\delta_c^2}{2\ln(1/\beta)} \sim \frac{0.4}{\ln(1/\beta)}.$$

We conclude that β is exponentially sensitive to δ_c or $\mathcal{P}_\mathcal{R}$, while $\mathcal{P}_\mathcal{R}$ is logarithmically sensitive to β or sensitive to the square of δ_c.

If we take the particular case of PBHs of one solar mass, with $f_{\rm PBH} = 1$ and $\beta = 10^{-8}$, we find $\mathcal{P}_\mathcal{R} \sim \frac{0.4}{\ln 10^8} \sim 10^{-2}$. On the other hand, the lowest possible PBH mass $M_{\rm PBH} \sim 10^{15}$ g, which would evaporate at present due to intense Hawking radiation, has been constrained with $\beta < 10^{-28}$ [50]. In this case, we find the lower value: $\mathcal{P}_\mathcal{R} \sim 8 \times 10^{-3}$. The amplitude of the power spectrum is then limited to:

$$\mathcal{P}_\mathcal{R} \gtrsim 10^{-2}. \tag{98}$$

This range is valid for all possible fractions $f_{\rm PBH}$. If one can somehow measure the value of $f_{\rm PBH}$, and hence deduce β, the amplitude of the power spectrum can be adjusted with some freedom. On the other hand, if one measures the amplitude of the power spectrum, this will impose a very fine-tuned constraint on β despite its exponential sensitivity to $\mathcal{P}_\mathcal{R}$. Similarly, β is exponentially sensitive to δ_c as can be seen from Eq. (95). Taking the case of PBH decaying today, with $5\sigma^2 \sim 10^{-2}$ using Eq. (97), we get:

$$\frac{\beta\left(\delta_{\rm c} = 0.4\right)}{\beta\left(\delta_{\rm c} = 1/3\right)} \simeq 10^{-5}. \tag{99}$$

Note that during the QCD transition phase, relevant for the formation of solar mass PBHs, the radiation pressure decreased significantly: $w = 1/3 \to 0.25$. Therefore, PBH

formation was easier and we obtain a collapse fraction amplified by several orders of magnitude [46].

We conclude that the production of PBHs in the early universe requires very fine-tuned conditions. In particular, comparing the result (98) to the CMB scales, we find:

$$\Delta\mathcal{P}_{\mathcal{R}} \equiv \frac{\mathcal{P}_{\mathcal{R}}\left(k_{\mathrm{PBH}}\right)}{\mathcal{P}_{\mathcal{R}}\left(k_{\mathrm{CMB}}\right)} \sim 10^{7}. \tag{100}$$

This implies that the primordial power spectrum needs to be amplified by several orders of magnitude. In Section 3.3, we will see how it is possible to produce such an amplification between CMB large scales and small PBH scales. Let us remember that the results found above are only valid for PBHs formed during the RDU and assuming Gaussian perturbations. Non-Gaussianity effects would have drastic implications on the outcome. This is related to the exponential sensitivity on δ_c, see Eq. (99). We refer to [49] for a discussion on the topic.

3.2 Observational constraints

Up to now, there is no confirmed direct evidence of the existence of PBHs. However, current observations have set limits on the allowed mass range of PBHs [50], [51]. The main constraints are shown in Figure 8. Gravitational constraints are usually expressed in terms of the DM fraction f_{PBH}. In the case of PBHs currently evaporating, Hawking radiation constraints appear and they are usually expressed in terms of the collapse fraction β [52]. Let us remember, however, the relation between the two fractions in Eq. (90). Based on the observational constraints, there is still a mass window where the entire Dark Matter content may consist in PBHs: $f_{\mathrm{PBH}} = 1$. This range spans from 10^{17} to 10^{22} g, or equivalently from 10^{-16} to $10^{-12}\, M_{\odot}$. It is often referred to as the "asteroid mass window".

The idea that PBHs could be small led Hawking to make the link between quantum mechanics and general relativity to study their quantum properties [54]. He found that BHs radiate thermally in the same way as a black body with a temperature proportional to the BH's surface area:

$$T_{\mathrm{BH}} = \frac{\hbar c^3 \mathrm{M}_{\mathrm{P}}^2}{M_{\mathrm{BH}} k} \propto \frac{1}{M_{\mathrm{BH}}},$$

Since a black body distribution emits radiation energy as T^4 per unit area, the total energy radiated by a BH is given by the surface area times T^4. Let us recall that a BH's radius is proportional to its mass, see Eq. (87). Therefore, the total energy radiated is given by:

$$E_{\mathrm{BH}} \propto \frac{1}{M_{\mathrm{BH}}^2} \;\Rightarrow\; \frac{dM_{\mathrm{BH}}}{dt} \propto \frac{1}{M_{\mathrm{BH}}^2},$$

The corresponding evaporating timescale of PBHs is found by integration and is given by:

$$\tau_{evap} \propto M_{\mathrm{PBH}}^3.$$

As mentioned earlier, PBHs with masses less than $M_{\mathrm{PBH}} \lesssim 10^{-18} M_{\odot} = 10^{15}$ g would have evaporated at the present time [55]. This kind of PBHs is formed before 10^{-23} s, see Eq. (92). Their size is comparable to that of a proton. PBHs decaying at the present time correspond to masses $10^{-18} M_{\odot} < M_{\mathrm{PBH}} \lesssim 10^{-16} M_{\odot}$. Such PBHs are drastically constrained by observation, see Figure 8. Smaller masses would have completely evaporated

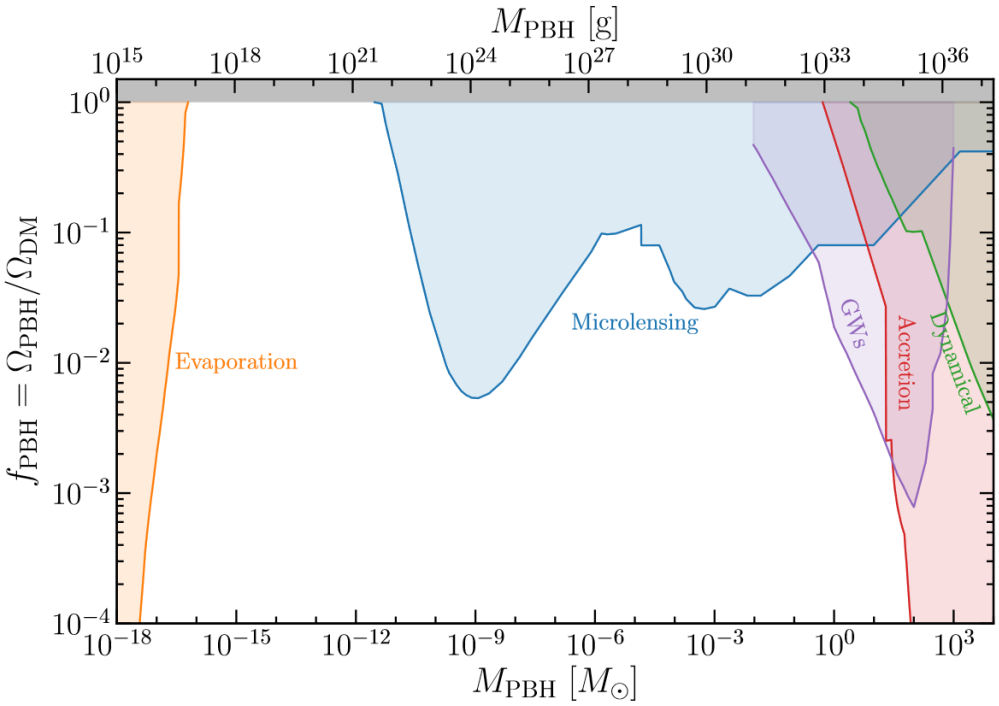

Figure 8: Direct constraints on the abundance of PBHs as a function of their mass. Coloured areas are forbidden due to the absence of detection by observational detectors. On the lower part of the mass spectrum in orange, constraints associated with PBH evaporation are shown. Microlensing constraints are represented in blue, and gravitational wave constraints for sub-solar mass PBHs in purple. Finally, constraints derived from PBH accretion in the CMB are illustrated in red. Pict. taken from [53].

today, while the Hawking radiation is negligible for higher masses.

When a massive object passes between an observer and a distant light source, the light rays from the background source are bent. This phenomenon is called microlensing. PBHs should act as lenses and produce specific features in the light-curve of the source. The intensity of the distortion depends on the mass of the PBH and its distance to the light source. The Hyper-Suprime Cam on the Subaru telescope has set microlensing constraints on PBH masses ranging from $10^{-12}M_\odot \lesssim M_{\rm PBH} \lesssim 10^{-6}M_\odot$. It has ruled out $f_{\rm PBH} = 1$ with a lower limit $f_{\rm PBH} \lesssim 10^{-2}$ for $M_{\rm PBH} \sim 10^{-9}M_\odot$ [56]. The higher mass range $10^{-6}M_\odot \lesssim M_{\rm PBH} \lesssim 1M_\odot$ has been constrained with older surveys such as OGLE, MACHO and EROS [57].

When we consider larger masses, current gravitational wave detectors become sensitive to mergers of binaries [58]. A wide number of merger events have been detected by LIGO/Virgo since 2015. The possibility that such binaries have a primordial origin has been raised. The mass range $1M_\odot \lesssim M_{\rm PBH} \lesssim 10^2M_\odot$ is strongly constrained with $f_{\rm PBH} \lesssim 10^{-3}$. Below in mass, the microlensing constraints are more restrictive. However, it is important to point out that these gravitational constraints are model-dependent. They require an estimate of the rate of PBH mergers in the early universe. In those models, it is assumed that PBH binaries are formed soon after PBH formation with a significant fraction remaining unchanged until today. Making the distinction between an astrophysical or cosmological origin of these gravitational wave observations will require

further advancement in our theoretical understanding of PBHs. However, the detection of a mass below the Chandrasekhar limit would exclude an astrophysical origin. Note that solar-mass PBHs can be potentially detected with the current gravitational wave detectors.

We expect PBHs to accrete gas in the early universe. At some point, radiation pressure exceeds the gravitational attraction, producing intense energetic radiation. Such radiation has been used, for instance, to make the first picture of the event horizon of a supermassive BH [59], [60]. In the early universe, this effect would heat and ionise the intergalactic medium. Depending on the number of PBHs, this would affect the CMB anisotropies. For masses $M_{\rm PBH} \gtrsim 1 M_\odot$, $f_{\rm PBH} = 1$ appears to be excluded. The constraint is lowered to $f_{\rm PBH} \lesssim 10^{-4}$ for $M_{\rm PBH} \gtrsim 10^2 M_\odot$ [61]. Note that accretion is not relevant for a smaller range of masses. Let us briefly mention the dynamical constraints, which are not very precise and are contained in the accretion constraints. For very massive PBHs, dynamical effects could modify or even suppress some cosmological objects, such as dwarf galaxies. This provides the constraints on the highest masses of PBHs.

3.3 Amplification of the perturbations

Let us summarise the key points introduced up to now. Inflation produced inflationary perturbations. Depending on the scale range, these perturbations were the seeds for the formation of the anisotropies in the CMB, the LSS, and possibly the PBHs. In this scenario, the abundance of PBHs is related to the amplitude of fluctuations in the inflaton field, see Eq. (93). During the quasi-de Sitter expansion regime of SR inflation, the SR parameters remain small and approximately constant, resulting in a nearly flat and scale-invariant spectrum of scalar perturbations, see Eq. (86). The formation of PBHs requires the amplitude of the field fluctuations to be significantly enhanced by several orders of magnitude w.r.t. what is typically measured from the CMB, see Eq. (100). The mechanism of enhancement must increase the amplitude of the shortest wavelength perturbations while preserving the features of CMB perturbations.

The necessary amplification of the inflationary fluctuations can be achieved through a phase of USR or CR inflation. In this transient phase, the conditions for slow-roll inflation are temporarily violated and the inflaton field evolves towards a de Sitter attractor, see Section 1.3.3. The USR phase can be realised in the presence of an inflection point in the inflaton potential [39], [62] which decelerates the inflaton field before the end of inflation, see Figure 9. The amplification can be achieved in two different ways, which we will investigate in this Section.

3.3.1 Constant SR parameters

The method presented below allows us to verify if conditions for the amplification of the perturbations are present. Such conditions are investigated by assuming a phase with nearly constant SR parameters. Let us first briefly explain in which context such an assumption can be made. SR parameters are found to be exactly constant in the de Sitter inflation and in the power law inflation. In the de Sitter case, H is constant and all the SR parameters are zero $\epsilon_i = 0$ for $i > 0$, see the definitions (33). In power law inflation, we have $a = t^{\rm cst.}$ and $H \propto t^{-1}$, so that ϵ_1 is constant and all the other SR parameters are

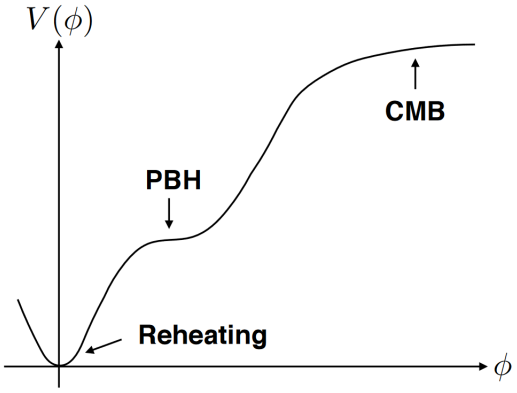

Figure 9: Introduction of an inflection point in the inflationary potential for the generation of PBHs. Pict. taken from [63].

zero. In addition, the SR parameters can be approximated as constant in the SR case, as the SR parameters are small. We can then use constant SR parameters during slow-roll provided that we expand the expressions to first order. However, it is still possible to make such an approximation for more general cases. For example in the case of CR, we have already mentioned that the asymptotic limits of the SR parameters have zero and constant values. Therefore, close to the USR attractor, we can also use the same results.

There also exists a wide variety of other transient phases having such behaviour in the large a limit. This limit can be satisfied during inflation, and correspondingly the SR parameters tend to zero and constant values for either even or odd indices. Let us illustrate this point by considering the condition [64]:

$$\epsilon_i = l_i + L_i(N) \quad \text{with} \quad \lim_{N\to\infty} L_i(N) = 0. \tag{101}$$

Due to their definition, we can express the SR parameters recursively as follows:

$$\epsilon_{i+1} \equiv \frac{d\epsilon_i/dN}{\epsilon_i} \overset{N\to\infty}{=} \frac{L_{i,N}(N)}{l_i + L_i(N)}.$$

In the same way, we can express the subsequent SR parameter as:

$$\epsilon_{i+2} \equiv \frac{d\epsilon_{i+1}/dN}{\epsilon_{i+1}} \overset{N\to\infty}{=} \frac{L_{i,NN}(N)}{L_{i,N}(N)} + \epsilon_{i+1}.$$

If we suppose $L_i(N) \propto \mathrm{e}^{-\gamma N} \sim a^{-\gamma}$, with $\gamma > 0$, we find the following limits:

$$\begin{aligned} \epsilon_{i+1} &\overset{N\to\infty}{=} 0, \\ \epsilon_{i+2} &\overset{N\to\infty}{=} -\gamma + \epsilon_{i+1}. \end{aligned}$$

As a result, the overall hierarchy behaviour alternates between constant and zero values:

$$\lim_{N\to\infty} \epsilon_i = l_i, \quad \lim_{N\to\infty} \epsilon_{i+1+2n} = 0, \quad \lim_{N\to\infty} \epsilon_{i+2n} = -\gamma. \tag{102}$$

Let us note that the condition $\lim_{N\to\infty} L_{i,N}(N) = 0$, in Eq. (101), is a necessary but not sufficient condition to obtain such limits. One can indeed verify that $L_i \propto N^{-\gamma}$ gives the

sequence $\lim_{N\to\infty}\epsilon_j = 0$ for $j > i$. Let us mention that due to the recursive definition of SR parameters, other hierarchies, such as the scalar field flow functions in Eqs. (34), may have the same behaviour.

The limit in Eq. (102) where the odd parameters are going to zero is the only one being able to produce an amplification in the presence of a minimally coupled inflaton:

$$\epsilon_1 = \epsilon_{2i+1} \to 0, \quad \epsilon_2 = \epsilon_{2i} \to \text{cst.}.$$

This has been the major conclusion from the article [64] and it can be easily checked by using the other limit. Therefore, in the present work, we adopt this result and we explicitly verify the amplification through the condition on the parameters Φ and $n_s - 1$, which we will define below. Since the de Sitter inflation has all its SR parameters $\epsilon_i = 0$, we will need a de Sitter attractor and the evolution toward it for the generation of the amplification. As we saw in Section 1.3.3, the CR and USR phases have such a de Sitter attractor.

3.3.2 Amplification from a growing solution

In SR inflation, we have seen that the curvature perturbation on super-Hubble evolution is given by a constant and a decaying mode, see 2.3.2. It means that on super-Hubble scales, the constant mode is dominant over the decreasing one. This gives the slightly red-tilted power spectrum in Figure 6. In USR, the situation can be radically different [22], [40]. As we saw before in Section 1.3.3, a USR phase has $\epsilon_1 \propto a^{-6} = e^{-6N}$. Therefore, taking the first expression of Eq. (73) with this new evolution of ϵ_1, we have:

$$R_k \propto A_k + C_k \int \frac{dt}{e^{-3Ht}} \propto e^{3Ht} \propto a^3. \tag{103}$$

In this scenario, when the scalar curvature perturbation exits the horizon, a growing solution which multiplies C_k is present. If we assume a USR phase for a small number of e-folds, only a small interval of perturbations are concerned with this growing solution. As we saw before, the largest scales we observe today exited the horizon much earlier than smaller scales. The solution C_k decreases much longer than it increases during the USR phase. Therefore, the growing phase of the solution does not affect large scales, for which the constant mode A_k remains dominant. During the RDU after inflation, the smallest scales are re-entering the horizon with an amplified amplitude. Thus we may find the favourable form of the power spectrum needed to produce PBHs. In Section 1.3.3, we saw that $\epsilon_2 \approx -6$ during USR. Let us mention that if it takes a different constant value, $\epsilon_2 = \text{cst.}$, it is still possible to have a growing solution on super-Hubble scales. In such a case, the first SR parameter is evolving as $\epsilon_1 \propto a^{\epsilon_2}$. Using Eq. (73), we see that the scalar perturbation R_k is growing on super-Hubble scales provided that:

$$\epsilon_2 < -3. \tag{104}$$

Let us now introduce a systematic and general way to solve the Mukhanov-Sasaki equation for the case of constant SR parameters. Doing so, we are going to find the necessary condition leading to the presence of a growing solution. We follow the procedure presented in [64]. Using the definition of the curvature perturbation in Eq. (64), we can rewrite the Mukhanov-Sasaki equation (59) as follows:

$$\mathcal{R}_k'' + 2\frac{z'}{z}\mathcal{R}_k + k^2\mathcal{R}_k = 0. \tag{105}$$

At this point, it is convenient to introduce the new dimensionless variable $\xi = k/(aH)$. Using the definition of conformal time, see Eq. (14), it is possible to express the first and second derivatives w.r.t. conformal time in terms of this new variable:

$$\frac{d}{d\eta} = aH\left(1-\epsilon_1\right)\xi\frac{d}{d\xi}, \tag{106}$$

$$\frac{d^2}{d\eta^2} = a^2H^2\left(1-\epsilon_1\right)^2\left[\xi^2\frac{d^2}{d\xi^2} + \frac{\epsilon_1\epsilon_2}{\left(1-\epsilon_1\right)^2}\xi\frac{d}{d\xi}\right], \tag{107}$$

where we used $\epsilon_1' = aH\epsilon_1\epsilon_2$, see Eq. (37), to express the second derivative w.r.t. to η.

Performing this change of variable in Eq. (105), we find:

$$\xi^2\frac{d^2\mathcal{R}_k}{d\xi^2} + \left(\frac{\epsilon_1\epsilon_2 - 2\left(1-\epsilon_1\right)\frac{1}{\mathcal{H}}\frac{z'}{z}}{\left(1-\epsilon_1\right)^2}\right)\xi\frac{d\mathcal{R}_k}{d\xi} + \frac{\xi^2}{\left(1-\epsilon_1\right)^2}\mathcal{R}_k = 0 \tag{108}$$

where we have used the conformal Hubble parameter, see the definition (22). Since $dN = d\ln a = aHd\eta$, we can write:

$$\frac{d\ln z}{dN} = \frac{z'}{z}\frac{1}{\mathcal{H}} \tag{109}$$

Eq. (108) is a homogeneous linear second-order differential equation. Let us now assume the long wavelength limit $\xi \to 0$, i.e. the super-Hubble regime. The last term of the differential equation (108) can be set to zero, it gives:

$$\xi^2\frac{d^2\mathcal{R}_k}{d\xi^2} = -\left(\frac{\epsilon_1\epsilon_2 - 2\left(1-\epsilon_1\right)\frac{d\ln z}{dN}}{\left(1-\epsilon_1\right)^2}\right)\xi\frac{d\mathcal{R}_k}{d\xi}.$$

This equation admits two solutions, one is the constant solution and one is of the form $R_k \propto \xi_k^\beta$ if the SR parameters are constant. Indeed, assuming this form, we obtain the solution:

$$\beta = \frac{\left(1-\epsilon_1\right)^2 - \epsilon_1\epsilon_2 + 2\left(1-\epsilon_1\right)\frac{d\ln z}{dN}}{\left(1-\epsilon_1\right)^2}.$$

The growing solution takes then the form [64]:

$$\mathcal{R}_k = \frac{v_k}{z} \propto \left(\frac{k}{aH}\right)^\beta \sim \mathrm{e}^{-\beta(1-\epsilon_1)N}.$$

We can therefore see that the solution ξ^β is increasing provided that the following condition is satisfied:

$$\Phi \equiv \beta\left(1-\epsilon_1\right) = \frac{1 - 2\epsilon_1 + \epsilon_1\left(\epsilon_1-\epsilon_2\right) + 2\left(1-\epsilon_1\right)\frac{d\ln z}{dN}}{\left(1-\epsilon_1\right)} < 0. \tag{110}$$

In this case, the amplitude of the power spectrum is amplified and the formation of PBHs is possible. In the other case, when $\Phi > 0$, the solution ξ^β decreases in time. The constant solution is then dominant in the long wavelength limit and we do not have super-horizon evolution.

3.3.3 Amplification from a blue-tilted spectrum

When the condition necessary for the generation of a growing solution is not satisfied, the rapid changes in the value of the SR parameters may still lead to amplified perturbations [65], [66]. The definition of the power spectrum (85) and the spectral index (86) are sensitive to the slow-roll parameters. These expressions, however, have been found in the context of SR inflation, and to the linear order in the SR parameters. They cannot be used to estimate the amplification in the case of CR or USR inflation. A complete analytical estimate of the spectrum is not possible and one needs to solve the Mukhanov-Sasaki equation numerically. Nonetheless, to get an idea of USR dynamics, let us use the same Eq. (85) in the USR case[18]. During USR, the first SR parameter evolves as $\epsilon_1 \propto a^{-6}$. Consequently, the power spectrum exhibits a growth pattern characterised by:

$$\mathcal{P}_{\mathcal{R}} \propto e^{6N}, \tag{111}$$

with additional corrections [22], [28]. Thus, the power spectrum is amplified very rapidly. Therefore, the rapid variation during the USR dynamics could produce amplification of the perturbation by generating a blue-tilted spectrum [23].

Now, we aim to generalise this procedure to scenarios where the SR parameters are constant. To determine the spectral index, we must revisit the Mukhanov equation (59). By performing the change of variable ξ once again, we can express it using Eqs. (106) and (107) in the following manner:

$$\left[\xi^2 \frac{d^2 v_k}{d\xi^2} + \frac{\epsilon_1 \epsilon_2}{(1-\epsilon_1)^2} \xi \frac{dv_k}{d\xi}\right] + \frac{\xi^2 - f_{\rm MS}(\epsilon_i)}{(1-\epsilon_1)^2} v_k = 0. \tag{112}$$

This equation is a linear second-order differential equation, which can be easily solved if SR parameters are constant. In addition, in the case of the long wavelength limit, the variable $\xi \to 0$ and one can neglect the ξ^2 term in the differential equation. Doing so, Eq. (112) admits two solutions of the form $v_k = \xi^\alpha$. Indeed, using this form, the differential equation is reduced to a simple second-order equation:

$$\alpha^2 + \left[\frac{\epsilon_1 \epsilon_2}{(1-\epsilon_1)^2} - 1\right] \alpha - \frac{f_{\rm MS}(\epsilon_i)}{(1-\epsilon_1)^2} = 0.$$

The solutions are given by the standard quadratic formula:

$$\alpha_{1,2} = \frac{-\left[\frac{\epsilon_1\epsilon_2}{(1-\epsilon_1)^2} - 1\right] \pm \sqrt{\left[\frac{\epsilon_1\epsilon_2}{(1-\epsilon_1)^2} - 1\right]^2 + 4\frac{f_{\rm MS}(\epsilon_i)}{(1-\epsilon_1)^2}}}{2}. \tag{113}$$

Since $v_k \sim \xi^\alpha$, we can express the curvature perturbation R_k in the following way:

$$v_k \sim k^{-1/2} \left(\frac{k}{aH}\right)^\alpha \;\Rightarrow\; R_k = \frac{v_k}{z} \sim k^{-1/2} k^\alpha.$$

[18] In SR inflation, the reference time is often chosen as the time of horizon exit, as perturbations are constant on super-horizon scales during this phase. Since we are in a similar situation where the modes are frozen, we still choose the time of horizon re-entry in Eq. (85). Let us note that when the modes are growing on super-horizon scale, as the perturbations do not freeze, the reference time needs to be chosen after the growing phase.

The factor $k^{-1/2}$ in front comes from the Bunch-Davies conditions (72). Using this form for the curvature perturbation, we can express Eq. (75) as:

$$\mathcal{P}_{\mathcal{R}} \propto k^{2+2\alpha}.$$

Finally, using Eq. (76), we can calculate the spectral index to be $n_s - 1 = 2 + 2\alpha$. We want to verify if we can have a blue-tilted spectrum in the presence of a decreasing solution. We need ξ^α to increase as $\xi \to 0$. This is the case when $\alpha < 0$. We therefore choose the negative solution α_2, in Eq. (113), and we check the condition for which the spectral index is positive[19]. So, the spectral index is blue-tilted when we have the following condition satisfied:

$$n_s - 1 = 2 - \left[\frac{\epsilon_1\epsilon_2}{(1-\epsilon_1)^2} - 1\right] - \sqrt{\left[\frac{\epsilon_1\epsilon_2}{(1-\epsilon_1)^2} - 1\right]^2 + 4\frac{f_{\rm MS}(\epsilon_i)}{(1-\epsilon_1)^2}} > 0. \tag{114}$$

Let us end this Section by remarking that both Eqs. (103) and (111) reinforce our statement about the duration of the USR phase, see Section 1.3.3. It must be short to prevent $\mathcal{P}_{\mathcal{R}}$ from approaching 1, where perturbations stop to be small, and cosmological perturbation theory breaks down. Because of quantum mechanics, this scenario could lead to eternal inflation in certain regions of the universe, as the inflaton field is just as likely to move backwards along the potential as it is to go down to the minimum.

[19]Let us remember that the spectral index is red-tilted when $n_s - 1 < 0$. This indicates that at short wavelengths or large wavenumbers k^{-1}, the power spectrum has an excess. While we say that the power spectrum is blue-tilted when $n_s - 1 > 0$.

4 Potential reconstruction for the generation of PBHs

In inflation, the choice of the potential V determines the evolution of the inflaton field and its quantum perturbations. As a consequence, different forms of the potential lead to different predictions for the subsequent universe. By imposing the formation of PBHs in the early universe, the form of the potential is constrained. Before we define the conditions on the potential, we first need to construct the inflationary potential compatible with the theory of inflation. There are several possibilities to do so. In Section 4.1, we will study the superpotential method, which allows the reconstruction of the inflationary potential. The idea is to use the homogeneous scalar field to parameterise the dynamics. This can be compared, for instance, with the reconstruction method presented in [64], where the scale factor is used instead. We will find the form of the potential leading to the amplification of perturbations in General Relativity and in some specific modified gravity theories, in Sections 4.2 and 4.3 respectively.

In the following Sections, we will use the notation ∂_μ to refer to the derivative w.r.t. the coordinates x^μ. We also adopt the following notations for the derivative of a quantity Q w.r.t. time and the field σ:

$$\begin{cases} \frac{dQ}{dt} & = \dot{Q} \\ \frac{dQ}{d\sigma} & = Q_{,\sigma} \end{cases} . \tag{115}$$

In Section 1.3.2, we introduce the concept of "attractor", which represents a point of stability that attracts the scalar field. During the CR and USR phases, the scalar field evolves towards a quasi-de Sitter attractor and a de Sitter attractor solution, respectively. In this context, we are interested in a monotonic evolution of the scalar field. This means that the inflaton is moving continuously towards the minimum of the potential, transitioning smoothly towards the attractor solutions. This implies that we can substitute the time evolution, in Eq. (115), with the evolution w.r.t. the field:

$$\dot{Q} = Q_{,\sigma}\dot{\sigma}. \tag{116}$$

It's important to note that our aim is finding the behaviour of the inflaton potential in the vicinity of the attractor. The reconstructed potential represents only a small part of the full SR inflaton potential. We refer to [23] for an example of a complete potential leading to the formation of PBHs.

4.1 Superpotential method

The superpotential method is presented in [67], and we review such method in this Section. We want to describe the formation of PBHs in General Relativity (GR) as well as in modified gravity theories in which the inflaton may be non-minimally coupled to gravity [68]. Therefore, we first generalise the inflationary formalism studied in Chapter 1.3 for GR. We shall refer to these modified gravity theories as the Jordan Frame (JF), while the case of GR will be referred to as the Einstein Frame (EF).

Non-minimally coupled scalar field models are of great interest, particularly in the context of inflation or to explain the presence of the present cosmic acceleration (Dark Energy). In such models, additional interactions are added to influence the dynamics of the early universe. The simple models are obtained by assuming a non-minimally coupled

scalar field to the Ricci scalar R. This interaction can be defined by a differentiable function $U(\sigma)$ that describes the interaction between the scalar field σ and the curvature. Note that we are going to use the notation σ for the scalar field when working in the JF. We will reserve the notation ϕ for the special case of GR. The inflation action, in Eq. (23), is generalised into:

$$S = \int d^4x\sqrt{-g}\left[U(\sigma)R - \frac{1}{2}g^{\mu\nu}\partial_\mu\sigma\partial_\nu\sigma + V(\sigma)\right], \tag{117}$$

where g is the determinant of the metric tensor $g_{\mu\nu}$, R is the Ricci scalar, and $V(\sigma)$ is the potential. In the context of GR, the scalar field is minimally coupled to gravity. We must recover the Einstein-Hilbert gravitational action of Eq. (23) by choosing U as a constant given by $U_0 = \mathrm{M_P^2}/2$.

Let us now assume the evolution of a homogeneous scalar field in a flat universe. The general line element for a flat FLRW spacetime is given by:

$$ds^2 = N_L(t)^2dt^2 - a^2(t)\left(dx_1^2 + dx_2^2 + dx_3^2\right),$$

where we have introduced the lapse function N_L because we are interested, in the next Sections, in mapping the EF and the JF by redefining the field and the metric [69]. Indeed, the mapping from one frame to another does not preserve the metric, meaning that the lapse function is not frame-invariant. Usually, we choose the case $N_L = 1$ so that the time t is the cosmic time in this particular frame. The choice $N_L = a$ gives a conformal metric $g_{\mu\nu} = a^2\eta_{\mu\nu}$, so that t is then the conformal time.

This metric has a determinant given by $\sqrt{-g} = N_L a^3$. With this metric, the Ricci scalar, given in Eq. (3), takes the form [68]:

$$R = -6\left(\frac{\ddot{a}}{aN_L^2} - \frac{\dot{N}\dot{a}}{aN_L^3} + \frac{\dot{a}^2}{a^2N_L^2}\right). \tag{118}$$

The dynamics of the homogeneous scalar field is described by the action (117). Inserting Eq. (118) and the expression for the determinant into the action, we find the following Lagrangian:

$$L = -6U\left(\frac{\ddot{a}a^2}{N_L^2} - \frac{\dot{N}_L\dot{a}a^2}{N_L^2} + \frac{\dot{a}^2a}{N_L}\right) - \frac{a^3\dot{\sigma}^2}{2N_L} + N_La^3V.$$

Integrating by parts the second term, we find after some algebra:

$$L = 6U\left(\frac{\dot{a}^2a}{N_L} + \frac{6a^2\dot{a}\dot{\sigma}U_{,\sigma}}{N_L} - \frac{a^3\dot{\sigma}^2}{2N_L} + N_LVa^3\right).$$

We can obtain the equations of motion by varying the action (117) w.r.t. the degrees of freedom. The variations w.r.t. the lapse function and the scale factor give, after some algebra, the first and second Friedmann equations in the Jordan frame respectively:

$$\frac{6U\dot{a}^2}{a^2} + \frac{6U_{,\sigma}\dot{a}\dot{\sigma}}{a} = \frac{1}{2}\dot{\sigma}^2 + N_L^2V,$$

$$\frac{4U\ddot{a}}{a} + \frac{2U\dot{a}^2}{a^2} + \frac{4U_{,\sigma}\dot{a}\dot{\sigma}}{a} - \frac{4U\dot{a}\dot{N}_L}{aN_L} + 2U_{,\sigma\sigma}\dot{\sigma}^2 + 2U_{,\sigma}\dot{\sigma} - \frac{2U_{,\sigma}\dot{\sigma}\dot{N}_L}{N_L} = -\frac{1}{2}\dot{\sigma}^2 + N_L^2V.$$

The Klein-Gordon equation is obtained by varying the action with respect to σ:

$$\ddot{\sigma} + \left(3\frac{\dot{a}}{a} - \frac{\dot{N}_L}{N_L}\right)\dot{\sigma} - 6U_{,\sigma}\left[\frac{\ddot{a}}{a} + \frac{\dot{a}^2}{a^2}\right] + 6\frac{\dot{a}\dot{N}_L}{aN_L}U_{,\sigma} + N_L^2 V_{,\sigma} = 0.$$

As mentioned before, we are free to choose a particular lapse function in a given frame. Let us choose $N_L = 1$ for simplicity. In this case, we find the following set of equations, as in [67]:

$$6UH^2 + 6\dot{U}H = \frac{1}{2}\dot{\sigma}^2 + V, \tag{119}$$

$$2U\left(2\dot{H} + 3H^2\right) + 4\dot{U}H + 2\ddot{U} + \frac{1}{2}\dot{\sigma}^2 - V = 0, \tag{120}$$

$$\ddot{\sigma} + 3H\dot{\sigma} + V_{,\sigma} = 6\left(\dot{H} + 2H^2\right)U_{,\sigma}. \tag{121}$$

where we used $\frac{\ddot{a}}{a} = \dot{H} + H^2$. Let us remember that each quantity is now defined in the JF.

Combining Eqs. (119) and (120), we find:

$$4U\dot{H} - 2\dot{U}H + 2\ddot{U} + \dot{\sigma}^2 = 0.$$

Using Eq. (116) for a monotonic scalar field evolution, we can rewrite this equation in terms of derivatives w.r.t. σ:

$$4UH_{,\sigma}G - 2HU_{,\sigma}G + 2U_{,\sigma\sigma}G^2 + 2U_{,\sigma}\ddot{\sigma} + G^2 = 0,$$

where we have defined the function $G = \dot{\sigma}$. As stated before, the evolution is described by the scalar field in the superpotential method. The Hubble parameter is also expressed as a function of the field $H(\sigma)$. Similarly, we can also write $\ddot{\sigma} = \dot{G} = G_{,\sigma}G$, so that we finally find:

$$4UH_{,\sigma} + 2\left(G_{,\sigma} - H\right)U_{,\sigma} + \left(2U_{,\sigma\sigma} + 1\right)G = 0. \tag{122}$$

The reconstruction method, aiming to reconstruct the potential of the theory, is based on this last equation. Indeed, the solution of this first-order linear differential equation gives the functions $G(\sigma)$ or $H(\sigma)$ once the other is chosen. When knowing $U(\sigma)$ and $G(\sigma)$, the solution is given by:

$$H(\sigma) = -\left[\int^{\sigma} \frac{2G_{,\tilde{\sigma}}U_{,\tilde{\sigma}} + \left(2U_{,\tilde{\sigma}\tilde{\sigma}} + 1\right)G}{4U^{3/2}}d\tilde{\sigma} + c_0\right]\sqrt{U}, \tag{123}$$

with c_0 an integration constant. While for a given $H(\sigma)$ and $U(\sigma)$, we find:

$$G(\sigma) = \left[\int^{\sigma} \frac{U_{,\tilde{\sigma}}H - 2UH_{,\tilde{\sigma}}}{U_{,\tilde{\sigma}}}e^{\Upsilon}d\tilde{\sigma} + \tilde{c}_0\right]e^{-\Upsilon(\sigma)}, \tag{124}$$

where we have defined:

$$\Upsilon(\sigma) \equiv \frac{1}{2}\int^{\sigma} \frac{2U_{,\tilde{\sigma}\tilde{\sigma}} + 1}{U_{,\tilde{\sigma}}}d\tilde{\sigma}.$$

and $\tilde{c}_0$ is another integration constant. Note that both $U(\sigma)$ and $V(\sigma)$ need to be differentiable functions of the scalar field σ.

Finally, we reconstruct the potential $V(\sigma)$ by inserting the functions G, U, and H into Eq. (119):

$$V(\sigma) = 6UH^2 + 6U_{,\sigma}GH - \frac{1}{2}G^2. \tag{125}$$

The field evolution $\sigma(t)$ can also be found from the integration of G.

When the scalar field approaches the USR or CR phase, the inflaton evolves towards a de Sitter attractor, and the inflaton tends to a fixed value. In other words, we are looking for a solution where the scalar field approaches asymptotically a constant attractor value σ_0. This condition is satisfied when the time variation of the field vanishes:

$$\lim_{\sigma \to \sigma_0} G = 0. \tag{126}$$

An important remark can now be made observing this result. Close to the attractor, the potential in Eq. (125) and the Hubble parameter in Eq. (123) have the following de Sitter behaviour:

$$\begin{cases} H^2 &= V/6U \\ H &= -c_0\sqrt{U} \end{cases} \quad \Rightarrow \; V = -6c_0^2U^2. \tag{127}$$

This implies that the desired de Sitter solution at the attractor results in a potential $V \propto U^2$. We will explicitly verify that the derivative of V/U^2 w.r.t. the field vanishes in the specific cases examined in the following Sections.

To summarise, the superpotential method is a technique that enables the reconstruction of the potential starting from a given ansatz [70]. The fundamental observations leading to reconstruction are outlined below:

1. The dynamical equations contain three functions (H, U, G), from which the potential can be reconstructed, see Equation (125).
2. $U(\sigma)$ determines the gravitational model (EF, JF).
3. $G(\sigma) = \dot{\sigma}$ determines the dynamics of the inflation.
4. H (or G) can be derived analytically through an integral, see Eq. (123) (Eq. (124)). U and H (or G) must be selected such that the integral can be exactly performed.
5. In proximity to the attractor, $\frac{dV/U^2}{d\sigma} \simeq 0$, see Equation (127).

The SR parameters are useful functions to describe the inflaton dynamics. Before applying the reconstruction method, we first illustrate how the two first SR parameters are expressed and used in the context of the reconstruction. The Hubble and scalar flow functions are defined recursively in Eqs. (33) and (34). Let us now express them as functions of the scalar field σ using G and H, which will simplify the derivation of the hierarchy:

$$\epsilon_1 = -\frac{GH_{,\sigma}}{H^2}, \tag{128}$$

$$\epsilon_{i+1} = \frac{G\epsilon_{i,\sigma}}{H\epsilon_i}. \tag{129}$$

$$\delta_1 = \frac{G}{H\sigma}, \tag{130}$$

$$\delta_{i+1} = \frac{G\delta_{i,\sigma}}{H\delta_i}. \tag{131}$$

Let us now express the second SR parameter in more detail using the expression of the first SR parameter. We can express the derivatives $\epsilon_{1,\sigma}$ and $\delta_{1,\sigma}$ as follows:

$$\epsilon_{1,\sigma} = \epsilon_1 \left(\frac{G_{,\sigma}}{G} + \frac{H_{,\sigma\sigma}}{H_{,\sigma}} - 2\frac{H_{,\sigma}}{H} \right), \quad \delta_{1,\sigma} = \delta_1 \left(\frac{G_{,\sigma}}{G} - \frac{H_{,\sigma}}{H} - \delta_1 \frac{H}{G} \right).$$

With this expression, the second slow-roll parameter takes the following form:

$$\epsilon_2 = 2\epsilon_1 - \frac{G}{H}\frac{H_{,\sigma\sigma}}{H_{,\sigma}} + \frac{G_{,\sigma}}{H}, \quad \delta_2 = -\delta_1 + \epsilon_1 + \frac{G_{,\sigma}}{H}.$$

We end up with the following expressions:

$$\epsilon_1 = -\frac{\sigma H_{,\sigma}}{H}\delta_1, \qquad \delta_1 = \frac{G}{H\sigma}, \tag{132}$$

$$\epsilon_2 = 2\epsilon_1 - \frac{\sigma^2 H_{,\sigma\sigma}}{H}\frac{\delta_1^2}{\epsilon_1} + \frac{G_{,\sigma}}{H}. \qquad \delta_2 = -\delta_1 + \epsilon_1 + \frac{G_{,\sigma}}{H}. \tag{133}$$

4.2 General Relativity

General Relativity is usually associated with a minimally coupled scalar field. We recover GR by defining the function U as constant:

$$U \equiv U_0 = \frac{\mathrm{M_P^2}}{2}. \tag{134}$$

For GR, let us use the conventional notation ϕ to denote the scalar field. Substituting Eq. (134) into the equations of motion in Eqs. (119), (120), and (121), we find:

$$3\mathrm{M_P^2}H^2 = \frac{1}{2}\dot{\phi}^2 + V, \tag{135}$$

$$4\mathrm{M_P^2}\dot{H} + 6\mathrm{M_P^2}H^2 + \frac{1}{2}\dot{\phi}^2 - V = 0, \tag{136}$$

$$\ddot{\phi} + 3H\dot{\phi} + V_{,\phi} = 0. \tag{137}$$

The first equation is the first Friedmann equation obtained in Section 1.3, in Eq. (29). The third one is the Klein-Gordon equation obtained in Eq. (24). Substituting Eq. (135) into Eq. (136), we recover the second Friedmann equation in Eq. (30):

$$\dot{H} = -\frac{1}{2\mathrm{M_P^2}}\dot{\phi}^2.$$

Using Eq. (116), we can further relate the function $G(\phi)$ and the derivative of the Hubble parameter w.r.t. ϕ:

$$G(\phi) = \dot{\phi} = -2\mathrm{M_P^2}H_{,\phi}. \tag{138}$$

This result is also consistent with Eq. (122) by substituting U_0. In addition, since the derivative of U_0 vanishes, the solution of the differential equation in Eq. (124) no longer exists. Instead, $G(\phi)$ can simply be obtained by differentiating H, as shown in Eq. (138). The other solution in Eq. (123) is equivalent to the result in Eq. (138):

$$H(\phi) = -\frac{1}{2\mathrm{M_P^2}}\int^{\phi} G d\tilde{\phi} - c_0\sqrt{U_0} \;\Rightarrow\; H_{,\phi} = -\frac{1}{2\mathrm{M_P^2}}G.$$

Potential reconstruction

The process of reconstruction of the potential is thus straightforward and exact, once we have fixed the expression of either $G(\phi)$ or $H(\phi)$. The potential, in Eq. (125), can then be written in terms of the Hubble parameter:

$$V(\phi) = 3\mathrm{M}_\mathrm{P}^2 H^2 - 2\mathrm{M}_\mathrm{P}^4 H_{,\phi}^2. \tag{139}$$

Note that we can express the relation close to the attractor, defined in Eq. (126), using Eq. (138):

$$\lim_{\phi\to\phi_0} G = 0 \Leftrightarrow \lim_{\phi\to\phi_0} H_{,\phi} = 0. \tag{140}$$

The Hubble parameter is constant close to the de Sitter attractor, in addition to the fixed scalar field.

The first slow-roll parameter, defined in Eq. (128), can be expressed using the expression of the function $G(\phi)$ in Eq. (138):

$$\epsilon_1 = \frac{G^2}{2\mathrm{M}_\mathrm{P}^2 H^2}. \tag{141}$$

Due to the simple relation between G and H in GR, we can use the general definition in Eq. (129) to derive the second slow-roll parameter:

$$\epsilon_2 = G\frac{\epsilon_{1,\phi}}{H\epsilon_1} = \frac{2\epsilon_1 G_{,\phi} - 2\epsilon_1 \frac{H_{,\phi}G}{H}}{H\epsilon_1} = \frac{2G_{,\phi}}{H} + 2\epsilon_1. \tag{142}$$

Similarly, let us express the third slow-roll parameter:

$$\epsilon_3 = G\frac{\epsilon_{2,\phi}}{H\epsilon_2} = \frac{\frac{2G_{,\phi\phi}G}{H} - 2G_{,\phi}\frac{H_{,\phi}G}{H^2} + 2\left(2\epsilon_1 G_{,\phi} + 2\epsilon_1^2 H\right)}{H\epsilon_2} = \frac{G_{,\phi\phi}G + 3G_{,\phi}\epsilon_1 H + 2\epsilon_1^2 H^2}{G_{,\phi}H + \epsilon_1 H^2}. \tag{143}$$

With Eq. (138), we can then express the three slow-roll parameters either with the function $G(\phi)$, with Eqs. (141), (142), and (143), or with the function $H(\phi)$:

$$\begin{aligned}
\epsilon_1 &= 2\mathrm{M}_\mathrm{P}^2\left(\frac{H_{,\phi}}{H}\right)^2, & \epsilon_1 &= \frac{G^2}{2\mathrm{M}_\mathrm{P}^2 H^2},\\
\epsilon_2 &= -\frac{4\mathrm{M}_\mathrm{P}^2 H_{,\phi\phi}}{H} + 2\epsilon_1, & \epsilon_2 &= \frac{2G_{,\phi}}{H} + 2\epsilon_1,\\
\epsilon_3 &= \frac{4\mathrm{M}_\mathrm{P}^4 H_{,\phi\phi\phi}H_{,\phi} - 6\mathrm{M}_\mathrm{P}^2 H_{,\phi\phi}\epsilon_1 H + 2\epsilon_1^2 H^2}{-2\mathrm{M}_\mathrm{P}^2 H_{,\phi\phi}H + \epsilon_1 H^2}. & \epsilon_3 &= \frac{G_{,\phi\phi}G + 3G_{,\phi}\epsilon_1 H + 2\epsilon_1^2 H^2}{G_{,\phi}H + \epsilon_1 H^2}.
\end{aligned} \tag{144}$$

Let us also express the first two scalar flow functions using Eqs. (132) and (133):

$$\begin{aligned}
\delta_1 &= -2\mathrm{M}_\mathrm{P}^2\frac{H_{,\phi}}{H\phi},\\
\delta_2 &= -2{\mathrm{M}_\mathrm{P}}^2\frac{H_{,\phi\phi}}{H} + \epsilon_1 - \delta_1.
\end{aligned}$$

We are interested in studying the form of the potential close to the attractor. Let us consider a Taylor expansion of the Hubble parameter H close to the attractor ϕ_0:

$$H(\phi) = \sum_{n=0}^{\infty} h_n\left(\frac{\phi}{\phi_0} - 1\right)^n \equiv \sum_{n=0}^{\infty} h_n\left(\frac{\delta\phi}{\phi_0}\right)^n, \tag{145}$$

where we assume that H is well-defined at ϕ_0. Before proceeding, we must first mention that h_0 must be positive to have inflation close to the attractor. Assuming that $H(\phi)$ is continuous and differentiable at ϕ_0, we can express the condition (140) as a condition on the first coefficient of the Taylor expansion: $h_1 = 0$.

Furthermore, by expressing G to leading order using Eq. (138), we find:

$$G \simeq -4\mathrm{M}_\mathrm{P}^2 \frac{h_2}{\phi_0}\left(\frac{\phi}{\phi_0} - 1\right), \tag{146}$$

This equation gives a new condition on h_2 to ensure ϕ_0 is an attractor: $h_2/\phi_0 > 0$. Indeed, when $h_2/\phi_0 > 0$ and ϕ is greater than ϕ_0 ($\phi > \phi_0$), then G is negative. Conversely, if ϕ is slightly less than ϕ_0 ($\phi < \phi_0$), then G is positive. In both cases, the field ϕ evolves towards its attractor ϕ_0.

With these three conditions on the coefficients of the Taylor expansion, we can find the asymptotic behaviours of the SR parameters when $\phi \to \phi_0$:

$$\epsilon_1(\phi_0) = \epsilon_3(\phi_0) = ... = 0, \tag{147}$$

$$\epsilon_2(\phi_0) = \epsilon_4(\phi_0) = ... = -8\frac{\mathrm{M}_\mathrm{P}^2}{\phi_0^2}\frac{h_2}{h_0}, \tag{148}$$

$$\delta_1(\phi_0) = \delta_3(\phi_0) = ... = 0, \tag{149}$$

$$\delta_2(\phi_0) = \delta_4(\phi_0) = ... = -4\frac{\mathrm{M}_\mathrm{P}^2}{\phi_0^2}\frac{h_2}{h_0}, \tag{150}$$

To obtain an amplified spectrum, the odd SR parameters must approach zero, while the even parameters must tend to a constant as ϕ approaches ϕ_0. From the set of SR parameters identified above, we observe that the parameters ϵ_2 and δ_2 tend towards a constant if the expansion of H includes a quadratic term: $h_2 \neq 0$. The subsequent SR parameters can be evaluated similarly as ϕ approaches ϕ_0. We have explicitly verified with Mathematica that the hierarchy alternates between zero and constant values. This result is consistent with the results in [64].

Finally, to obtain the evolution of $\phi(t)$, we integrate the function G in Eq. (146):

$$\phi(t) \simeq \phi_0\left(1 + \mathrm{e}^{-4\mathrm{M}_\mathrm{P}^2 h_2 \phi_0^{-2} t}\right) \simeq 1 + e^{-\gamma N}, \tag{151}$$

where in the last equality, we defined $\gamma = 4\mathrm{M}_\mathrm{P}^2\phi_0^{-2}\frac{h_2}{h_0}$. The Hubble parameter, expressed to second order in Eq. (145), is given by:

$$H(t) \sim h_0 + h_2\mathrm{e}^{-8\mathrm{M}_\mathrm{P}^2 h_2 \phi_0^{-2} t} \sim h_0 + h_2 e^{-2\gamma N}.$$

To summarise, in GR, we have found conditions on the Taylor expansion of H to express the behaviour close to the attractor possibly producing an amplified spectrum. One can find the corresponding conditions on G starting from the expansion:

$$H(\phi) = \sum_n h_n \left(\frac{\phi}{\phi_0} - 1\right)^n \quad \text{with } h_0 > 0 \text{ and } h_2 \neq 0, \tag{152}$$

$$G(\phi) = \sum_n g_n \left(\frac{\phi}{\phi_0} - 1\right)^n \quad \text{with } g_0 = 0 \text{ and } g_1 \neq 0, \tag{153}$$

and relating the Taylor coefficients of the series through the relation between G and H, see Eq. (138). The Hubble parameter needs to have a vanishing Taylor first-order coefficient.

We can also explicitly verify that the set of SR parameters, expressed in terms of $G(\phi)$ in Eqs. (144), is consistent with the condition that the function G contains a linear term in $(\phi/\phi_0 - 1)$, as was obtained in Eq. (146). Note that it should not contain a constant value in the limit of ϕ which tends to ϕ_0.

Let us express the potential (139) using the expression $H = h_0 + h_2 \left(\frac{\phi}{\phi_0} - 1\right)^2$ as exact. We then find the potential leading to the formation of PBHs:

$$V(\phi) = 3\mathrm{M}_\mathrm{P}^2 \left(h_0 + h_2 \left(\frac{\phi}{\phi_0} - 1\right)^2\right)^2 - 8\mathrm{M}_\mathrm{P}^4 \frac{h_2^2}{\phi_0^2} \left(\frac{\phi}{\phi_0} - 1\right)^2. \tag{154}$$

Amplification of the perturbations

The asymptotic limit of the SR parameters in Eqs. (149), (150), (147), and (148) are necessary conditions for the generation of PBHs. However, to effectively verify the amplification of the perturbations, we need to explicitly satisfy the conditions expressed either by the parameter Φ or the spectral index found in Eqs. (110) and (114), respectively. Let us remember that the function z, present in the Sasaki-Mukhanov equation (59), is a time-dependent function which varies according to the specific model of inflation considered. In the case of GR, with a minimally coupled inflaton, $z \propto a\sqrt{\epsilon_1}$, see Eq. (63). The corresponding functions z'/z and z''/z are derived in annex A.1.

Let us first check if the amplification can be obtained through the presence of a growing solution. Using the result (263) from the annex:

$$\frac{z'}{z} = aH \left[1 + \frac{1}{2}\epsilon_2\right],$$

in Eq. (110), we can express the parameter Φ in the case of GR as:

$$\Phi \equiv \beta\,(1 - \epsilon_1) = \frac{3 - 4\epsilon_1 + \epsilon_2 + \epsilon_1\,(\epsilon_1 - 2\epsilon_2)}{(1 - \epsilon_1)}.$$

Evaluating Φ w.r.t. the hierarchies in Eqs. (148) and (147), only constants and terms linear in the SR parameters ϵ_2 remain:

$$\Phi = 3 + \epsilon_2 = 3 - \frac{8\mathrm{M}_\mathrm{P}^2}{\phi_0^2}\frac{h_2}{h_0} = 3 - 2\gamma. \tag{155}$$

The growing solution exists for $\Phi < 0$, i.e. $\epsilon_2 < -3$ as found in Eq. (104). If we assume $\phi_0 > 0$ without loss of generality, we find the following condition on h_2:

$$\gamma > \frac{3}{2} \;\Rightarrow\; h_2 > \frac{3\phi_0^2}{8\mathrm{M}_\mathrm{P}^2} h_0. \tag{156}$$

If this condition is satisfied, it ensures the presence of a growing solution and the amplification of the perturbation required for the formation of PBHs. Let us remember that we impose $h_0 > 0$ to have an expanding universe during inflation.

On the other hand, we can still have amplification in the absence of the growing solution but with a blue-tilted spectrum. The power spectrum can be expressed in Eq. (114) through the function f_{MS} defined in (62). This function is derived in Eq. (264):

$$\frac{z''}{z} = a^2H^2\left[2-\epsilon_1+\epsilon_2\left(\frac{3}{2}+\frac{\epsilon_2}{4}-\frac{\epsilon_1}{2}+\frac{\epsilon_3}{2}\right)\right] \equiv a^2H^2 f_{\rm MS}\left(\epsilon_i\right).$$

Imposing now the particular limit of the SR parameters found above, we can evaluate f_{MS} close to the attractor as:

$$f_{MS} = 2+\frac{3\epsilon_2}{2}+\frac{\epsilon_2^2}{4}.$$

Using the condition $\gamma < \frac{3}{2}$, we finally express the spectral index in Eq. (114) as:

$$n_s - 1 = 3 - \sqrt{9+6\epsilon_2+\epsilon_2^2} = 3 - |3+\epsilon_2| = -\epsilon_2 = 2\gamma. \tag{157}$$

It leads to a blue-tilted spectrum when $n_s - 1 > 0$, corresponding to the interval:

$$0 < \gamma < \frac{3}{2}. \tag{158}$$

This is indeed the case for $h_2 > 0$, as it was for ϕ_0. Note that the condition $h_2/\phi_0 > 0$ on G, see Eq. (146), is thus well satisfied.

Note also that we obtain the same result as presented in the article [23]. Specifically, they demonstrated the possibility of generating a blue-tilted spectrum with CR inflation provided that $-\frac{3}{2} < -3-\alpha < 0$, see Eq. (42) for the definition of α. As we approach the attractor, we find $\delta_2 \to \frac{\ddot{\phi}}{H\dot{\phi}} = -3-\alpha$, as indicated in Eq. (133). Furthermore, in the context of GR, the limit of the second SR parameters are related by $\delta_2 = \frac{\epsilon_2}{2}$, see Eq. (150). Hence, the condition investigated in [23] can be expressed in the same way, close to the attractor as Eq. (157): $-\frac{3}{2} < \frac{\epsilon_2}{2} < 0$. In ref. [64], the authors used a different method for the reconstruction of the potential, parametrising the evolution with the scale factor instead of the scalar field:

$$H(a) = H_0\left(\alpha+\frac{A}{a^n}\right)^m \;\Rightarrow\; H \sim \alpha^m H_0\left(1+\frac{mA}{\alpha a^n}\right) \;\text{ when }\; \frac{A}{\alpha a^n} \ll 1. \tag{159}$$

They found that the condition to have a growing solution, $\Phi < 0$, is $n > 3$, see Eq. (37) in [64]. The blue-tilted condition for the spectral index is $0 < n < 3$, see Eq. (38) in [64]. By comparing with the conditions found above, see Eqs. (156) and (157) respectively, we find the following relation between the two reconstruction methods:

$$n = \frac{8\mathrm{M_P^2}h_2}{\phi_0^2 h_0}. \tag{160}$$

Note that we can also verify that the expression for the evolution of the scalar field in terms of the scale factor gives the same result. Starting from equation (138), we can indeed determine the evolution of $\phi(a)$ using Eq. (17):

$$H\frac{\mathrm{d}\phi}{\mathrm{d}\ln a} = -2\mathrm{M_P^2}\frac{H_{,\phi}}{H}.$$

Using the Taylor expansion of H in Eq. (152) to leading order, we can integrate this expression to find:

$$\frac{\phi(a)}{\phi_0} - 1 = e^1 \left(\frac{a_0}{a}\right)^{\frac{4M_P^2 h_2}{\phi_0^2 h_0}} .$$

Inserting this result back into the Taylor expansion of H, we obtain:

$$H(a) = h_0 + h_2 e^2 \left(\frac{a_0}{a}\right)^{\frac{8M_P^2 h_2}{\phi_0^2 h_0}} .$$

Comparing with the Taylor expansion of H from [64], taken in Eq. (159), we find the same n as before, in Eq. (160).

To conclude this Section, let us analyse a specific case by choosing particular values for h_2 and h_0. For simplicity, we set $M_P^2 = 1$ and select an arbitrary attractor value $\phi_0 = 5$. We first choose the specific parameters $h_0 = 1$ and $h_2 = 10$, defining the Hubble parameter. In this case, Eq. (155) yields $\Phi = -1/5$. The corresponding potential, in Eq. (154), is illustrated in Figure 10. This potential produces a growing solution since the condition $\Phi < 0$ is satisfied, see Eq. (156). Figure 11 illustrates the parameter α defined in the Klein-Gordon equation (42). We have an evolution similar to CR inflation close to the attractor, with a constant parameter $\alpha = -1.42$. The trajectory of the scalar field in the phase space diagram is simply represented by a linear decreasing function, see Eq. (146). As ϕ_0 has been chosen positive, the function G decreases towards ϕ_0, consistently with the fact that ϕ_0 is indeed an attractor. Finally, one can use Eq. (127) to verify that near the attractor, we indeed observe a de Sitter behaviour: $V/U_0^2 \propto$ cst. , see Figure 12.

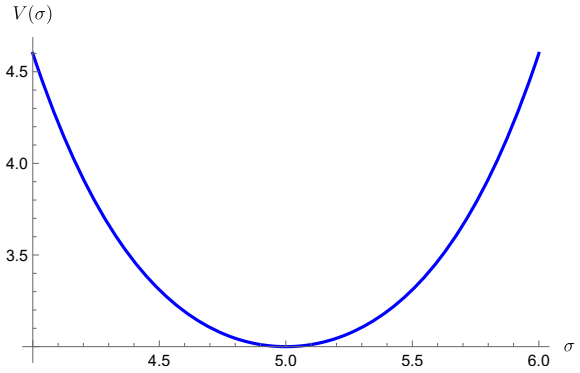

Figure 10: Potential for the particular case $H = h_0 + h_2 \left(\frac{\phi}{\phi_0} - 1\right)^2$ with the parameters chosen as $M_P^2 = 1$, $\phi_0 = 5$, $h_0 = 1$, and $h_2 = 1$.

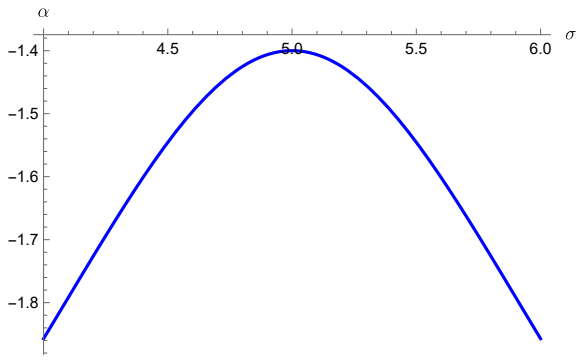

Figure 11: Plot of the parameter $\alpha = \frac{V_{,\phi}}{HG}$. Close to the attractor, it remains nearly constant, around $\alpha = -1.42$.

Let us now illustrate the USR case for the same value of the attractor $\phi_0 = 5$. We can indeed fine-tune the parameters h_0 and h_2 to recover the USR $\alpha = 0$ around the attractor, see Eq. (42). Indeed, taking the limit of the SR parameters in Eqs. (149) and (147) into Eq. (133), we have $\delta_2 \to \frac{\ddot{\phi}}{H\dot{\phi}}$. We can then impose the following condition to recover USR:

$$\delta_2 = -4\frac{M_P^2}{\phi_0^2}\frac{h_2}{h_0} = -3 \;\Rightarrow\; \frac{h_2}{h_0} = \frac{3\phi_0^2}{4}.$$

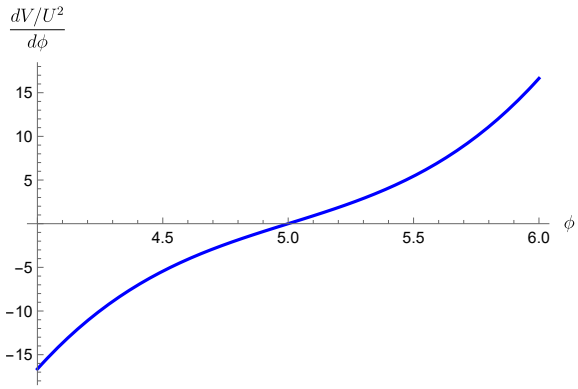

Figure 12: Derivative of V/U_0^2 w.r.t. ϕ. We do indeed have a de Sitter behaviour close to the attractor, i.e. $\frac{dV/U_0^2}{d\phi} = 0$, see Eq. (127).

Let us choose $h_0 = 4/5$ and $h_2 = 15$. In this case, the potential is flattened close to the attractor, see Figure 13. The CR parameter α is then null, and we find an evolution close to the attractor which resemble to the one of USR, see Figure 14. We also verify the condition ensuring the presence of a growing solution since $\Phi = -3$.

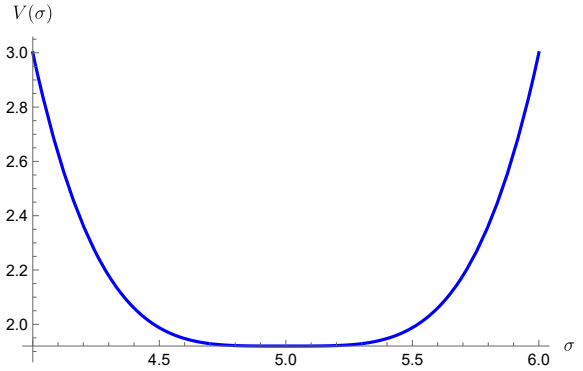

Figure 13: Potential for the particular case $H = h_0 + h_2\left(\frac{\phi}{\phi_0} - 1\right)^2$ with the parameters chosen as $M_P^2 = 1$, $\phi_0 = 5$, $h_0 = 4/5$ and $h_2 = 15$.

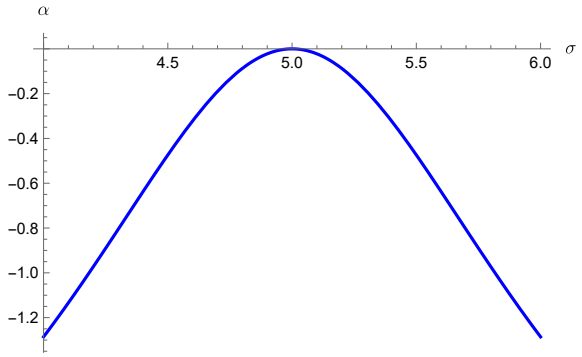

Figure 14: Plot of the parameter $\alpha = \frac{V_{,\phi}}{HG}$. It vanishes close to the attractor when considering the choice $M_P^2 = 1$, $\phi_0 = 5$, $h_0 = 4/5$ and $h_2 = 15$.

Note that we can also impose conditions to find the SR case, for which $\alpha \approx -3$. However, this corresponds to setting $\delta_2 \approx 0$, so we need to impose $h_2 \approx 0$. With our particular form of the Hubble parameter H, this results in a nearly constant Hubble parameter. SR inflation is therefore reduced to the de Sitter inflation case, with $\Phi > 0$ and a flat power spectrum $n_s - 1 \approx 0$, see [64].

Stability

The USR or CR phase, induced by the inflaton potential, deviates the dynamics of the inflaton field from the typical slow-roll evolution. During this phase, the inflaton field relaxes towards a de Sitter attractor. However, one needs to verify that the solutions found above are stable. Indeed, if the solution is unstable, it is impossible to approach the de Sitter attractor and obtain any amplification. Therefore, we will verify that homogeneous

perturbations, $\delta\phi$, tend to zero.

Using the relation $\frac{d^2}{dt^2} = HH_{,N}\frac{d}{dN} + H^2\frac{d^2}{dN^2}$, we can first express the homogeneous Klein-Gordon equation (137) in terms of e-folds as:

$$HH_{,N}\phi_{,N} + H^2\phi_{,NN} + 3H^2\phi_{,N} + V_{,\phi} = 0 \tag{161}$$

We can then extract the Hubble parameter from Eq. (135): $H = \sqrt{\frac{V/3}{\mathrm{M_P^2} - \phi_{,N}^2/6}}$. Using this result in Eq. (161) and expanding to linear order around the attractor $\phi \to \phi_0 + \delta\phi$, we find:

$$3\mathrm{M_P^2}V_{,\phi}(\phi_0) + \left(V(\phi_0)\delta\phi_{,NN} + 3V(\phi_0)\delta\phi_{,N} + 3\mathrm{M_P^2}V_{,\phi\phi}(\phi_0)\delta\phi\right) = 0, \tag{162}$$

where $|\delta\phi|\,\mathrm{M_P} \ll 1$. Using the expression of the potential in Eq. (154), we have that $V(\phi_0) = 3\mathrm{M_P^2}h_0^2$ and:

$$V_{,\phi}(\phi_0) = 0, \tag{163}$$

$$V_{,\phi\phi}(\phi_0) = 12\frac{\mathrm{M_P^2}}{\phi_0^2}h_0h_2\left(1 - \frac{4}{3}\frac{h_2}{h_0}\frac{\mathrm{M_P^2}}{\phi_0^2}\right) = \frac{V(\phi_0)}{3\mathrm{M_P^2}}\gamma\left(3-\gamma\right). \tag{164}$$

The linearised equation for $\delta\phi$, in Eq. (162), is a second-order differential equation with constant coefficients. Therefore, its general solution is given by the sum of two independent exponential solutions:

$$\delta\phi = c_1\exp^{-N(3-\gamma)} + c_2\exp^{-\gamma N}. \tag{165}$$

In the previous Section, we have started from one of these two solutions and we have reconstructed the corresponding potential. From the result (165), we see that besides such a solution, one also has a second solution which can also be found by the replacement:

$$\gamma \to 3 - \gamma. \tag{166}$$

This corresponds to make the substitution:

$$h_2 \to -h_2 + 3\phi_0^2h_0/(4\mathrm{M_P^2}). \tag{167}$$

The two independent solutions found by linearising the KG equation close to ϕ_0, are associated to the invariance of the potential w.r.t. the transformation (167). Therefore, both solutions give the same reconstructed potential. We can explicitly check that $V(\phi_0)$ and $V_{,\phi\phi}(\phi_0)$, present in Eq. (162), are invariant w.r.t. this transformation. Let us note that the substitution (167) can be deduced by observing that the coefficient $\frac{3}{4\mathrm{M_P^2}}$ is equal to $-\frac{1}{2}$ multiplied by the ratio between the coefficient in front of H^2 and that in front of $H_{,\phi}^2$ in Eq. (139). In the following, we will use this last result to find the invariance of the potential for non-minimal coupling cases.

Let us now discuss the stability of the solutions in Eq. (165). As the field approaches the de Sitter attractor, the homogeneous perturbations $\delta\phi$ need to decrease in time to ensure stability. In cases where both solutions are decreasing in time, the solution is stable. On the other hand, if one solution is increasing, the system is unstable. However, the system may still evolve towards the de Sitter attractor provided fine-tuned initial conditions are chosen. The case of USR is of this kind with one solution evolving towards

the de Sitter attractor and one moving away from it. Depending on the initial conditions, the decreasing solution can dominate for a certain period. This is the reason why getting amplification with an USR phase is not straightforward and requires special initial conditions. The SR phase preceding the USR phase needs to bring the conditions to have the unstable solution negligible.

For GR, the stability condition is respected for any choice of the initial conditions c_1 and c_2 if:

$$\gamma < 3. \tag{168}$$

In the case $\gamma < 3/2$, the second exponential will decrease more slowly, becoming dominant close to the attractor. The second exponential will also dominate for a non-negligible amount of time when $3/2 < \gamma < 3$, provided that $c_1 \ll c_2$. In such a case, one essentially finds the previous solution (151) and the expressions (155) and (157). On the other hand, the first exponential will dominate close to the attractor if the condition $3/2 < \gamma < 3$ is satisfied. It will also overcome the first exponential for a non-negligible amount of time if $\gamma < 3/2$ and $c_2/c_1 \ll 1$. In such a case, one needs to make the replacement found above, see Eq. (166), in Eqs. (148) and (150), to find the corresponding SR parameters for this second solution. It gives:

$$\epsilon_1(\phi_0) = \epsilon_3(\phi_0) = ... = 0, \qquad \delta_1(\phi_0) = \delta_3(\phi_0) = ... = 0,$$
$$\epsilon_2(\phi_0) = \epsilon_4(\phi_0) = ... = 2\delta_2. \qquad \delta_2(\phi_0) = \delta_4(\phi_0) = ... = -3 + \gamma.$$

The corresponding conditions for the generation of PBHs are determined using the same approach, based on Eqs. (155) and (157):

$$\Phi = 2\gamma - 3,$$
$$n_s - 1 = 6 - 2\gamma.$$

Let us introduce a general method to check the stability of the solutions in a systematic way [71], [72], without solving again Eq. (162). The equilibrium point of the potential can be found by solving $V_{,\phi}(\phi_0) = 0$, as in Eq. (163). Stability is verified if the potential has a positive concavity $V_{,\phi\phi}(\phi_0) > 0$. One may check that Eq. (168) is equivalent to this condition, see Eq. (164). Note that for non-minimally coupled scalar fields, one needs to define an effective potential to check the stability.

4.3 Jordan Frames

We now want to consider a more general case with non-minimally coupled inflaton $U(\sigma)$. In such cases, the simple connection between the functions G and $H_{,\phi}$ defined and found in the EF, see Eq. (138), no longer holds. Indeed, we now have to consider the differential equation (122), containing both the first derivatives of G and H. Therefore, we need to use its solutions (124) and (123). The potential and the SR parameters are no longer expressed in terms of a single function and its derivative. The missing function can be obtained analytically through integration, provided that the two others are chosen properly. Indeed, they need to be such that the integral can be performed exactly. Let us try in this context to derive some results for more general frames, in which U is not constant. Note that we henceforth return to the notation with σ indicating the inflaton field and the Hubble parameter H and the function G are now defined in the JF. Using

Eq. (122), we can write:

$$\frac{G_{,\sigma}}{H} = 1 - 2\frac{U}{U_{,\sigma}}\frac{H_{,\sigma}}{H} - \left(\frac{U_{,\sigma\sigma}}{U} + \frac{1}{2U_{,\sigma}}\right)\frac{G}{H}.$$

So, we can express the second scalar field flow parameter in Eq. (133) as:

$$\delta_2 = \epsilon_1 - \delta_1 + 1 - 2\frac{U}{U_{,\sigma}}\frac{H_{,\sigma}}{H} - \left(\frac{U_{,\sigma\sigma}}{U} + \frac{1}{2U_{,\sigma}}\right)\delta_1\sigma.$$

The case of Induced Gravity is defined by $U(\sigma) = \frac{\xi\sigma^2}{2}$. Using it in the previous relation, we find:

$$\delta_2 = \epsilon_1 - \frac{\epsilon_1}{\delta_1} - \frac{4\xi+1}{2\xi}\delta_1 + 1.$$

This relation can be inverted, it gives back the well-known relation between SR parameters in Induced Gravity, see [73] for instance:

$$\epsilon_1 = \frac{\delta_1}{1+\delta_1}\left(\frac{\delta_1}{2\xi} + 2\delta_1 + \delta_2 - 1\right). \tag{169}$$

Performing the same procedure, we can generalise this result to more general modified gravity theories, in which $U(\sigma) = \frac{\xi\sigma^2}{2} + J$. We find:

$$\epsilon_1 = \frac{\delta_1}{1+\delta_1+\frac{2J}{\xi\sigma^2}}\left(\frac{\delta_1}{2\xi} + 2\delta_1 + \delta_2 - 1\right). \tag{170}$$

In both cases, Eqs. (169) and (170), we find that when $\delta_1 \to 0$, when G is linear in $(\sigma/\sigma_0 - 1)$, $\epsilon_1 \sim -\delta_1$. Starting from this relation and using the definition of the two first SR parameters, see Eqs. (128) and (130), we find:

$$\frac{dH}{H} \sim \frac{d\sigma}{\sigma} \;\Rightarrow\; \frac{H}{H_0} \sim \frac{\sigma}{\sigma_0} \;\Rightarrow\; H \sim H_0\left[\left(\frac{\sigma}{\sigma_0}+1\right) - 1\right]. \tag{171}$$

Therefore, we find here a different result from that of GR, see (152). In the next Section, we are going to complete the discussion for IG and more general modified gravity theories employing another method. We are going to use the mapping between the EF and the JF. This method turns out to be easier to deal with the problem of amplification of the fluctuation.

5 Non-minimally coupled scalar fields

A non-minimally coupled model can be mapped into the corresponding Einstein Frame through a conformal transformation of the metric and a field redefinition[20]. In this way, it is possible to express G and H in the JF in terms of their counterparts in the EF. The main advantage of this method is that the relation (138), defined for GR (EF), will still be used to describe the dynamics in the JF. Therefore, the reconstruction of the potential in the JF will be obtained in terms of the Hubble parameter in the EF and its derivative. In this Section, the tilted notation refers to quantities expressed in the EF, with ϕ the inflaton in that frame. We first review how the two actions in both frames are linked to one another following the same approach as [39]. Then, we construct the mapping between the two frames, i.e. we relate the quantities G and H with $\tilde{G}$ and $\tilde{H}$ defined in the JF and EF, respectively.

5.1 Weyl transformation

A Weyl transformation, or conformal transformation, is a mathematical transformation applied to the metric tensor of general relativity. This transformation influences the measurements of timelike and spacelike intervals. However, it preserves the light cones, meaning that the causal structure remains unchanged. It is defined as follows [76]:

$$g_{\mu\nu} = \Omega^{-2}(x)\tilde{g}_{\mu\nu} = \frac{U_0}{U}\tilde{g}_{\mu\nu} \;\Rightarrow\; \Omega^2 = \frac{U}{U_0}. \tag{172}$$

where Ω^2 is a non-vanishing, regular function of spacetime coordinates and U_0 is defined for the EF in (134). The determinant of the metric is then given by: $\sqrt{-g} = \Omega^{-4}\sqrt{-\tilde{g}}$.

The line element can be expressed in the two frames as follows [74]:

$$ds^2 = N_L^2(t)dt^2 - a^2(t)(dx^2 + dy^2 + dz^2) = \tilde{N}_L^2(t)dt^2 - \tilde{a}^2(t)(dx^2 + dy^2 + dz^2).$$

From the metric in Eq. (172), we can relate the JF (σ, U, N_L, a) and the EF $\left(\phi, U_0, \tilde{N}_L, \tilde{a}\right)$ at the homogeneous level. Indeed, the lapse function and the scale factor are related by the following relations:

$$\tilde{N}_L = \Omega N_L, \tag{173}$$

$$\tilde{a} = \Omega a. \tag{174}$$

Performing a Weyl transformation, defined in Eq. (172), one can express the corresponding transformation of the Ricci scalar [76], [77]:

$$R = \Omega^2\left(\tilde{R} + 3\frac{\Box\Omega^2}{\Omega^4} - \frac{3}{2}\tilde{g}^{\mu\nu}\frac{\partial_\mu\Omega^2}{\Omega^2}\frac{\partial_\nu\Omega^2}{\Omega^2}\right) = \Omega^2\left(\tilde{R} + 3\frac{\Box\Omega^2}{\Omega^4} - \frac{3}{2}\left(\nabla\log\Omega^2\right)^2\right) \tag{175}$$

where the d'Alembertian is defined as $\Box = g^{\mu\nu}\partial_\mu\partial_\nu = \Omega^2\tilde{g}^{\mu\nu}\partial_\mu\partial_\nu$.

[20]For this reason, EF and JF are mathematically equivalent [74]. However, in practice, these different frames can still generate different predictions [75], i.e. predictions may not be frame-independent.

Let us transform the action in the JF, see Eq. (117), into that of the EF. We first use the conformal transformation defined in Eq. (172) to express U and g in the EF:

$$S = \int d^4x \frac{\sqrt{-\tilde{g}}}{\Omega^4} \left[U_0 \Omega^2 R - \frac{1}{2} \Omega^2 \tilde{g}^{\mu\nu} \partial_\mu \sigma \partial_\nu \sigma + V(\sigma) \right],$$

We can then use the definition of the Ricci scalar in Eq. (175). Using the fact that the integral on the second term $\int \sqrt{-\tilde{g}} \Box \Omega^2$ vanishes due to the Gauss's theorem, we are left with:

$$S = \int d^4x \sqrt{-\tilde{g}} \left(U_0 \tilde{R} - \frac{1}{2} \left(\frac{1}{\Omega^2} + 3U_0 \left(\frac{d \log \Omega^2}{d\sigma} \right)^2 \right) \tilde{g}^{\mu\nu} \partial_\mu \sigma \partial_\nu \sigma + \tilde{V}(\sigma) \right),$$

where the potential in the Einstein frame is defined as:

$$\tilde{V}(\sigma) = \frac{V(\sigma)}{\Omega^4}.$$

Now, we can perform the following scalar field transformation, and introduce the new scalar field ϕ [67]:

$$\frac{d\phi}{d\sigma} = \sqrt{\frac{1}{\Omega^2} + 3U_0 \left(\frac{\Omega^2_{,\sigma}}{\Omega^2} \right)^2} = \sqrt{\frac{U_0}{U} + 3U_0 \frac{U^2_{,\sigma}}{U^2}}. \tag{176}$$

Doing so, we recover the action for a minimally coupled scalar field ϕ, or the EF action:

$$S = \int d^4x \sqrt{-\tilde{g}} \left[\frac{M_P^2}{2} \tilde{R} - \frac{1}{2} \tilde{g}^{\mu\nu} \partial_\mu \phi \partial_\nu \phi + \tilde{V}(\phi) \right].$$

5.2 Jordan and Einstein frame mapping

Let us see how the conformal transformation modifies the expression (138) in the JF. Starting from the field transformation in Eq. (176), we can express the function $\tilde{G}$ as follows:

$$\tilde{G} = \frac{d\phi}{\tilde{N}_L dt} = \frac{d\phi}{d\sigma} \frac{d\sigma}{\Omega N_L dt} = \frac{U_0}{U} \frac{\sqrt{U_0 \left(U + 3U^2_{,\sigma} \right)}}{U} G. \tag{177}$$

We can do the same for the Hubble parameter using the transformation in Eqs. (173) and (174):

$$\tilde{H} = \frac{d\tilde{a}}{\tilde{a}\tilde{N}_L dt} = \frac{d(\Omega a)}{\Omega^2 a N_L dt} = \frac{1}{\Omega^2} \frac{d\Omega}{N_L dt} + \frac{1}{\Omega} \frac{da}{a N_L dt} = \sqrt{\frac{U_0}{U}} \left(H + \frac{U_{,\sigma}}{2U} G \right). \tag{178}$$

where, in the last equality, we used Eq. (172).

Using Eq. (138) defined in the EF, we can express $\tilde{G}$ as follows:

$$\tilde{G} = -4U_0 \tilde{H}_{,\phi} = -\frac{4U_0 U}{\sqrt{U_0 \left(U + 3U'^2 \right)}} Y_{,\sigma}, \tag{179}$$

where in the last equation, we used again the field transformation (176) to express the derivative in the JF. We have also introduced the function $Y(\sigma) \equiv \tilde{H}(\phi(\sigma))$ to underline

the different functional dependencies, when expressing $\tilde{H}$ in terms of the scalar field in the JF with Eq. (176).

We can now invert the function $\tilde{G}$ in Eq. (177) to find the corresponding expression in the Jordan frame $G(\sigma)$. Using Eq. (179), and after some algebra, we find:

$$G = -\sqrt{\frac{2U}{\mathrm{M_P^2}}}\frac{4UY_{,\sigma}}{1+3U_{,\sigma}^2/U}. \tag{180}$$

Inverting Eq. (178) and using Eq. (180), we find the expression of H in the JF:

$$H = \sqrt{\frac{2U}{\mathrm{M_P^2}}}\left(Y + \frac{2U_{,\sigma}Y_{,\sigma}}{1+3U_{,\sigma}^2/U}\right). \tag{181}$$

By substituting these two expressions for H and G in the JF, we can explicitly check that they satisfy Eq. (122).

Therefore, the reconstruction procedure in the JF can be done by assuming a given non-singular Hubble parameter $Y(\sigma) \equiv \tilde{H}(\phi(\sigma))$ in the EF, expressed through the scalar field σ through the relation $\phi(\sigma)$ obtained with Eq. (176). The functions G and H in the JF are expressed with Eqs. (180) and (181) respectively. Knowing the three functions, we can correspondingly express the JF potential using Eq. (125) and find the specific inflationary evolution in the JF. In practice, we will impose the conditions found previously for the amplification of the perturbations in the EF, and we will use the results of this Section to translate them into the JF.

5.3 Induced Gravity

Induced gravity is a particular modified gravity theory in which the Newton constant is associated with the expectation value of a scalar field, similarly to the Brans-Dicke theory [78]. The traditional Einstein-Hilbert term, which describes gravity in terms of the curvature of spacetime, is replaced by a mass-like term associated with a scalar field [32], [73]. In this theory, the function $U(\sigma)$ is given by:

$$U(\sigma) = \frac{\xi}{2}\sigma^2. \tag{182}$$

Using the conformal mapping, we can express the functions G and H for this case, using Eqs. (180) and (181):

$$G = -\alpha\sigma^3 Y_{,\sigma}, \tag{183}$$

$$H = \beta\sigma Y + \alpha\sigma^2 Y_{,\sigma}, \tag{184}$$

where we have defined $\beta \equiv \sqrt{\xi}/\mathrm{M_P}$ and $\alpha \equiv 2\xi\beta/(1+6\xi)$.

Potential reconstruction

With the expressions of G, H, and U, we can reconstruct the potential using Eq. (125):

$$\begin{aligned} V &= 3\xi\sigma^4\left(\beta Y + \alpha\sigma Y_{,\sigma}\right)^2 - 6\xi\sigma^4\left(\alpha\sigma Y_{,\sigma}\right)\left(\beta Y + \alpha\sigma Y_{,\sigma}\right) - \frac{\sigma^4}{2}\left(\alpha\sigma Y_{,\sigma}\right)^2 \\ &= \frac{\xi^2\sigma^4\left[3(1+6\xi)Y^2 - 2\xi\sigma^2 Y_{,\sigma}^2\right]}{\mathrm{M_P^2}(1+6\xi)}. \end{aligned} \tag{185}$$

To proceed with the study of the generation of PBHs, we search for specific patterns in the hierarchies of the SR parameters. For IG, it is easier to work with the scalar field flow functions. We can express the first two scalar field flow functions using Eqs. (130) and (131):

$$\delta_1 = \frac{G}{\sigma H} = -\frac{\alpha\sigma Y_{,\sigma}}{\beta Y + \alpha\sigma Y_{,\sigma}}, \tag{186}$$

$$\delta_2 = \sigma\delta_{1,\sigma} = -\frac{\beta Y\delta_1 + \left[2\alpha\left(1+\delta_1\right) + \delta_1\beta\right]\sigma Y_{,\sigma} + \alpha\left(1+\delta_1\right)\sigma^2 Y_{,\sigma\sigma}}{\beta Y + \alpha\sigma Y_{,\sigma}}. \tag{187}$$

As before, we assume that the inflaton approaches a particular attractor value σ_0, which we take as positive without loss of generality. We have expressed all the quantities in terms of the EF Hubble parameter Y. Let us now expand Y around the attractor σ_0 and impose the conditions on the Taylor coefficients of Y, leading to the suitable hierarchy required for the amplification of the perturbations:

$$Y(\sigma) = \sum_n y_n \left(\frac{\sigma}{\sigma_0} - 1\right)^n \quad \text{with } y_0 > 0 \text{ and } y_2 \neq 0. \tag{188}$$

In this case, when the field approaches the attractor, we have that $Y \to y_0$, $Y_{,\sigma} \to 0$, and $Y_{,\sigma\sigma} \to \frac{2y_2}{\sigma_0^2}$. Using these results in Eqs. (186) and (187), we find the following limit for the SR parameters:

$$\begin{aligned} \delta_1(\sigma_0) &= 0, \\ \delta_2(\sigma_0) &= -2\frac{\alpha}{\beta}\frac{y_2}{y_0}. \end{aligned} \tag{189}$$

In the vicinity of σ_0, we find that Y has the following behaviour $Y \sim y_0 + y_2\left(\sigma/\sigma_0 - 1\right)^2$. Thus, a straightforward potential that could result in an amplification can be obtained by taking this truncated second-order Taylor expansion as an exact function Y. In this scenario, $\sigma Y_{,\sigma} = \frac{2y_2\sigma}{\sigma_0}\left(\sigma/\sigma_0 - 1\right)$, and the potential in Eq. (185) becomes:

$$V = \frac{\xi^2\sigma^4 y_2^2}{\mathrm{M_P^2}(1+6\xi)}\left(3(1+6\xi)\left[\frac{y_0}{y_2} + \left(\frac{\sigma}{\sigma_0} - 1\right)^2\right]^2 - 8\xi\frac{\sigma^2}{\sigma_0^2}\left(\frac{\sigma}{\sigma_0} - 1\right)^2\right). \tag{190}$$

Let us now examine the behaviour of G and H in the vicinity of σ_0, using this same expression for Y in Eqs. (183) and (184):

$$G \simeq -2y_2\alpha\sigma_0^2\left(\frac{\sigma}{\sigma_0} - 1\right), \tag{191}$$

$$H \simeq \beta\sigma_0 y_0\left[1 + \left(1 + 2\frac{\alpha y_2}{\beta y_0}\right)\left(\frac{\sigma}{\sigma_0} - 1\right)\right]. \tag{192}$$

As found before in Eq. (171), it's worth noting that the Hubble parameter H approaches a constant value linearly as the field σ evolves. This is very different from the EF behaviour, in which Y has no linear term as an essential condition for the generation of PBHs. In contrast, G has the same form as in the EF in Eq. (146), so that $\sigma(t)$ evolves in a similar way as in GR, see Eq. (151).

Let us now consider the equations of motion, and in particular, we observe that the linear combination of Eqs. (119)/3 + (120) gives the following result:

$$4U\left(\dot{H}+2H^2\right)=-6\dot{U}H-2\ddot{U}-\frac{1}{3}\dot{\sigma}^2+\frac{4}{3}V.$$

Using this relation in the Klein-Gordon equation (121), we find after some algebra:

$$(\ddot{\sigma}+3H\dot{\sigma})\left(1+3\frac{U_{,\sigma}^2}{U}\right)+\frac{U_{,\sigma}}{2U}\dot{\sigma}^2\left(1+6U_{,\sigma\sigma}\right)+\left(V_{,\sigma}-2\frac{U_{,\sigma}}{U}V\right)=0. \tag{193}$$

Using the expression of U in Eq. (182) for the case of Induced Gravity, in this reformulated Klein-Gordon equation, we find the relation:

$$\ddot{\sigma}+3H\dot{\sigma}+\frac{\dot{\sigma}^2}{\sigma}=-\frac{V_{\text{eff},\sigma}}{1+6\xi},$$

where $V_{\text{eff},\sigma}=dV/d\sigma-4V/\sigma$. When one can neglect $\dot{\sigma}^2$, this equation is similar to the equation of motion in GR for USR, see Eq. (137). In this latter case, the scalar field is stuck at the minimum of the potential, $V_{,\sigma}=0$. In IG, the situation is different, the scalar field can be constant at $V_{\text{eff},\sigma}=0$:

$$\frac{dV}{d\sigma}=\frac{4V}{\sigma}\;\Rightarrow\;\sigma\frac{d\ln V}{d\sigma}=4. \tag{194}$$

We will use this expression to check our results for IG.

Amplification of the perturbations

Let us now work with the Mukhanov-Sasaki equation, in Eq. (59), to find the conditions leading to the formation of PBHs. In the case of IG, the generalised function z, defined in Eq. (61), is given by [79]:

$$z=a\phi\delta_1\frac{\sqrt{1+6\xi}}{1+\delta_1},$$

where we have defined $Z=\frac{1+6\xi}{(1+\delta_1)^2}$.

As before, we begin studying the amplification checking the presence of a growing solution. In Eq. (266) from the annex A.2, we have expressed the function z'/z in terms of the SR parameters:

$$\frac{z'}{z}=aY\left[1+\delta_1+\delta_2-\frac{\delta_1\delta_2}{1+\delta_1}\right],$$

We can express the parameter Φ using this result and Eq. (109) in Eq. (110):

$$\Phi=\left[1-\epsilon_1-\frac{\epsilon_1\epsilon_2}{(1-\epsilon_1)}+2\left(1+\delta_1+\delta_2-\frac{\delta_1\delta_2}{1+\delta_1}\right)\right]$$

With our hierarchies of slow-roll parameters, see Eqs. (189), we then find:

$$\Phi=3+2\delta_2=3-\frac{4\alpha y_2}{\beta y_0}, \tag{195}$$

Imposing the condition for the existence of the growing solution $\Phi < 0$, we find:

$$3 < \frac{4\alpha y_2}{\beta y_0} \;\Rightarrow\; \frac{y_2}{y_0} > \frac{3\beta}{4\alpha} = \frac{3(1+6\xi)}{8\xi}. \tag{196}$$

If the growing solution is absent, we need to check if the spectrum is blue-tilted. In Eq. (267), the derivation of the function f_{MS} can be found, it is given by:

$$f_{\rm MS} = \delta_1^2 + \delta_2^2 + (3-\epsilon_1)(1+\delta_1+\delta_2) + \delta_2\delta_3 + \frac{\delta_1\delta_2\left(\epsilon_1 + \delta_1 - 3\delta_2 - \delta_3 + \frac{2\delta_1\delta_2}{1+\delta_1}\right)}{1+\delta_1} - 1.$$

In the limit $\delta_1 \to 0$ and $\delta_3 \to 0$, it can be simplified as follows:

$$f_{\rm MS} = 2 + 3\delta_2 + \delta_2^2.$$

The scalar spectral index, in Eq. (114), then takes the form:

$$n_s - 1 = 3 - \sqrt{9 + 12\delta_2 + 4\delta_2^2} = 3 - |3 + 2\delta_2| = -2\delta_2 = 4\frac{\alpha y_2}{\beta y_0}, \tag{197}$$

where in the last equality, we used the condition $3 > \frac{4\alpha y_2}{\beta y_0}$. Therefore, we have a blue-tilted spectrum if the following condition is satisfied:

$$0 < \frac{4\alpha y_2}{\beta y_0} < 3 \;\Rightarrow\; 0 < \frac{y_2}{y_0} < \frac{3\beta}{4\alpha} = \frac{3(1+6\xi)}{8\xi}. \tag{198}$$

Let us now consider a particular case, choosing some specific values for $y_2 = 1$ and $y_0 = 1$. As before, let us choose $\mathrm{M_P^2} = 1$, $\xi = 1$, and an arbitrary attractor value $\sigma_0 = 1$. For this choice of values, we find, from Eq. (195), $\Phi = 13/7 > 0$. Consequently, we have a constant and decreasing solution. Eq. (197) for the spectral index gives $n_s - 1 = 8/7 > 0$ which is blue-tilted. The potential for induced gravity, using $Y \sim y_0 + y_2(\sigma/\sigma_0 - 1)^2$, is shown in Figure 15. We have also plotted the logarithmic derivative of the potential, as derived in Eq. (194). We see that the derivative of the effective potential w.r.t. the scalar field vanishes for $\sigma = \sigma_0$. In addition, it asymptotically tends to $+8$ as $\sigma \to \pm\infty$, which can be analytically obtained using the expression for the potential in Eq. (190). Figure 17 illustrates the phase space and the attractor value $\sigma_0 = 1$. We have also verified the de Sitter relation in Eq. (127) near the attractor, see Figure 18.

Finally, as for the minimal coupling, let us check that our conditions for the generation of amplification are compatible with the results in [64]. In that article, the condition $3 < 2n$ was found in order to have the growing solution, and the condition $0 < 2n < 3$ for the blue-tilted spectrum, see Eqs. (78) and (81) in [64]. Comparing with our previous conditions, see Eqs. (196) and (197) respectively, we find the following relation between the two reconstruction methods:

$$n = \frac{2\alpha y_2}{\beta y_0}. \tag{199}$$

Starting from Eq. (191), using H in Eq. (192) at leading order together with Eq. (17), we can express the evolution of the scalar field in terms of the scale factor:

$$\frac{d\sigma}{d\ln a} = -\frac{2y_2\alpha\sigma_0}{\beta y_0}\left(\frac{\sigma}{\sigma_0} - 1\right) \;\Rightarrow\; \frac{\sigma(a)}{\sigma_0} - 1 = \left(\frac{a_0}{a}\right)^{\frac{2\alpha y_2}{\beta y_0}}.$$

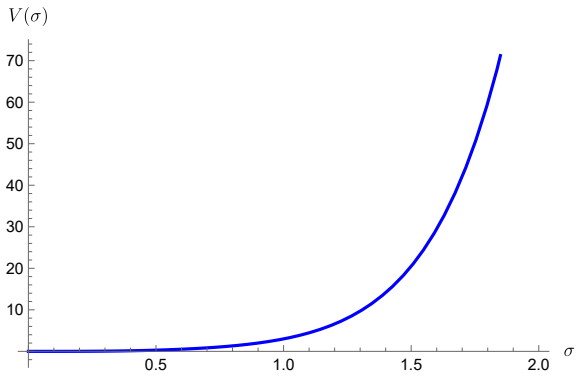

Figure 15: Potential reconstructed in Induced Gravity using the parameters: $M_P = 1$, $y_0 = 1$, $y_2 = 1$, $\sigma_0 = 1$, and $\xi = 1$.

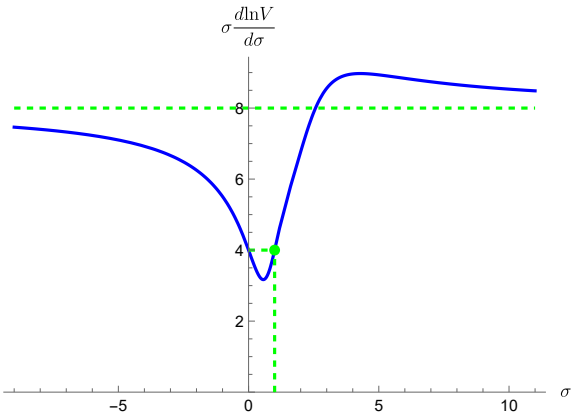

Figure 16: Plot of the function $\sigma d\ln V/d\sigma$. It takes value 4 at the attractor $\sigma = \sigma_0$ and at $\sigma = 0$, as expected from Eq. (194).

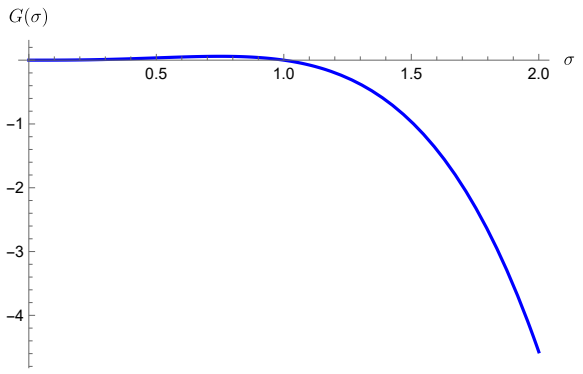

Figure 17: Phase space diagram for the simple potential of order two with the particular choice $M_P^2 = 1$, $\sigma_0 = 1$, $y_0 = 1$ and $y_2 = 1$. The scalar field σ is evolving towards its attractor $\sigma_0 = 1$.

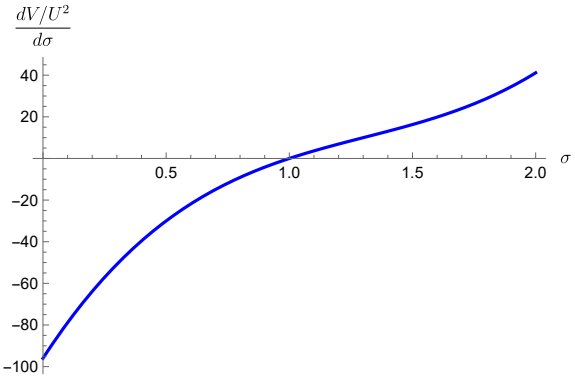

Figure 18: Derivative of V/U^2 w.r.t. σ. We do well have a de Sitter behaviour close to the attractor, i.e $\frac{dV/U^2}{d\sigma} = 0$, see Eq. (127).

From the expression of H in Eq. (192) for IG and substituting this last result, we find:

$$H \simeq \beta\sigma_0 y_0 \left[1 + \left(1 + 2\frac{\alpha y_2}{\beta y_0}\right)\left(\frac{a_0}{a}\right)^{\frac{2\alpha y_2}{\beta y_0}}\right].$$

Comparing it with the Taylor expansion of H from [64], see Eq. (159), we do indeed find the same Hubble evolution with the scale factor, w.r.t. a power n given by Eq. (199).

Stability

Using the same arguments as in GR, see Section 4.2, we can apply an analogous procedure to find the second perturbed solution, see Eq. (165), and the stability conditions. Starting from the expression of the potential in Eq. (185), we can deduce its invariance by taking the same combination of the coefficients of the potential as in GR, i.e. the ratio between the coefficients of Y^2 and that of $\sigma^2 Y_{,\sigma}^2$, divided by -2:

$$y_2 \to -y_2 + \frac{3\,(1+6\xi)}{4\xi} y_0 = -y_2 + \frac{3\beta}{2\alpha} y_0.$$

Note that the potential is indeed invariant close to the attractor. Therefore, one needs to expand the expression (190) in order to check explicitly the invariance. Applying this replacement in Eqs. (195) and (197), we find the following conditions for the amplification when the second solution is dominant.

$$\begin{aligned}\Phi =&\frac{4\alpha y_2}{\beta y_0}-3,\\ n_s-1=&6-\frac{4\alpha y_2}{\beta y_0}.\end{aligned}$$

5.4 General Jordan frames action

Let us now consider more general Jordan frame actions for which the gravitational interaction is described by the function [80]:

$$U(\sigma)=\frac{\xi\sigma^2}{2}+J. \tag{200}$$

Note that this coupling is equivalent to a quadratic polynomial form [70].

$$U(\sigma)=\frac{\xi\sigma^2}{2}+C_1\sigma+J_0.$$

Indeed, defining $\sigma_0=-\frac{C_1}{\xi}, J=J_0-\frac{C_1^2}{2\xi}$, we can rewrite it as: $U(\sigma)=\frac{\xi}{2}\left(\sigma-\sigma_0\right)^2+J$. Therefore, by redefining $\sigma-\sigma_0\to\sigma$ one recovers (200).

Using our results for the mapping between JF and EF in Eqs. (180) and (181), this coupling gives the following functions in the Jordan frame:

$$G=-\frac{2^{7/2}}{\mathrm{M_P}}\frac{U^{5/2}Y_{,\sigma}}{(1+6\xi)\,\xi\sigma^2+2J}, \tag{201}$$

$$H=\frac{\sqrt{2U}}{\mathrm{M_P}}\left(Y+\frac{4\xi U\sigma Y_{,\sigma}}{(1+6\xi)\,\xi\sigma^2+2J}\right). \tag{202}$$

Potential reconstruction

The potential is then obtained from Eq. (125):

$$V=\frac{\left(\xi\sigma^2+2J\right)^2}{\mathrm{M_P^2}}\left(3Y^2-\frac{2\left(\xi\sigma^2+2J\right)^2Y_{,\sigma}^2}{\xi(1+6\xi)\sigma^2+2J}\right). \tag{203}$$

Let us proceed in the same manner as usual. We can represent the scalar field flow functions as defined in Eq. (130) and (131):

$$\delta_1=-\frac{8U^2Y_{,\sigma}}{\xi(1+6\xi)\sigma^3Y+2J\sigma Y+4\xi U\sigma^2Y_{,\sigma}}, \tag{204}$$

$$\begin{aligned}\delta_2=&-\frac{4U\left(4\xi\sigma Y_{,\sigma}+2UY_{,\sigma\sigma}\right)}{(2J+\xi(1+6\xi)\sigma^2)Y+4\xi\sigma UY_{,\sigma}}\\ &-\delta_1\frac{(2J+3\xi(1+6\xi)\sigma^2)\,Y+(2J(1+4\xi)\sigma+\xi(1+14\xi)\sigma^3)\,Y_{,\sigma}+4\xi\sigma^2UY_{,\sigma\sigma}}{(2J+\xi(1+6\xi)\sigma^2)Y+4\xi\sigma UY_{,\sigma}}.\end{aligned} \tag{205}$$

Let us now suppose that the inflaton evolves to the same attractor σ_0, with the same assumption $\sigma_0 > 0$ and the same constrained Taylor expansion for Y, see Eq. (188). With this condition, we find the following limit for the SR parameters:

$$\begin{aligned}\delta_1(\sigma_0) &= 0,\\ \delta_2(\sigma_0) &= -\frac{4y_2}{\sigma_0^2 y_0}\frac{\left(\xi\sigma_0^2+2J\right)^2}{\xi(1+6\xi)\sigma_0^2+2J}.\end{aligned} \tag{206}$$

We can again find a simple potential leading to an amplification using the truncated Taylor expansion at second order $Y = y_0 + y_2\left(\sigma/\sigma_0 - 1\right)^2$ as exact:

$$V = \frac{y_2^2\left(\xi\sigma^2+2J\right)^2}{\mathrm{M_P^2}}\left(3\left[\frac{y_0}{y_2}+\left(\frac{\sigma}{\sigma_0}-1\right)^2\right]^2 - \frac{\frac{8}{\sigma_0^2}\left(\xi\sigma^2+2J\right)^2\left(\frac{\sigma}{\sigma_0}-1\right)^2}{\xi(1+6\xi)\sigma^2+2J}\right). \tag{207}$$

The behaviour in the vicinity of σ_0 gives:

$$G \simeq -\frac{4y_2}{\mathrm{M_P}\sigma_0^2}\frac{\left(\xi\sigma_0^2+2J\right)^{5/2}}{\left(\xi(6\xi+1)\sigma_0^2+2J\right)}\left(\frac{\sigma}{\sigma_0}-1\right), \tag{208}$$

$$H \simeq \frac{y_0}{\mathrm{M_P}}\sqrt{\xi\sigma_0^2+2J} + \left(\frac{4y_2}{\mathrm{M_P}}\frac{\xi\left(\xi\sigma_0^2+2J\right)^{3/2}}{\xi(6\xi+1)\sigma_0^2+2J} + \frac{y_0}{\mathrm{M_P}}\frac{\xi\sigma_0^2}{\sqrt{\xi\sigma_0^2+2J}}\right)\left(\frac{\sigma}{\sigma_0}-1\right). \tag{209}$$

It's worth noting that we still find the linear behaviour of the Hubble parameter H approaching the attractor in the JF. Additionally, the time dependence of $\sigma(t)$ still remains similar to that in the EF, see Eq. (146). Note also that we can explicitly check that the previous results for the case of Induced Gravity can be recovered by taking $J = 0$ in the JF. In addition, the results in the EF can be recovered by taking $\xi = 0$ and $J = \frac{\mathrm{M_P^2}}{2}$. In particular, using these values in the general expression of the potential in Eq. (203), we recover the potential in GR found in Eq. (139) and the one for IG in Eq. (185).

Developing Eq. (193) for the JF using Eq. (200), we find:

$$\left(\ddot{\sigma}+3H\dot{\sigma}\right)\left(1+6\frac{\xi^2\sigma^2}{\xi\sigma^2+2J}\right)+\frac{\xi\sigma\left(1+6\xi\right)}{\xi\sigma^2+2J}\dot{\sigma}^2 = -V_{\text{eff},\sigma}.$$

where $V_{\text{eff},\sigma} = \left(V_{,\sigma} - \frac{4\xi\sigma}{\xi\sigma^2+2J}V\right)$. The derivative of the effective potential vanishes when:

$$\frac{d\ln V}{d\sigma} = \frac{4\xi\sigma}{\xi\sigma^2+2J}. \tag{210}$$

When such a condition is satisfied, the scalar field can be constant, with $\dot{\sigma} \approx \ddot{\sigma} \approx 0$, and it is possible to have a de Sitter behaviour.

Amplification of the perturbations

The function z, present in the Mukhanov-Sasaki equation in Eq. (61), for the JF has the following form [80]:

$$z = a\phi\delta_1\frac{\sqrt{1+\frac{3\dot{U}^2}{\dot{\phi}^2U}}}{1+\frac{\dot{U}}{2HU}},$$

where the function Z is defined as $Z = \left(1 + \frac{3\dot{U}^2}{\dot{\phi}^2 U}\right) / \left(1 + \frac{\dot{U}}{2HU}\right)^2$.

In the annex A.3 in Eq. (271), we have derived the function z'/z in terms of the SR parameters:

$$\frac{z'}{z} = \mathcal{H}\left[1 + \gamma_1 + \gamma_2 - \gamma_3 + \gamma_4\right],$$

where the functions γ_i are defined in Eqs. (270). The amplification through the presence of a growing solution is verified through the value of Φ, defined in Eq. (110) and having the following form:

$$\Phi = \left[1 - \epsilon_1 + \frac{\epsilon_1^2 - \epsilon_1\epsilon_2}{(1-\epsilon_1)} + 2\left(1 + \gamma_1 + \gamma_2 - \gamma_3 + \gamma_4\right)\right].$$

The parameters δ_i have been defined in terms of the SR parameters in Eq. (275). Using our hierarchies of SR parameters in (206), we then find:

$$\Phi = 3 + 2\delta_2 = 3 - \frac{8y_2}{\sigma_0^2 y_0}\frac{\left(\xi\sigma_0^2 + 2J\right)^2}{\xi(1+6\xi)\sigma_0^2 + 2J}, \tag{211}$$

and the growing solution can exist for:

$$3 < \frac{8y_2}{\sigma_0^2 y_0}\frac{\left(\xi\sigma_0^2 + 2J\right)^2}{\xi(1+6\xi)\sigma_0^2 + 2J}. \tag{212}$$

Otherwise, we need to continue with the derivation of the spectral index. The function f_{MS} is derived in Eq. (272) and is given by:

$$f_{\rm MS} = \left[\left(1 + \gamma_1 + \gamma_2 - \gamma_3 + \gamma_4\right)\left(2 + \gamma_2 - \gamma_3 + \gamma_4\right)\right].$$

Using Eqs. (275) and (206), we find the following result close to the de Sitter attractor:

$$f_{\rm MS} = 2 + 3\delta_2 + \delta_2^2.$$

The scalar spectral index in Eq. (114) then takes the form:

$$n_s - 1 = 3 - |3 + 2\delta_2| = -2\delta_2 = \frac{8y_2}{\sigma_0^2 y_0}\frac{\left(2J + \xi\sigma_0^2\right)^2}{\left(2J + \xi\sigma_0^2(6\xi+1)\right)}, \tag{213}$$

where in the first equality, we used the fact that the condition (212) is not satisfied. Therefore, the spectrum is blue-tilted if the following condition is satisfied:

$$3 > \frac{8y_2}{\sigma_0^2 y_0}\frac{\left(\xi\sigma_0^2 + 2J\right)^2}{\xi(1+6\xi)\sigma_0^2 + 2J} > 0 \;\Rightarrow\; \frac{3\sigma_0^2}{8}\frac{\xi(1+6\xi)\sigma_0^2 + 2J}{\left(\xi\sigma_0^2 + 2J\right)^2} > \frac{y_2}{y_0} > 0. \tag{214}$$

Note that we can find this result using the second method of the derivation of the function f_{MS} in Eq. (268) or from the spectral index in Eq. (276).

Let us take some particular coefficients $y_2 = 1/3$ and $y_0 = 1$. We choose $\mathrm{M_P^2} = 1$, $\xi = J = 1$ and an attractor value $\sigma_0 = 1$. We find, with Eq. (211), $\Phi = 8/7 > 0$, which gives a constant and decreasing solution. The associated spectral index, Eq. (213), is $n_s - 1 = 8/3 > 0$ which is blue-tilted. The behaviour of the potential close to the attractor, in Eq. (207), is shown in Figure 19. The de Sitter relation in Eq. (127) close to the attractor is verified, see Figure 22. Figure 21 represents the phase space of the scalar field.

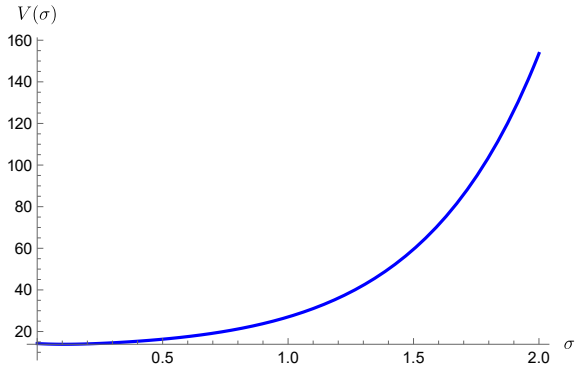

Figure 19: Potential reconstructed in the JF using the parameters: $M_P = 1$, $y_0 = 1$, $y_2 = 1/3$, $\sigma_0 = 1$, and $\xi = J = 1$

.

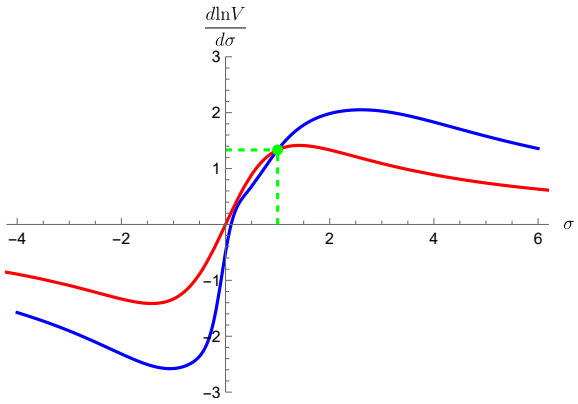

Figure 20: Figure representing $\frac{d\ln V}{d\sigma}$ in blue and $\frac{4\xi\sigma}{\xi\sigma^2+2J}$ in red. They intersect at the attractor value $\sigma_0 = 1$, at 4/3, see Eq. (210).

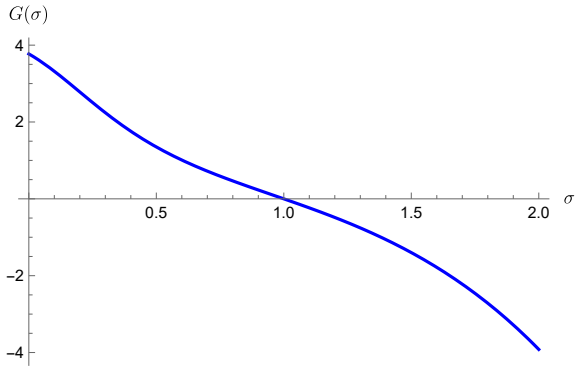

Figure 21: Phase space diagram for the simple potential of order two. The scalar field σ is evolving towards its attractor $\sigma_0 = 1$.

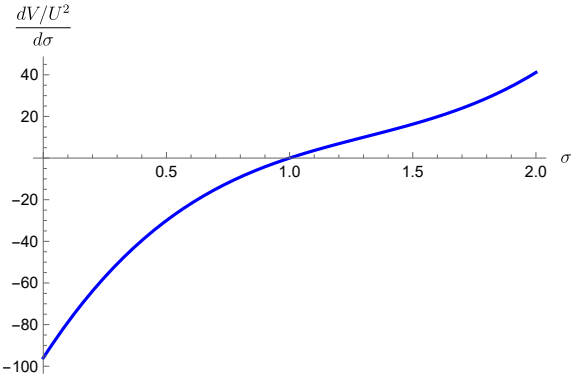

Figure 22: Derivative of V/U^2 w.r.t. σ. We do well have a de Sitter behaviour close to the attractor, i.e. $\frac{dV/U^2}{d\sigma} = 0$, see Eq. (127).

Stability

The invariance of the potential in the JF, see Eq. (203), can be found, as in the previous cases, by considering the ratio between the coefficients of Y^2 and $\sigma^2 Y_{,\sigma}^2$, divided by -2:

$$y_2 \to -y_2 + \frac{3\sigma_0^2\left(\xi(1+6\xi)\sigma_0^2+2J\right)}{4\left(\xi\sigma_0^2+2J\right)^2}y_0.$$

Applying this replacement in Eqs. (211) and (213) one obtains the second solution which yields the following conditions on the amplification:

$$\begin{aligned}\Phi =& \frac{8y_2}{\sigma_0^2 y_0}\frac{\left(\xi\sigma_0^2+2J\right)^2}{\xi(1+6\xi)\sigma_0^2+2J}-3,\\ n_s-1 =& 6-\frac{8y_2}{\sigma_0^2 y_0}\frac{\left(\xi\sigma_0^2+2J\right)^2}{\xi(1+6\xi)\sigma_0^2+2J}.\end{aligned}$$

5.5 Conformal coupling

Let us now study a particular case in which the coupling is conformal together with a nonzero Einstein–Hilbert term [81]. It corresponds to taking $\xi = -1/6$ in the general

expression Eq. (200):

$$U = J - \frac{\sigma^2}{12}.$$

We can express the functions G and H using the results found for the general JF, see Eqs. (201) and (202):

$$G = -\frac{2^{5/2}U^{5/2}Y_{,\sigma}}{\mathrm{M_P}J}, \tag{215}$$

$$H = \frac{\sqrt{2U}}{\mathrm{M_P}}\left(Y - \frac{U\sigma Y_{,\sigma}}{3J}\right). \tag{216}$$

Potential reconstruction

The potential can be obtained from Eq. (203):

$$V = \frac{1}{36\mathrm{M_P^2}}\left(12J - \sigma^2\right)^2\left(3Y^2 - \left(12J - \sigma^2\right)^2\frac{Y_{,\sigma}^2}{36J}\right). \tag{217}$$

Using $\xi = -1/6$ in Eqs. (204) and (205), we find the SR parameters in this particular coupling:

$$\begin{aligned}\delta_1 =& -\frac{\left(\sigma^2 - 12J\right)^2 Y_{,\sigma}}{36J\sigma Y + \left(\sigma^2 - 12J\right)\sigma^2 Y_{,\sigma}}\\ \delta_2 =& -\frac{\left(\sigma^2 - 12J\right)\left(4\sigma Y_{,\sigma} + \left(\sigma^2 - 12J\right)Y_{,\sigma\sigma}\right)}{36JY + \left(\sigma^2 - 12J\right)\sigma Y_{,\sigma}}\\ &- \delta_1\frac{\left(\sigma^2 - 12J\right)\sigma^2 Y_{,\sigma\sigma} + 4\left(3J + \sigma^2\right)\sigma Y_{,\sigma} + 36JY}{36JY + \left(\sigma^2 - 12J\right)\sigma Y_{,\sigma}}\end{aligned}$$

Assuming in the same way as before $\sigma_0 > 0$ and considering the constrained Taylor expansion for Y, we obtain the following limits:

$$\begin{aligned}\delta_1(\sigma) &= 0,\\ \delta_2(\sigma_0) &= -\frac{y_2}{\sigma_0^2 y_0}\frac{\left(\sigma_0^2 - 12J\right)^2}{18J}.\end{aligned} \tag{218}$$

As usual, we write the potential that might lead to an amplification close to the attractor, by using the second-order truncated Taylor expansion as the exact function $Y = y_0 + y_2\left(\sigma/\sigma_0 - 1\right)^2$ in Eq. (217):

$$V = \frac{y_2^2}{36\mathrm{M_P^2}}\left(12J - \sigma^2\right)^2\left(3\left[\frac{y_0}{y_2} + \left(\frac{\sigma}{\sigma_0} - 1\right)^2\right]^2 - \frac{\left(12J - \sigma^2\right)^2}{9J\sigma_0^2}\left(\frac{\sigma}{\sigma_0} - 1\right)^2\right). \tag{219}$$

The behaviour of the functions G and H, see Eqs. (215) and (216), close to σ_0 is given by:

$$\begin{aligned}G &\simeq -\frac{y_2}{\mathrm{M_P}}\frac{\left(12J - \sigma_0^2\right)^{5/2}}{18\sqrt{6}J\sigma_0}\left(\frac{\sigma}{\sigma_0} - 1\right),\\ H &\simeq \frac{y_0}{\mathrm{M_P}}\frac{\sqrt{12J - \sigma_0^2}}{\sqrt{6}} + \left(\frac{y_0}{\mathrm{M_P}}\frac{\sigma_0\sqrt{12J - \sigma_0^2}}{\sqrt{6}(\sigma_0^2 - 12J)} - \frac{y_2}{\mathrm{M_P}}\frac{(12J - \sigma_0^2)^{3/2}}{36\sqrt{6}J}\right)\left(\frac{\sigma}{\sigma_0} - 1\right).\end{aligned}$$

Amplification of the perturbations

Using the asymptotic limit of the SR parameters in Eqs. (218), we find the parameter Φ:

$$\Phi = 3 - \frac{y_2}{\sigma_0^2 y_0}\frac{\left(\sigma_0^2 - 12J\right)^2}{9J}. \tag{220}$$

The growing solution exists provided that the following condition is satisfied:

$$3 < \frac{y_2}{\sigma_0^2 y_0}\frac{\left(\sigma_0^2 - 12J\right)^2}{9J}. \tag{221}$$

In the case where the condition (221) is not satisfied, the scalar spectral index takes the form:

$$n_s - 1 = 3 - \left|3 - \frac{y_2}{\sigma_0^2 y_0}\frac{\left(\sigma_0^2 - 12J\right)^2}{9J}\right| = \frac{y_2}{\sigma_0^2 y_0}\frac{\left(\sigma_0^2 - 12J\right)^2}{9J}. \tag{222}$$

The spectrum is blue-tilted when we have the condition:

$$3 > \frac{y_2}{\sigma_0^2 y_0}\frac{\left(\sigma_0^2 - 12J\right)^2}{9J} > 0 \;\Rightarrow\; \frac{27\sigma_0^2 J}{8\left(\sigma_0^2 - 12J\right)^2} > \frac{y_2}{y_0} > 0. \tag{223}$$

We take some particular coefficients $y_2 = 2$ and $y_0 = 1$ to illustrate the conformal coupling case. We choose $M_P^2 = J = 1$ and an attractor value $\sigma_0 = 2$. We find with Eq. (220), $\Phi = -5/9 < 0$, which gives a growing solution. The behaviour of the potential close to the attractor, in Eq. (219), is shown in Figure 23. The de Sitter relation in Eq. (127) is verified in Figure 26.

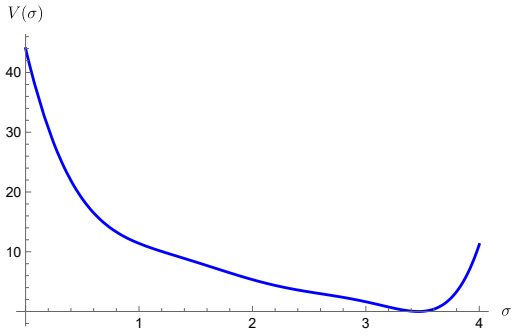

Figure 23: Potential reconstructed in the JF using the parameters: $M_P = J = 1$, $y_0 = 1$, $y_2 = 2$, $\sigma_0 = 1$, and $\xi = -1/6$

.

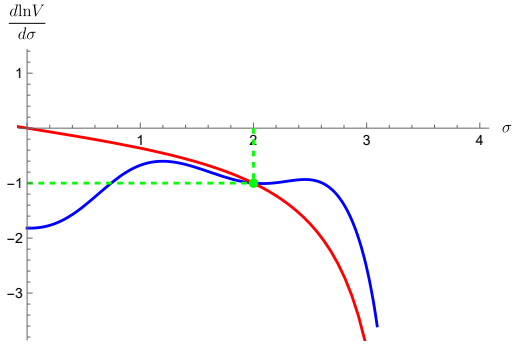

Figure 24: Figure representing $\frac{d\ln V}{d\sigma}$ in blue and $\frac{4\xi\sigma}{\xi\sigma^2+2J}$ in red. They intersect at the attractor value $\sigma_0 = 2$, at -1, see Eq. (210).

Stability

The invariance of the potential in the JF, see Eq. (217), is given for:

$$y_2 \to -y_2 + \frac{54J\sigma_0^2}{\left(\sigma_0{}^2 - 12J\right)^2}y_0.$$

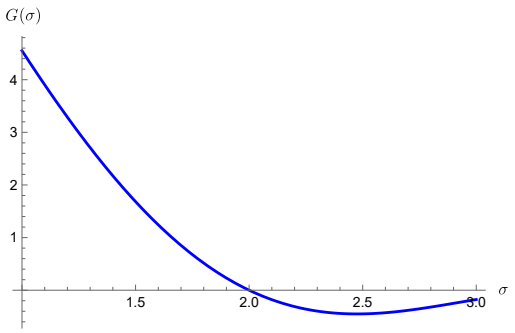

Figure 25: Phase space diagram for the simple potential of order two. The scalar field σ is evolving towards its attractor $\sigma_0 = 2$.

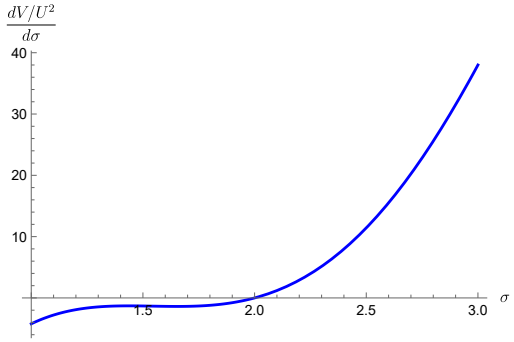

Figure 26: Derivative of V/U^2 w.r.t. σ. We do well have a de Sitter behaviour close to the attractor, i.e $\frac{dV/U^2}{d\sigma} = 0$, see Eq. (127).

Applying this replacement in Eqs. (220) and (222) we obtain the second solution which yields the following conditions on the amplification:

$$\begin{aligned}\Phi =& \frac{y_2}{\sigma_0^2 y_0}\frac{\left(\sigma_0^2 - 12J\right)^2}{9J} - 3,\\ n_s - 1 =& 6 - \frac{y_2}{\sigma_0^2 y_0}\frac{\left(\sigma_0^2 - 12J\right)^2}{9J}.\end{aligned}$$

6 f(R) cosmological models

In this Section, we consider another class of modified gravity theories generalising GR, called $f(R)$ gravity theories. In this class of models, the action is modified by replacing the simple Ricci scalar R term with a more general function $f(R)$ [82], [83]. These theories have a modified gravitational dynamics, which can explain various cosmological problems, such as inflation and dark energy[21]. The action for $f(R)$ gravity models is given by [82]:

$$S_R = \int d^4x\sqrt{-g}f(R), \tag{224}$$

where $f(R)$ is the function of the Ricci scalar R and needs to be double differentiable. Let us consider a new auxiliary scalar field φ described by the following action, without a kinetic term:

$$S_R = \int d^4x\sqrt{-g}\left[f_{,\varphi}(\varphi)(R-\varphi) + f(\varphi)\right]. \tag{225}$$

This action is equivalent to the original action (224). Indeed, the equation of motion for the scalar field is given by:

$$f_{,\varphi\varphi}(\varphi)(R-\varphi) = 0.$$

As we assumed f to be double differentiable, we have $f_{,\varphi\varphi}(\varphi) \neq 0$ which imposes $\varphi = R$. Therefore, the new degree of freedom is constrained by its "equation of motion" which is not dynamical, and the two actions are equivalent. The important point is that the action (225) is defined on the spacetime as the original action (224).

As before, we want to use the superpotential method with the goal to describe the conditions for the amplification of the perturbations. To do so, we can first describe the dynamics with the action (225). This action is that of a non-minimally coupled scalar field with a field potential and no kinetic term:

$$S_R = \int d^4x\sqrt{-g}\left[F(\varphi)R - V(\varphi)\right] \tag{226}$$

where we have defined $F(\varphi) \equiv \frac{df(\varphi)}{d\varphi}$ and the potential as:

$$V = F(\varphi)\varphi - f(\varphi). \tag{227}$$

As in the case of a non-minimally coupled scalar field model, we can perform a field and metric transformations to obtain a minimally coupled scalar field action. The metric transformation is a conformal transformation, see Eq. (172), which is defined as:

$$g_{\mu\nu} = \Omega^{-2}(x)\tilde{g}_{\mu\nu} = \frac{\mathrm{M_P^2}}{2F(\varphi)}\tilde{g}_{\mu\nu} \;\Rightarrow\; \Omega^2 = \frac{2F(\varphi)}{\mathrm{M_P^2}}. \tag{228}$$

[21] Observations show us that the expansion of the universe is actually accelerating. It requires breaking the SEC, as we saw before in annex 1.2, with the presence of a fluid with $w < -\frac{1}{3}$ to get $\frac{\ddot{a}}{a} > 0$, see Eq. (7). Dark energy has been introduced to account for this missing fluid and cannot be composed of ordinary matter. Since observations indicate $w_{DE} \sim -1$, dark energy is consistent with the cosmological constant Λ, note, however, the new Dark Energy Survey showing deviation from these values [84]. The theories $f(R)$ can offer a unified framework for both the accelerated expansion dynamics in the early universe and in the late universe.

Using this transformation and the corresponding Ricci transformation in Eq. (175), we find the following action:

$$S_E = \int d^4x\sqrt{-\tilde{g}}\left[\frac{\mathrm{M_P^2}}{2}\tilde{R} - \frac{1}{2}\left(\frac{3F}{\Omega^2}\left(\frac{d\log\Omega^2}{d\varphi}\right)^2\right)\tilde{g}^{\mu\nu}\partial_\mu\varphi\partial_\nu\varphi - \tilde{V}\right], \tag{229}$$

where we have defined the potential in the EF as:

$$\tilde{V} = \frac{V}{\Omega^4} = \mathrm{M_P^4}\frac{F\varphi - f}{4F^2}.$$

To recover the minimal coupling action, one finally needs to define the field as:

$$\frac{d\phi}{d\varphi} = \sqrt{\frac{3F}{\Omega^2}}\frac{\Omega^2_{,\varphi}}{\Omega^2} = \sqrt{\frac{3}{2}}\mathrm{M_P}\frac{F_{,\varphi}}{F} \;\Rightarrow\; \phi = \sqrt{\frac{3}{2}}\mathrm{M_P}\ln\left(\frac{2}{\mathrm{M_P^2}}F(\varphi)\right). \tag{230}$$

Inserting this new field into Eq. (229), we indeed obtain an EF action with a minimally coupled scalar field ϕ:

$$S_E = \int d^4x\sqrt{-g}\left[\frac{\mathrm{M_P^2}}{2}\tilde{R} - \frac{1}{2}\tilde{g}^{\mu\nu}\partial_\mu\phi\partial_\nu\phi - \tilde{V}(\phi)\right].$$

At this point, one could proceed in the same way as previously. However, in this context, the goal is reconstructing the form of f. A major difference comes from the fact that the potential in the JF depends on the form of the function $f(\varphi)$. To recover the potential in Eq. (226), one needs to find the form of $f(\varphi)$. We follow the steps presented in [85]. Before going into the reconstruction procedure, let us note that not all potentials in the EF can be analytically transformed in the JF. Indeed, the functions f and R can be expressed only parametrically in terms of $\tilde{V}$ as [83]:

$$R = \left[\frac{\sqrt{6}}{\mathrm{M_P}}\tilde{V}_{,\phi} + \frac{4\tilde{V}}{\mathrm{M_P^2}}\right]\mathrm{e}^{\frac{\sqrt{6}\phi}{3\mathrm{M_P}}}, \tag{231}$$

$$f = \frac{\mathrm{M_P^2}}{2}\left[\frac{\sqrt{6}}{\mathrm{M_P}}\tilde{V}_{,\phi} + \frac{2\tilde{V}}{\mathrm{M_P^2}}\right]\mathrm{e}^{2\frac{\sqrt{6}\phi}{3\mathrm{M_P}}}. \tag{232}$$

So, the function f in Eq. (232) and the corresponding potential in the JF can only be obtained in an analytical form for some specific choices of the potential in the EF. If we choose, for instance, the following form for the function R:

$$R = C_1 + C_k\mathrm{e}^{\frac{k\phi}{\mathrm{M_P}}}, \tag{233}$$

with C_1 and $C_k \neq 0$ being some arbitrary constants, Eq. (231) becomes a linear first-order differential equation. Its solution gives the form of the potential $\tilde{V}$ in the EF:

$$\left[\frac{\sqrt{6}}{\mathrm{M_P}}\frac{d\tilde{V}}{d\phi} + \frac{4\tilde{V}}{\mathrm{M_P^2}}\right]\mathrm{e}^{\frac{\sqrt{6}}{3}\frac{\phi}{\mathrm{M_P}}} = C_1 + C_k\mathrm{e}^{k\frac{\phi}{\mathrm{M_P}}}$$

$$\Rightarrow\; \tilde{V}(\phi) = \frac{\mathrm{M_P^2}}{2}\left(C_2\mathrm{e}^{-2\frac{\sqrt{6}\phi}{3\mathrm{M_P}}} + C_1\mathrm{e}^{-\frac{\sqrt{6}\phi}{3\mathrm{M_P}}} + C_\omega\mathrm{e}^{\frac{6}{3\mathrm{M_P}}\phi}\right), \tag{234}$$

where we have defined C_2 as the integration constant, $\omega = \sqrt{6}k/2 - 1$, and $C_\omega = \frac{\sqrt{6}C_k}{\sqrt{6}+3k} = \frac{C_k}{\omega+2}$. Using this result in Eqs. (231) and (232), we find:

$$R = C_\omega(\omega+2)\mathrm{e}^{(\omega+1)\frac{\sqrt{6}\phi}{3\mathrm{M_P}}} + C_1,$$
$$f = \frac{\mathrm{M_P^2}}{2}\left(C_\omega(\omega+1)\mathrm{e}^{(\omega+2)\frac{\sqrt{6}\phi}{3\mathrm{M_P}}} - C_2\right).$$

which combined gives finally the analytical expression of the function $f(R)$, see:

$$f(R) = \frac{\mathrm{M_P^2}}{2}\left[C_\omega(\omega+1)\left(\frac{R-C_1}{C_\omega(\omega+2)}\right)^{\frac{\omega+2}{\omega+1}} - C_2\right]. \tag{235}$$

where C_2 is an integration constant, $\omega = \sqrt{6}k/2 - 1$, and $C_\omega = \frac{\sqrt{6}C_k}{\sqrt{6}+3k} = \frac{C_k}{\omega+2}$.

The reconstruction procedure to find the function $f(R)$ in Eq. (235), and thus the potential V in (227), can be fulfilled if the form of the potential in the EF is given by Eq. (234). Let us remember that in our case, we are interested in a potential having a de Sitter behaviour close to an attractor ϕ_0. We assume the following form of the Hubble parameter in the EF:

$$\tilde{H}(\phi) = y_a\mathrm{e}^{a\sqrt{\frac{3}{2}}\frac{\phi-\phi_0}{\mathrm{M_P}}} + y_b\mathrm{e}^{b\sqrt{\frac{3}{2}}\frac{\phi-\phi_0}{\mathrm{M_P}}}. \tag{236}$$

This form is the same as Eq. (16) in [85], providing the following relations between the parameters: $W_a \equiv y_a\mathrm{e}^{-a\sqrt{\frac{3}{2}}\frac{\phi_0}{\mathrm{M_P}}}$ and $W_b \equiv y_b\mathrm{e}^{-b\sqrt{\frac{3}{2}}\frac{\phi_0}{\mathrm{M_P}}}$. Using this form for the Hubble parameter, we find the corresponding potential in the EF using Eq. (139):

$$\tilde{V} = 3\mathrm{M_P^2}\left(\left(1-a^2\right)y_a^2 e^{\sqrt{6}a\frac{(\phi-\phi_0)}{\mathrm{M_P}}} + 2y_a y_b(1-ab)e^{\sqrt{\frac{3}{2}}(a+b)\frac{(\phi-\phi_0)}{\mathrm{M_P}}} + \left(1-b^2\right)y_b^2 e^{\sqrt{6}b\frac{(\phi-\phi_0)}{\mathrm{M_P}}}\right),$$

which is formally analogous to Eq. (234). To obtain an analytical expression for $f(R)$, it is necessary to compare this potential with the one in Eq. (234), obtained with R defined in Eq. (233). An appropriate analytical expression can be found only for some specific parameters a and b, and the result has been presented in Tab. 1 from [85].

6.1 Frame mapping

We can now constrain further the form of the potential for the amplification of the perturbations. We start by expressing the scalar evolution and the Hubble parameter in the EF, in the same way as Eqs. (177) and (178) for the previous JF:

$$\tilde{G} = \frac{d\phi}{\tilde{N}_L dt} = \frac{d\phi}{d\varphi}\frac{d\varphi}{\Omega N_L dt} = \frac{\sqrt{3}}{2}\mathrm{M_P^2}\frac{F_{,\varphi}}{F^{3/2}}G. \tag{237}$$

where we have used the field transformation in Eq. (230) and Eqs. (173) and (174). The Hubble parameter is given by:

$$\tilde{H} = \frac{d\tilde{a}}{\tilde{a}\tilde{N}_L dt} = \frac{1}{\Omega^2}\frac{d\Omega}{N_L dt} + \frac{1}{\Omega}\frac{da}{aN_L dt} = \frac{\mathrm{M_P}}{2\sqrt{2}}\frac{F_{,\varphi}}{F^{3/2}}G + \frac{\mathrm{M_P}}{\sqrt{2F}}H. \tag{238}$$

Let us now use the scalar field evolution in the EF, as in Eq. (138):

$$\tilde{G} = -2\mathrm{M_P^2}\tilde{H}_{,\phi} = -\frac{2\sqrt{2}}{\sqrt{3}}\mathrm{M_P}\frac{F}{F_{,\varphi}}Y_{,\varphi}. \tag{239}$$

where in the last equation, we used the field transformation (230) to express the derivative in the JF. In addition, the function F can be expressed inverting Eq. (230) as follows:

$$F = \frac{\mathrm{M_P^2}}{2} e^{\sqrt{\frac{2}{3}}\frac{\phi}{\mathrm{M_P}}} \;\Rightarrow\; \Omega^2 = \frac{2F}{\mathrm{M_P^2}} = e^{\sqrt{\frac{2}{3}}\frac{\phi}{\mathrm{M_P}}}, \tag{240}$$

where we used it to express the Weyl transformation defined in Eq. (228).

We can now invert Eq. (237) to express the scalar evolution G in the JF, and substituting Eq. (239) one obtains:

$$G = -\frac{4}{\sqrt{3}}\frac{F^{3/2}}{F_{,\varphi}}\tilde{H}_{,\phi} = -\frac{4\sqrt{2}}{3\mathrm{M_P}}\frac{F^{5/2}}{F_{,\varphi}^2}Y_{,\varphi}. \tag{241}$$

Inverting Eq. (238) and using Eqs. (240) and (241), we finally find the expression of H in the JF:

$$H = \mathrm{e}^{\frac{\phi}{\sqrt{6}\mathrm{M_P}}}\left(\tilde{H} + \sqrt{\frac{2}{3}}\mathrm{M_P}\tilde{H}_{,\phi}\right) = \frac{\sqrt{2F}}{\mathrm{M_P}}\left(Y + \frac{2}{3}\frac{F}{F_{,\varphi}}Y_{,\varphi}\right). \tag{242}$$

Potential reconstruction

Starting from Eqs. (241) and (242), one can express the first and second SR parameters in terms of $Y(\phi(\varphi))$ and its derivatives. In a way similar to the previous non-minimal coupling case, we could use the Taylor expansion of the Hubble parameter in terms of the scalar field in the JF. Doing so, we would find the conditions on the coefficients of the expansion. We could also find expressions similar to Eqs. (208) and (209) close to the attractor. However, we now have a constrained Hubble parameter in the EF, see Eq. (236), which leads to an analytical expression for the potential. So, instead of using the Taylor expansion of $Y(\varphi)$, we can Taylor expand w.r.t. the scalar field in the EF, $\tilde{H}(\phi)$. Let us now find the SR parameters in terms of $\tilde{H}(\phi)$ and its derivatives. The first SR parameter is found by taking the derivative of the first expression in Eq. (242):

$$\epsilon_1 = -\frac{1}{H^2}\frac{dH}{N_L dt} = -\Omega\tilde{G}\frac{H_{,\phi}}{H^2} = 2\mathrm{M_P^2}\tilde{H}_{,\phi}\frac{\frac{\tilde{H}}{\sqrt{6}\mathrm{M_P}} + \frac{4}{3}\tilde{H}_{,\phi} + \sqrt{\frac{2}{3}}\mathrm{M_P}\tilde{H}_{,\phi\phi}}{\left(\tilde{H} + \sqrt{\frac{2}{3}}\mathrm{M_P}\tilde{H}_{,\phi}\right)^2}. \tag{243}$$

Differentiating of the first SR parameter, we can then find the second SR parameter:

$$\begin{aligned}\epsilon_2 &= \Omega\tilde{G}\frac{\epsilon_{1,\phi}}{H\epsilon_1} \\ &= \frac{2\mathrm{M_P^2}\tilde{H}_{,\phi}}{\tilde{H} + \sqrt{\frac{2}{3}}\mathrm{M_P}\tilde{H}_{,\phi}}\left(\frac{\tilde{H}_{,\phi\phi}}{\tilde{H}_{,\phi}} - 2\frac{\tilde{H}_{,\phi} + \sqrt{\frac{2}{3}}\mathrm{M_P}\tilde{H}_{,\phi\phi}}{\tilde{H} + \sqrt{\frac{2}{3}}\mathrm{M_P}\tilde{H}_{,\phi}} + \frac{\frac{\tilde{H}_{,\phi}}{\sqrt{6}\mathrm{M_P}} + \frac{4}{3}\tilde{H}_{,\phi\phi} + \sqrt{\frac{2}{3}}\mathrm{M_P}\tilde{H}_{,\phi\phi\phi}}{\frac{\tilde{H}}{\sqrt{6}\mathrm{M_P}} + \frac{4}{3}\tilde{H}_{,\phi} + \sqrt{\frac{2}{3}}\mathrm{M_P}\tilde{H}_{,\phi\phi}}\right).\end{aligned} \tag{244}$$

Amplification of the perturbations

As usual, let us suppose that the scalar field evolves towards some attractor $\phi_0 > 0$, without loss of generality. We need to evaluate the behaviour of the SR parameters close to the attractor ϕ_0 and impose the condition to get amplification. The first SR parameter

in Eq. (243) needs to vanish close to the attractor. This requires to impose $\tilde{H}_{,\phi}(\phi_0) = 0$. Using Eq. (236), we find:

$$\tilde{H}_{,\phi}(\phi_0) = \sqrt{\frac{3}{2}}\frac{1}{\mathrm{M_P}}(a y_a + b y_b) = 0 \;\Rightarrow\; y_b = -\frac{a}{b} y_a. \tag{245}$$

The second SR parameter needs to go to a constant $\epsilon_2 \to$ cst. , so that $\tilde{H}_{,\phi\phi}(\phi_0) \neq 0$, and $\tilde{H}(\phi_0) > 0$ to ensure inflation:

$$\begin{aligned} \tilde{H}(\phi_0) &= y_a + y_b = \frac{(b-a)y_a}{b} > 0, \\ \tilde{H}_{,\phi\phi}(\phi_0) &= \frac{3}{2\mathrm{M_P^2}}\left(a^2 y_a + b^2 y_b\right) = \frac{3}{2\mathrm{M_P^2}} a(a-b) y_a \neq 0. \end{aligned} \tag{246}$$

Using these results in Eqs. (243) and (244), we find the following asymptotic limits:

$$\begin{aligned} \epsilon_1(\phi_0) &= 0, \\ \epsilon_2(\phi_0) &= 3ab. \end{aligned} \tag{247}$$

We are looking for solutions where ϕ_0 is an attractor. Close to the attractor ϕ_0, the scalar field ϕ in the EF must evolve toward ϕ_0 linearly at leading order, see Eq. (153):

$$\tilde{G}(\phi) \sim \tilde{g}_0 \left(\frac{\phi}{\phi_0} - 1\right),$$

with $\tilde{g}_0 < 0$ to ensure the attraction, as we assumed $\phi_0 > 0$. Substituting the constrained Taylor expansion, see Eq. (152), up to the second order:

$$\tilde{H}(\phi) \sim h_0 + h_2 \left(\frac{\phi}{\phi_0} - 1\right) = \tilde{H}(\phi_0) + \frac{\tilde{H}_{,\phi\phi}(\phi_0)}{2}(\phi - \phi_0)^2,$$

in the first expression in Eq. (239), we find:

$$\tilde{G}(\phi) \sim -2{\mathrm{M_P}}^2 \tilde{H}_{,\phi\phi}(\phi_0)(\phi - \phi_0) = 3a(b-a) y_a (\phi - \phi_0) = 3ab\phi_0 \tilde{H}(\phi_0)\left(\frac{\phi}{\phi_0} - 1\right).$$

In the second equality, we used Eqs. (245) and (246). The condition $\tilde{g}_0 = 3ab\phi_0\tilde{H}(\phi_0) < 0$ is satisfied when a and b have opposite signs. This condition is also compatible with the de Sitter condition, $\tilde{H}(\phi_0) > 0$, when considering $y_a > 0$, see Eq. (246).

To summarise, the generation of amplification in $f(R)$ theories requires the solutions to have $y_a > 0$, $(b-a)/b > 0$ and $a \cdot b < 0$. Imposing all these conditions in Tab. 1 from [85], we are left with a restricted range of possible analytical solutions, which are presented in Tab. 2. Let us remind that the requirement of the existence of the de Sitter attractor has changed the Hubble parameter in the EF, see Eq. (236), with $W_a \equiv y_a \exp\left(-a\sqrt{3/2}\,\phi_0/\mathrm{M_P^2}\right)$.

The function z, present in the Sasaki-Mukhanov equation in Eq. (61), for the $f(R)$ models is defined as follows [86]:

$$z = a\sqrt{\frac{3\mathrm{M_P^2}}{2}}\frac{\dot{F}}{\sqrt{F}\left(H + \dot{F}/2F\right)},$$

a	b	$y_b = -\frac{a}{b} y_a$	$f(R)$	$F(R)$	$\epsilon_2 = 3ab$
$-\frac{2}{3}$	1	$\frac{2}{3} y_a$	$20 y_a^2 \left(\frac{3R}{100 y_a^2}\right)^{5/3} - \frac{10 y_a^2}{3}$	$\left(\frac{3R}{100 y_a^2}\right)^{2/3}$	-2
-1	$\frac{1}{3}$	$3 y_a$	$96 y_a^2 \left(\frac{R}{144 y_a^2} - \frac{1}{3}\right)^{3/2}$	$\sqrt{\frac{R}{144 y_a^2} - \frac{1}{3}}$	-1
$-\frac{1}{3}$	1	$\frac{1}{3} y_a$	$\frac{32}{3} y_a^2 \left(\frac{R}{16 y_a^2} - \frac{1}{3}\right)^{3/2}$	$\sqrt{\frac{R}{16 y_a^2} - \frac{1}{3}}$	-1
$-\frac{7}{3}$	1	$\frac{7}{3} y_a$	$160 y_a^2 \left(\frac{3R}{400 y_a^2}\right)^{5/6} - \frac{280}{3} y_a^2$	$\left(\frac{3R}{400 y_a^2}\right)^{-1/6}$	-7
$-\frac{5}{3}$	1	$\frac{5}{3} y_a$	$\frac{128}{3} y_a^2 \left(\frac{R}{32 y_a^2} - \frac{5}{3}\right)^{3/4}$	$\left(\frac{R}{32 y_a^2} - \frac{5}{3}\right)^{-1/4}$	-5

Table 2: Analytical expressions for $f(R)$ from Tab. 1 in [85], imposing the conditions $y_a > 0$, $(b-a)/b > 0$ and $a \cdot b < 0$ for the amplification of the perturbations. Note that the first solution in [85], with $b = 0$ is not included, as the condition (245) is undefined. The second and third cases are equivalent, substituting $y_a \leftrightarrow y_a/3$.

In the annex A.4, we have derived the function z'/z and z''/z using two different methods. Substituting the limit of the SR parameters in the vicinity of the attractor, see Eqs. (247), into Eq. (289), it gives:

$$\frac{z'}{z} \to 1 + \epsilon_2.$$

The parameter Φ, defined in Eq. (110) becomes:

$$\Phi = 3 + 2\epsilon_2. \tag{248}$$

The amplification through the growing solution occurs when:

$$\epsilon_2 < -\frac{3}{2}. \tag{249}$$

The function f_{MS} is derived in Eq. (290). Imposing the limit for the SR parameters, it reduces to the form:

$$f_{\rm MS} \to 2 + 3\epsilon_2 + 2\epsilon_2^2.$$

The scalar spectral index in Eq. (114) becomes:

$$n_s - 1 = -2\epsilon_2, \tag{250}$$

which is blue-tilted if the following condition is satisfied:

$$-3/2 < \epsilon_2 < 0. \tag{251}$$

Let us analyse the first case in Table 2, with $a = -\frac{2}{3}$ and $b = 1$. Using the expression (248), we find an increasing solution: $\phi = -1$. The corresponding potential in the JF can be found with Eq. (227) and is presented in Figure 27.

6.2 de Sitter solutions in $f(R)$ theories

In the previous Section, we applied the superpotential method to reconstruct $f(R)$ theories for the amplification of the perturbations. The results were quite limited. However, a wider range of $f(R)$ models have been studied in the literature, and it is therefore useful

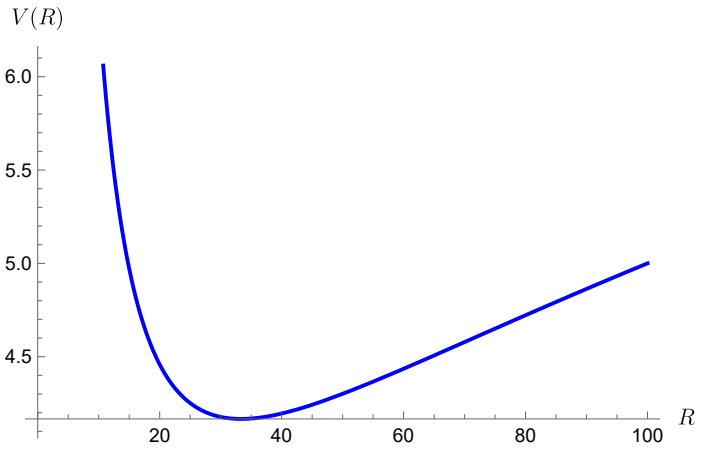

Figure 27: Reconstructed potential in Eq. (227) for the first case, $a = -\frac{2}{3}$ and $b = 1$, in Table 2 with $y_a = \mathrm{M_P^2} = 1$.

to enlarge the analysis. To do so, one can adopt a more specific approach compared to the general reconstruction method. Starting from a particular model, it is indeed possible to verify explicitly the existence of a de Sitter attractor and subsequently the possibility of an enhancement of the primordial spectrum. In addition, we can check the stability of the solutions. The reconstruction methods previously applied in the EF and JF frames cannot indeed be straightforwardly applied in the reconstruction of $f(R)$ theories. Let us remember that a de Sitter phase corresponds to eternal inflation with constant expansion. Therefore, the first SR parameter vanishes. Since we can express the Ricci scalar in Eq. (3) in terms of the first SR parameter:

$$R = 6\left(\frac{\ddot{a}}{a} + \frac{\dot{a}^2}{a^2}\right) = 6(2-\epsilon_1)H^2, \tag{252}$$

we deduce that the de Sitter attractor $R \equiv R_0$ is a positive constant $R_0 \propto H^2 = \text{cst.} > 0$.

The field equations in $f(R)$ gravity can be obtained by varying the action (224) w.r.t. $g_{\mu\nu}$ [86]:

$$F(R)R_{\mu\nu}(g) - \frac{1}{2}f(R)g_{\mu\nu} - \nabla_\mu\nabla_\nu F(R) + g_{\mu\nu}\Box F(R) = 0.$$

In the flat FLRW metric, the field equations are given by [86]:

$$3FH^2 = (FR - f)/2 - 3H\dot{F}, \tag{253}$$

$$-2F\dot{H} = \ddot{F} - H\dot{F}, \tag{254}$$

Using Eq. (252) and introducing the notation $n_x \equiv \frac{R}{x}\frac{dx}{dR}$, it is possible to write Eq. (253) in the following way:

$$1 = (2-\epsilon_1)\frac{n_f - 1}{n_f} - \frac{\dot{R}}{HR}n_F. \tag{255}$$

The existence of the de Sitter attractor implies the condition can then be reformulated as:

$$n_f(R_0) = 2. \tag{256}$$

Differentiating Eq. (255), we obtain a Klein-Gordon-like equation of the form:

$$\ddot{F} + 3H\dot{F} + \frac{2f - RF}{3} = 0,$$

for the homogeneous field F. The last term in the last equation is the potential gradient:

$$V_{,F} = \frac{2f - RF}{3}. \tag{257}$$

Thus, the stability of the de Sitter solution with respect to homogeneous perturbations can be studied using the potential implicitly defined by Eq. (257). The equilibrium point given by $V_{,F}(R_0) = 0$ is the de Sitter attractor found in Eq. (256). The stability condition is $V_{,FF}(R_0) > 0$, and we find a new condition on n_F:

$$V_{,FF}(R_0) = \frac{dR}{dF}\frac{dV_{,F}}{dR}\bigg|_{R=R_0} = \frac{R}{3}\left(\frac{1 - n_F}{n_F}\right)\bigg|_{R=R_0} > 0 \;\Rightarrow\; 0 < n_F(R_0) < 1, \tag{258}$$

provided that $R_0 > 0$. Expressing n_F using its definition $F(R) = \frac{df(R)}{dR}$, we can rewrite this stability condition in terms of the function $f(R)$ and its derivative:

$$\frac{f_{,R} - Rf_{,RR}}{f_{,RR}}\bigg|_{R=R_0} > 0 \;\Rightarrow\; 0 < f_{,RR}|_{R=R_0} < \frac{f_{,R}}{R}\bigg|_{R=R_0},$$

when $f_{,R}(R_0) > 0$.

Instead of solving the Klein-Gordon equation for homogeneous perturbations as in GR, see Eq. (162), one may differentiate Eq. (255) to find the two solutions $\epsilon_2^{(1,2)}$. By doing so and imposing the usual limit of SR parameters, with the odd parameters $\epsilon_{2i+1} \to 0$, and the de Sitter condition $n_f(R_0) \to 2$, one finds:

$$\epsilon_2^{(1,2)}(R_0) = -\frac{1}{2}\left(3 \pm \sqrt{25 - \frac{16}{n_F(R_0)}}\right). \tag{259}$$

The real limit of ϵ_2 only exists when $n_F(R_0) \geq 16/25$. By comparison with the stability condition (258), we finally have that the interval $16/25 < n_F(R_0) \leq 1$ ensures a stable solution. The second SR parameter then takes the corresponding extreme values $-3 < \epsilon_2^{(1)} < -3/2$ and $-3/2 < \epsilon_2^{(2)} < 0$. In such cases, the SR parameters may approach the de Sitter attractor $\epsilon_1 \to 0$, while $\epsilon_2 \to$ cst.. When $0 < n_F(R_0) \leq 16/25$, the solutions are still stable, but ϵ_2 becomes imaginary and solutions oscillate.

When the stability condition is not satisfied, the solution $\epsilon_2^{(1)}$ is the only one having the appropriate constant behaviour for amplification, corresponding to a decreasing $\epsilon_1 \to 0$. When $n_F(R_0) > 1$, we find indeed the extreme value $-4 < \epsilon_2^{(1)} < -3$, corresponding to $n_F(R_0) = +\infty$ and $n_F(R_0) = 1$, respectively. Instead, $0 < \epsilon_2^{(2)} < 1$ does not respect the condition required for amplification, see Eqs. (249) and (251). The case $n_F(R_0) < 0$ leads to the range $-\infty < \epsilon_2^{(1)} < -4$, corresponding to $n_F(R_0) = 0^-$ and $n_F(R_0) = -\infty$, respectively. As before, $1 < \epsilon_2^{(2)} < +\infty$ is outside the condition for amplification.

The conditions for the generation of PBHs in Eqs. (248) and (250) can be then extended with the two possible $\epsilon_2^{(1,2)}$. Close to the attractor, one has:

$$\Phi^{(1,2)} = 3 + 2\epsilon_2^{(1,2)} = \mp\sqrt{25 - \frac{16}{n_F(R_0)}}, \tag{260}$$

and

$$n_s^{(1,2)} - 1 = -2\epsilon_2^{(1,2)} = 3 \pm \sqrt{25 - \frac{16}{n_F(R_0)}}. \tag{261}$$

Therefore, with this method, we first need to find the de Sitter solution by solving Eq. (256) and then find the corresponding parameter $n_F(R_0)$ to determine the expression of the second SR parameter, see Eq. (259). Then, we can check the stability and the amplification of the perturbations with Eqs. (258), (260) and (261). By applying this procedure, we can extend the solutions found with the superpotential method in Table 2. The results are presented in Table 3. We see that the first three cases are stable, while the last two are unstable with $n_F(R_0) < 0$. In the next Sections, we analyse different models found in the literature using this method.

a	b	$f(R)$	R_0	$n_F(R_0)$	$\epsilon_2^{(1)}$	$\epsilon_2^{(2)}$
$-\frac{2}{3}$	1	$20y_a^2\left(\frac{3R}{100y_a^2}\right)^{5/3} - \frac{10y_a^2}{3}$	$\frac{100y_a^2}{3}$	$\frac{2}{3}$	-2	-1
-1	$\frac{1}{3}$	$96y_a^2\left(\frac{R}{144y_a^2} - \frac{1}{3}\right)^{3/2}$	$192y_a^2$	$\frac{2}{3}$	-2	-1
$-\frac{7}{3}$	1	$160y_a^2\left(\frac{3R}{400y_a^2}\right)^{5/6} - \frac{280}{3}y_a^2$	$\frac{400y_a^2}{3}$	$-\frac{1}{6}$	-7	/
$-\frac{5}{3}$	1	$\frac{128}{3}y_a^2\left(\frac{R}{32y_a^2} - \frac{5}{3}\right)^{3/4}$	$\frac{256y_a^2}{3}$	$-\frac{2}{3}$	-5	/

Table 3: Stability of the $f(R)$ solutions found in Table 2 found with the superpotential method.

6.2.1 Scale-invariant model

The Starobinsky inflation is based on a modification of general relativity by including a term in the action that involves the square of the Ricci scalar [19]. Let us consider this model with the function $f(R)$ defined as:

$$f(R) = \alpha R^2,$$

which directly gives $n_f(R_0) = \left.\frac{R}{f}\frac{df}{dR}\right|_{R=R_0} = 2$. It essentially means that the de Sitter attractor R_0 can take all positive values. Since $n_F(R_0) = \left.\frac{R}{F}\frac{dF}{dR}\right|_{R_0} = 1$, the stability condition (258) is not satisfied, similarly to what occurs for USR inflation, see Section 4.2. Therefore, only $\epsilon_2^{(1)}$ can exist as an unstable solution. One can indeed check that $\epsilon_2^{(2)} = 0$. Using Eq. (259), we find:

$$\epsilon_2^{(1)} = -3.$$

It gives $\Phi^{(1)} = -3 < 0$, using Eq. (260). The amplification of the spectrum is therefore generated by the existence of an increasing solution for the curvature perturbations. This model is the simplest model for the generation of amplification.

6.2.2 Powers of R binomial

Let us analyse the specific model [87]:

$$f(R) = R + \alpha\, R^n / M^{2n-2}.$$

The de Sitter attractor is found by solving Eq. (256):

$$R_0 = M^2 \left(\frac{1}{\alpha(n-2)} \right)^{1/(n-1)}. \tag{262}$$

To ensure $R_0 > 0$, this solution requires $\alpha(n-2) > 0$. Using this result, we find:

$$n_F(R_0) = \frac{n}{2}.$$

The solutions are stable provided that $0 < n < 2$, using Eq. (258). Beyond this range, $n > 2$ and $n < 0$, the de Sitter solution in Eq. (262) exists but is unstable. In this case, only $\epsilon_2^{(1)}$ approaches the de Sitter limit.

The definition of the second SR parameter in Eq. (259) becomes:

$$\epsilon_2^{(1,2)} = -\frac{1}{2} \left(3 \pm \sqrt{25 - \frac{32}{n}} \right).$$

Therefore, one also needs $n \geq 32/25$ to have a definite second SR parameter, the interval $32/25 < n < 1$ has a stable definite limit. Using Eqs. (259) and (261), we can finally deduce the conditions for the amplification studying the behaviour of:

$$\Phi = \mp \sqrt{25 - \frac{32}{n}} \quad \text{and} \quad n_s - 1 = 3 \pm \sqrt{25 - \frac{32}{n}},$$

on varying n.

6.2.3 Second-order polynomial in R

Let us now consider an extension of the Starobinsky model of the form:

$$f(R) = \alpha M^2 + \beta R + \gamma R^2 / M^2.$$

The first term corresponds to a cosmological constant, i.e. $\Lambda = \alpha M^2 R^0 = \alpha M^2$.

Following the same procedure used above, one finds that the de Sitter solution exists provided that $\alpha \cdot \beta < 0$:

$$R_0 = -2M^2 \frac{\alpha}{\beta}.$$

Correspondingly, one finds:

$$n_F(R_0) = -\frac{4\alpha\gamma}{\beta^2 - 4\alpha\gamma},$$

Assuming β real, the stability condition is satisfied for the ranges $0 < \beta^2 < 4\alpha\gamma$ or $4\alpha\gamma < 0 < \beta^2$. In such a case, one find:

$$\epsilon_2^{(1,2)} = -\frac{1}{2} \left(3 \pm \sqrt{25 + \frac{4\,(\beta^2 - 4\alpha\gamma)}{\alpha\gamma}} \right),$$

$$\Phi^{(1,2)} = \mp \sqrt{25 + \frac{4\,(\beta^2 - 4\alpha\gamma)}{\alpha\gamma}} \quad \text{and} \quad n_s - 1^{(1,2)} = 3 \pm \sqrt{25 + \frac{4\,(\beta^2 - 4\alpha\gamma)}{\alpha\gamma}}.$$

6.2.4 n-order trinomial

Let us now consider a similar case to the previous one but with a more general form of the function $f(R)$:

$$f(R) = R + \alpha \frac{R^2}{M^2} + \beta \frac{R^n}{M^{2n-2}}.$$

This model is a power-law extension of the Starobinsky model, see [88]. In the same way as before, the de Sitter solution is given by:

$$R_0 = M^2 \left(\frac{1}{\beta(n-2)} \right)^{1/(n-1)},$$

as found in the literature [89]. Therefore, it exists if $\beta(n-2) > 0$. Correspondingly, the stability condition becomes:

$$n_F(R_0) = \frac{1 + \frac{M^2 n(n-1)}{2R_0\alpha(n-2)}}{1 + \frac{M^2(n-1)}{2R_0\alpha(n-2)}} \equiv \frac{1+n\nu}{1+\nu} \quad \text{where} \quad \nu = \frac{M^2(n-1)}{2R_0\alpha(n-2)}.$$

In the case $n > 1$, the stability condition is respected if $-1/n < \nu < 0$ and $\nu < -1$. While the case $n < 2$ requires $\nu > 0$ to have a stable solution. We find that:

$$\epsilon_2^{(1,2)} = -\frac{1}{2}\left(3 \pm \sqrt{25 - \frac{16(1+\nu)}{1+n\nu}}\right),$$
$$\Phi^{(1,2)} = \mp\sqrt{25 - \frac{16(1+\nu)}{1+n\nu}} \quad \text{and} \quad n_s - 1^{(1,2)} = 3 \pm \sqrt{25 - \frac{16(1+\nu)}{1+n\nu}}.$$

Conclusion

Primordial black holes may be very promising candidates for explaining several astrophysical and cosmological observations. Since PBHs behave as cold and collision-less matter, they could form the entire dark matter content in the universe. In addition, their primordial origin could have seeded the formation of supermassive BHs in the centre of galaxies [45]. The current and future gravitational wave detectors have increased the hope of detecting their existence, leading to a regain of interest since their introduction in the 70s [90].

In this thesis, we have investigated a possible mechanism for generating the amplification of inflationary perturbations leading to the formation of PBHs. The latest observations of the LSS and the CMB with PLANCK have so far confirmed the predictions of the SR inflation scenario at large scales. During SR inflation, the perturbations are frozen on the super-horizon regime with a slightly red-tilted power spectrum. By introducing a de Sitter attractor in the inflaton potential, the inflationary dynamics became completely different at small scales. In particular, the amplification of perturbations is possible during inflationary phases very similar to USR and CR inflation because of the large variation in the dynamical quantities. A negative value of the parameter Φ ensures the existence of a growing solution of the Mukhanov-Sasaki equation, see Eq. (110). On the other hand, in absence of such a growing solution, a blue-tilted spectral index could still produce amplification, see Eq. (114).

During CR or USR inflationary dynamics, when the inflaton field approaches the de Sitter attractor, the odd SR parameters go to zero while the even ones go to a constant different from zero. In such scenarios, the conditions for the amplification could be obtained. By expressing the SR parameters in terms of the Hubble parameter, one can deduce the conditions on the form of the Taylor expansion of the Hubble parameter necessary for the amplification. With the form of the resulting Hubble parameter, the inflaton potential was constrained to generate the amplification of the perturbations. We have then explicitly verified the existence of the growing solution or of the blue-tilted power spectrum.

We have applied this statement to the inflationary dynamics reconstructed with the superpotential method. This method is a technique allowing the reconstruction of the potential starting from some ansatz. The dynamical equations contain three functions (H, U, G), from which the potential can be reconstructed, see Eq. (125). The function H (or G) can be obtained analytically by integration, see Eq. (123) or Eq. (124), once U and G (or H) are given. The functions which must be integrated can be defined in such a way that exact integration can be performed. Such a technique has been found to be very useful, compared to other reconstruction methods. It leads to quite general predictions for the shape of the inflaton potential needed for the amplification close to the attractor. Moreover, it is applicable to a wide class of models.

The case of inflation in the context of General Relativity has first been investigated. The simple relation relating the functions H and G, see Eq. (138), allowed us to reconstruct the dynamics in an easy and straightforward way. The formation of PBHs is possible provided that one of the two conditions in Eqs. (156) or (158) is satisfied. Exploiting the Jordan-Einstein frame transformation, the analysis has been extended to the

case of a non-minimally coupled inflaton. Indeed, using the mapping between these two frames, we are still able to use the relation (138) in the EF to find the condition in the JF. In the case of IG, the conditions in Eqs. (196) or (198) are found. The general Jordan frame case, of the form $U = \frac{\xi\sigma^2}{2} + J$, has then been investigated. The conditions on the generation of amplification are given in Eqs. (212) or (214). Studying the particular case $\xi = -1/6$ for the conformal coupling, we obtained the conditions (221) or (223). Finally, $f(R)$ gravity theories were studied in detail. In these theories, the reconstruction method is slightly different and more complicated due to the new function $f(R)$. The reconstruction can lead to models with exact solutions only for some specific reversible $f(R)$ gravity models. The requirement of amplification gave the conditions in Eqs. (249) and (251). To broaden the analysis, specific models have been studied verifying the existence of the de Sitter attractor directly.

The monotonic evolution of the inflaton field towards the de Sitter attractor may not be stable. In Section 4.2, we have found the stability conditions for the two possible solutions of the homogeneous perturbation of the inflaton field. We applied a similar analysis for the case of Induced Gravity and general Jordan frames. In $f(R)$ gravity theories, we checked the stability for the models obtained with the specific requirement of the de Sitter attractor.

Reconstructing a realistic inflationary model with a phase leading to an amplification of the power spectrum of the curvature perturbations is not straightforward. Calculating the exact features of the inflaton potential needed for the enhancement is a useful tool for the inflationary model building.

Acknowledgements

I would like to warmly thank my supervisor, Alessandro Tronconi, for his support and guidance in the field of cosmology. I am deeply grateful to him for the time and effort he devoted to supervising me throughout the year and for introducing me to the world of academic research.

I would also like to express my sincere thanks to Jean-René Cudell who agreed to be my local co-supervisor and to evaluate this thesis. I am grateful to Maxime Fays, Guillaume Mahler and Peter Schlagheck for agreeing to read and assess my work. My thanks go to the University of Bologna for hosting me during this research, and to the University of Liège and the Master in Space Science programme for their openness to such a project.

This work marks the end of a long journey as a Master's student. I would like to particularly thank Dominique Lambert, Silvia Pascoli, Prasanta Char and Jean-René Cudell for their precious help and advice during times of doubt and concern.

A Annex: Mukhanov-Sasaki equation

A.1 General Relativity

In GR, the variable z is defined by the scale factor a and the first slow-roll parameter ϵ_1 as:

$$z \propto a\sqrt{\epsilon_1}.$$

Using the definition of the SR parameters defined in conformal time, see Eqs. (37), we have:

$$\begin{aligned}\epsilon_1' &= \mathcal{H}\epsilon_1\epsilon_2,\\ \epsilon_2' &= \mathcal{H}\epsilon_2\epsilon_3.\end{aligned}$$

Using these definitions, we can express the first derivatives of z w.r.t. conformal time:

$$z' \propto a'\sqrt{\epsilon_1} + \frac{a}{2}\frac{\epsilon_1'}{\sqrt{\epsilon_1}} = a'\sqrt{\epsilon_1} + \frac{a'}{2}\frac{\epsilon_1\epsilon_2}{\sqrt{\epsilon_1}}.$$

Thus, we find:

$$\frac{z'}{z} = \mathcal{H}\left[1 + \frac{1}{2}\epsilon_2\right], \tag{263}$$

$$\begin{aligned}\frac{z''}{z} &= \frac{a''}{a} + \mathcal{H}^2\frac{\epsilon_2}{2} + \frac{a''}{a}\frac{\epsilon_2}{2} + \mathcal{H}^2\frac{\epsilon_2^2}{4} + \mathcal{H}^2\frac{\epsilon_2\epsilon_3}{2},\\ &= \mathcal{H}^2\left[2 - \epsilon_1 + \epsilon_2\left(\frac{3}{2} + \frac{\epsilon_2}{4} - \frac{\epsilon_1}{2} + \frac{\epsilon_3}{2}\right)\right].\end{aligned} \tag{264}$$

where in the last equality, we used the definition (36) to express the second derivative of the scale factor w.r.t. conformal time:

$$\frac{a''}{a} = \mathcal{H}^2 + \mathcal{H}' = (2 - \epsilon_1)\,\mathcal{H}^2. \tag{265}$$

A.2 Induced Gravity

In IG, the variable z is defined by the scale factor, the scalar field σ, and the Hubble parameter as:

$$z = \frac{a\dot{\sigma}}{H}\frac{\sqrt{1+6\gamma}}{1+\delta_1} = a\sigma\delta_1\frac{\sqrt{1+6\gamma}}{1+\delta_1}.$$

Using the scalar field functions in Eqs. (38) and (39), the first derivatives of z w.r.t. conformal time becomes:

$$z' = a'\sigma\delta_1\frac{\sqrt{1+6\gamma}}{1+\delta_1}\left(1 + \delta_1 + \delta_2 - \frac{\delta_1\delta_2}{1+\delta_1}\right).$$

Thus, we find:

$$\frac{z'}{z} = \mathcal{H}\left[1+\delta_1+\delta_2-\frac{\delta_1\delta_2}{1+\delta_1}\right], \tag{266}$$

$$\begin{aligned}\frac{z''}{z} =& \frac{a''}{a}\left(1+\delta_1+\delta_2-\frac{\delta_1\delta_2}{1+\delta_1}\right)+\mathcal{H}^2\left(\delta_1+\delta_2-\frac{\delta_1\delta_2}{1+\delta_1}\right)+\mathcal{H}^2\left(\delta_1^2+2\delta_1\delta_2-\frac{\delta_1^2\delta_2}{1+\delta_1}\right)\\ &+\mathcal{H}^2\left(\delta_1\delta_2+\delta_2^2-\frac{\delta_1\delta_2^2}{1+\delta_1}\right)-\mathcal{H}^2\left(\frac{\delta_1^2\delta_2}{1+\delta_1}+2\frac{\delta_1\delta_2^2}{1+\delta_1}+\frac{\delta_1\delta_2\delta_3}{1+\delta_1}-\frac{\delta_1^2\delta_2^2}{(1+\delta_1)^2}\right)\\ =&\mathcal{H}^2\left[\delta_1^2+\delta_2^2+(3-\epsilon_1)(\delta_1+\delta_2+1)+\delta_2\delta_3+\frac{\delta_1\delta_2}{1+\delta_1}\left(\epsilon_1+\delta_1-3\delta_2-\delta_3+\frac{2\delta_1\delta_2}{1+\delta_1}\right)-1\right].\end{aligned} \tag{267}$$

where in the last equality, we used Eq. (265).

A.3 General Jordan frame

First method

In JF, we can define the function z as follows [80]:

$$z = a\phi\delta_1\frac{\sqrt{1+\frac{3\dot{U}^2}{\dot{\phi}^2U}}}{1+\frac{\dot{U}}{2HU}} = a\phi\delta_1\frac{\sqrt{U^2+3\xi^2\sigma^2U}}{U+\frac{\xi\sigma^2}{2}\delta_1} = a\phi\delta_1\frac{\sqrt{N_1}}{D_1}.$$

Using the above definition, we can derive the first derivative of z w.r.t. conformal time.

$$z' = a'\phi\delta_1\frac{\sqrt{N_1}}{D_1}(1+\delta_1+\delta_2)-\frac{1}{2}a\phi\delta_1\frac{N_1'}{\sqrt{N_1}D_1}-a\phi\delta_1\frac{\sqrt{N_1}D_1'}{D_1^2}$$

It allows us to find the quantity of interest in the same way as for the IG case:

$$\begin{aligned}\frac{z'}{z} &= \mathcal{H}\left[1+\delta_1+\delta_2-\delta_1\left(\frac{1}{2}\frac{N_2}{N_1}+\frac{D_2}{D_1}\right)\right],\\ \frac{z''}{z} &= \mathcal{H}^2\left[\delta_1^2+\delta_2^2+(3-\epsilon_1)(\delta_1+\delta_2+1)+3\delta_1\delta_2+\delta_2\delta_3-1\right.\\ &\quad-\delta_1\left(\frac{3}{2}\frac{N_2}{N_1}+3\frac{D_2}{D_1}\right)-\delta_1^2\left(\frac{N_2}{N_1}+2\frac{D_2}{D_1}-\frac{3}{4}\frac{N_2^2}{N_1^2}+\frac{D_2^2}{D_1^2}+\frac{1}{2}\frac{N_3}{N_1}+\frac{D_3}{D_1}\right)\\ &\quad\left.-\delta_1\delta_2\left(\frac{3}{2}\frac{N_2}{N_1}+3\frac{D_2}{D_1}\right)+\epsilon_1\delta_1\left(\frac{1}{2}\frac{N_2}{N_1}+\frac{D_2}{D_1}\right)\right].\end{aligned} \tag{268}$$

where we have defined:

$$\begin{aligned}N_1 &= \frac{\xi^2\sigma^4}{4}(1+6\xi)+\xi\sigma^2J(1+3\xi)+J^2,\\ N_2 &= \xi^2\sigma^4(1+6\xi)+2\xi\sigma^2J(1+3\xi),\\ N_3 &= 4\xi^2\sigma^4(1+6\xi)+4\xi\sigma^2J(1+3\xi),\end{aligned}$$

$$\begin{aligned}D_1 &= \frac{\xi\sigma^2}{2}(1+\delta_1)+J,\\ D_2 &= \xi\sigma^2(1+\delta_1)+\frac{\xi\sigma^2}{2}\delta_2,\\ D_3 &= 2\xi\sigma^2(1+\delta_1)+2\xi\sigma^2\delta_2+\frac{\xi\sigma^2}{2}\frac{\delta_2\delta_3}{\delta_1}.\end{aligned}$$

They have been defined on the basis of the conformal derivatives of the numerator N_1

and the denominator D_1, with the goal of extracting the SR parameters:

$$\frac{1}{\mathcal{H}^2}\frac{N_1'}{N_1} = \frac{\delta_1}{\mathcal{H}}\frac{N_2}{N_1}, \qquad \frac{1}{\mathcal{H}^2}\frac{D_1'}{D_1} = \frac{\delta_1}{\mathcal{H}}\frac{D_2}{D_1},$$
$$\frac{1}{\mathcal{H}^2}\frac{N_1''}{N_1} = -\epsilon_1\delta_1\frac{N_2}{N_1} + \delta_1\delta_2\frac{N_2}{N_1} - \delta_1^2\frac{N_2^2}{N^2} - \delta_1^2\frac{N_3}{N_1}, \quad \frac{1}{\mathcal{H}^2}\frac{D_1''}{D_1} = -\epsilon_1\delta_1\frac{D_2}{D_1} + \delta_1\delta_2\frac{D_2}{D_1} - \delta_1^2\frac{D_2^2}{N^2} - \delta_1^2\frac{D_3}{D_1}.$$

and where we defined $N_2' = \mathcal{H}\delta_1 N_3$ and $D_2' = \mathcal{H}\delta_1 D_3$.

Second method

Let us now verify this calculation with another method. Let us restart by redefining the function z in a slightly different way:

$$z \equiv \frac{a\dot{\phi}}{H}\frac{\sqrt{1+\frac{3\dot{U}^2}{\dot{\phi}^2 U}}}{\left(1+\frac{\dot{U}}{2HU}\right)} = \frac{a\dot{\phi}}{H\sqrt{F}}\frac{\sqrt{E}}{(1+\gamma_3)} \tag{269}$$

where we have defined $E \equiv 2U\left(1+\frac{3\dot{U}^2}{\dot{\phi}^2 U}\right)$ and a new hierarchy of parameters γ_i:

$$\gamma_1 \equiv -\frac{\dot{H}}{H^2}, \quad \gamma_2 \equiv \frac{\ddot{\phi}}{H\dot{\phi}}, \quad \gamma_3 \equiv \frac{\dot{U}}{2HU}, \quad \gamma_4 \equiv \frac{\dot{E}}{2HE}. \tag{270}$$

Using these definitions, we can find the first derivative of z w.r.t. conformal time:

$$z' = a\dot{z} = a\left(\frac{\dot{a}\dot{\phi}}{H\sqrt{F}}\frac{\sqrt{E}}{(1+\gamma_3)} + \frac{a\ddot{\phi}}{H\sqrt{F}}\frac{\sqrt{E}}{(1+\gamma_3)} - \frac{a\dot{\phi}\dot{H}}{H^2\sqrt{F}}\frac{\sqrt{E}}{(1+\gamma_3)} - \frac{1}{2}\frac{a\dot{\phi}\dot{F}}{HF^{3/2}}\frac{\sqrt{E}}{(1+\gamma_3)} + \frac{1}{2}\frac{a\dot{\phi}}{H\sqrt{F}}\frac{\dot{E}}{\sqrt{E}(1+\gamma_3)}\right).$$

The quantities of interest in the Mukhanov-Sasaki equation are then expressed as follows:

$$\frac{z'}{z} = \frac{a\dot{z}}{z} = \mathcal{H}\left[1+\gamma_1+\gamma_2-\gamma_3+\gamma_4\right], \tag{271}$$
$$\frac{z''}{z} = \frac{a\dot{a}\dot{z}+a^2\ddot{z}}{z} = \mathcal{H}^2\left[(1+\gamma_1+\gamma_2-\gamma_3+\gamma_4)(2+\gamma_2-\gamma_3+\gamma_4)\right], \tag{272}$$

where we are considering situation where the parameters γ_i are constant, and therefore the following relations have been used:

$$\begin{aligned}
\dot{H} = \frac{\ddot{a}}{a} - \frac{\dot{a}^2}{a^2} \;&\Rightarrow\; \frac{\ddot{a}}{aH^2} = 1-\gamma_1, \\
H\dot{\gamma}_1 = -\frac{\ddot{H}}{H} + 2\frac{\dot{H}^2}{H^2} = 0 \;&\Rightarrow\; \frac{\ddot{H}}{H} = 2\frac{\dot{H}^2}{H^2}, \\
H\dot{\gamma}_2 = \frac{\dddot{\phi}}{\dot{\phi}} - \frac{\dot{H}\ddot{\phi}}{H\dot{\phi}} - \frac{\ddot{\phi}^2}{\dot{\phi}^2} = 0 \;&\Rightarrow\; \frac{\dddot{\phi}}{\dot{\phi}} = -\gamma_1\gamma_2 H^2 + \gamma_2^2, \\
H\dot{\gamma}_3 = \frac{1}{2}\frac{\ddot{F}}{F} - \frac{1}{2}\frac{\dot{H}\dot{F}}{HF} - \frac{1}{2}\frac{\dot{F}^2}{F^2} = 0 \;&\Rightarrow\; \frac{1}{2}\frac{\ddot{F}}{F} = -\gamma_1\gamma_3 H^2 + 2\gamma_3^2, \\
H\dot{\gamma}_4 = \frac{1}{2}\frac{\ddot{E}}{E} - \frac{1}{2}\frac{\dot{H}\dot{E}}{HE} - \frac{1}{2}\frac{\dot{E}^2}{E^2} = 0 \;&\Rightarrow\; \frac{1}{2}\frac{\ddot{E}}{E} = -\gamma_1\gamma_4 H^2 + 2\gamma_4^2.
\end{aligned} \tag{273}$$

Let us now assume $|\gamma_i| \ll 1$ for $(i = 1, 2, 3, 4)$, we can then find the spectral index of curvature perturbations at leading order in γ_i:

$$n_s - 1 \approx 3 - \sqrt{1 + 4\frac{f_{MS}}{(1-\epsilon_1)^2}} \approx 3 - \sqrt{1 + 4(2 + 2\gamma_1 + 3\gamma_2 - 3\gamma_3 + 3\gamma_4)(1 + 2\epsilon_1)}$$
$$\approx 3 - 3\left(1 + \frac{2}{9}(6\gamma_1 + 3\gamma_2 - 3\gamma_3 + 3\gamma_4)\right) \simeq -4\gamma_1 - 2\gamma_2 + 2\gamma_3 - 2\gamma_4, \qquad (274)$$

where we used the Taylor expansion to eliminate the two exponents.

In particular, for the non-minimal coupling case, we can relate the γ_i parameters, defined in Eqs. (270), to the SR hierarchies ϵ_i and δ_i. Indeed, using the definitions in Eqs. (200) and (133), we can write:

$$\gamma_1 = \epsilon_1, \quad \gamma_2 = \delta_1 + \delta_2 - \epsilon_1, \quad \gamma_3 = \frac{\delta_1}{1+\rho}, \quad \gamma_4 = \frac{(1+6\xi)\delta_1}{\rho + 1 + 6\xi}. \qquad (275)$$

where we have defined $\rho \equiv \frac{\mathrm{M_P^2}}{\xi\phi^2}$. The approximated scalar spectral index of the scalar perturbations, in Eq. (274), with these expressions becomes:

$$n_s - 1 = -2\left(\epsilon_1 + \delta_1 + \delta_2 - \frac{\delta_1}{1+\rho} + \frac{(1+6\xi)\delta_1}{\rho + 1 + 6\xi}\right), \qquad (276)$$

and we recover the result in [80].

A.4 $f(R)$ gravity

First method

In $f(R)$ gravity theories, we introduce the quantity $E = 3\dot{F}^2\mathrm{M_P^2}/2$ and define the function z as follows:

$$z = a\frac{\sqrt{E}}{\sqrt{F}H\,(1+\gamma_3)} = a\sqrt{\frac{3\mathrm{M_P^2}}{2}}\frac{\dot{F}}{\sqrt{F}H\,(1+\gamma_3)}, \qquad (277)$$

where $\gamma_3 = \frac{\dot{F}}{2HF}$. Remembering that the field kinetic term $\dot{\phi}^2$ is not present in the action (225), we conclude that the parameter γ_2, defined in Eq. (270), vanishes. We can now also write $\gamma_4 = \frac{\dot{E}}{2HE} = \frac{\ddot{F}}{H\dot{F}}$.

Using these definitions, we can find the first derivative of z w.r.t. conformal time:

$$z' = a\dot{z} = \frac{a}{(1+\epsilon_3)}\sqrt{\frac{3\mathrm{M_P^2}}{2}}\left(\dot{a}\frac{\dot{F}}{\sqrt{F}H} + a\frac{\ddot{F}}{\sqrt{F}H} - \frac{1}{2}a\frac{\dot{F}^2}{F^{3/2}H} - a\frac{\dot{F}\dot{H}}{\sqrt{F}H^2}\right).$$

We then find:

$$\frac{z'}{z} = \frac{a\dot{z}}{z} = \mathcal{H}\left[1 + \gamma_1 - \gamma_3 + \gamma_4\right],$$
$$\frac{z''}{z} = \frac{a\dot{a}\dot{z} + a^2\ddot{z}}{z} = \mathcal{H}^2\left[2 + 2\gamma_1 - 3\gamma_3 + 3\gamma_4 - 2\gamma_1\gamma_3 + \gamma_1\gamma_4 - 3\gamma_3\gamma_4 + 3\gamma_3^2 + \gamma_4^2\right], \qquad (278)$$

where we used that $\frac{\ddot{F}}{F} = 2H^2\gamma_3\gamma_4$. Substituting Eq. (273) in Eq. (278), we find the result in Eq. (272) with $\gamma_2 = 0$. We could have deduced these results by comparing the definition of the function z in the first equality of Eq. (277) with Eq. (269). They are the same when $\gamma_2 = 0$.

Let us now assume that we have $|\gamma_i| \ll 1$ for $(i = 1, 3, 4)$. We can then find the spectral index of curvature perturbations to leading order in the parameters γ_i:

$$n_s - 1 \approx 3 - \sqrt{1 + 4\frac{f_{MS}}{(1-\epsilon_1)^2}} \approx 3 - 3\left(1 + \frac{2}{9}(2\gamma_1 - 3\gamma_3 + 3\gamma_4)(1 + 2\epsilon_1)\right) \simeq -4\gamma_1 + 2\gamma_3 - 2\gamma_4, \tag{279}$$

where we used the Taylor expansion to eliminate the two exponents. This approximated expression is the same as in [86].

We can then use the definition of the Ricci scalar, see Eq. (3), and express the first and second derivatives w.r.t. cosmic time:

$$R = 6\left(\frac{\ddot{a}}{a} + \frac{\dot{a}^2}{a^2}\right) = 6(2 - \epsilon_1)H^2 \tag{280}$$

$$\frac{dR}{dt} = -2\epsilon_1 H R, \tag{281}$$

$$\frac{d^2R}{dt^2} = +6\epsilon_1^2 H^2 R, \tag{282}$$

where we have restricted the framework to a particular set of solutions for which $\epsilon_1 = 0$.

We can introduce the first and second derivatives of F w.r.t. cosmic time:

$$\frac{dF}{dt} = \frac{dF}{dR}\frac{dR}{dt} = -2\epsilon_1 H \frac{dF}{dR} R, \tag{283}$$

$$\frac{d^2F}{dt^2} = \frac{d^2F}{dR^2}\left(\frac{dR}{dt}\right)^2 + \frac{dF}{dR}\frac{d^2R}{dt^2} = 4\epsilon_1^2 H^2 \frac{d^2F}{dR^2} R^2 + 6\epsilon_1^2 H^2 \frac{dF}{dR} R, \tag{284}$$

where in the last equality, we used the result for the Ricci scalar in Eqs. (281) and (282). We can express the first SR parameter in terms of the derivatives introduced above, in Eqs. (283) and (284):

$$\gamma_1 = \epsilon_1 = -\frac{\dot{H}}{H^2} = \frac{\ddot{F} - H\dot{F}}{2FH^2} = 2\epsilon_1^2 \frac{d^2F}{dR^2}\frac{R^2}{F} + 3\epsilon_1^2 \frac{dF}{dR}\frac{R}{F} + \epsilon_1 \frac{dF}{dR}\frac{R}{F},$$

where in the second equality, we used the field equation to express $\dot{H}$, see Eq. (254). We can then extract the expression of the first SR parameter and the parameters present in the MS equation can be expressed in the same way:

$$\gamma_1 = \frac{1 - \frac{dF}{dR}\frac{R}{F}}{2\frac{d^2F}{dR^2}\frac{R^2}{F} + 3\frac{dF}{dR}\frac{R}{F}}, \tag{285}$$

$$\gamma_3 = \frac{1}{2}\frac{\dot{F}}{HF} = -\frac{dF}{dR}\frac{R}{F}\epsilon_1, \tag{286}$$

$$\gamma_4 = \frac{\ddot{F}}{H\dot{F}} = \frac{4\epsilon_1^2 H^2 \frac{d^2F}{dR^2} R^2 + 6\epsilon_1^2 H^2 \frac{dF}{dR} R}{-2\epsilon_1 H^2 \frac{dF}{dR} R} = \left(-2R\frac{d^2F}{dR^2}\Big/\frac{dF}{dR} - 3\right)\epsilon_1. \tag{287}$$

Let us now assume an ansatz on the form of the function $f(R) = \alpha R^n$ $(n > 0)$. In this case, we have:

$$\begin{aligned} F =& \frac{df}{dR} = n\alpha R^{n-1}, \\ \frac{dF}{dR} =& (n-1)\frac{F}{R}, \\ \frac{d^2F}{dR^2} =& (n-1)(n-2)\frac{F}{R^2}. \end{aligned}$$

Using these results in Eqs. (285), (286) and (287), we find the result in [86], i.e. constant parameters γ_i $(i = 1, 3, 4)$ expressed thought n:

$$\begin{aligned} \gamma_1 &= \frac{2-n}{(n-1)(2n-1)}, \\ \gamma_3 &= -(n-1)\epsilon_1 = \frac{n-2}{2n-1}, \\ \gamma_4 &= -(2n-1)\epsilon_1 = \frac{n-2}{n-1}. \end{aligned}$$

Instead of using the approximate expression in Eq. (279), we can use the exact expression of the spectral index, see Eq. (114). We find the same result as in the reference [86]:

$$n_s - 1 = -\frac{2(n-2)^2}{2n^2 - 2n - 1}.$$

In figure 28, the plot of this spectral index and the one of the parameter Φ is represented in a range of n leading to inflation. Therefore, there is no amplification possible when considering the parameters γ_i constant.

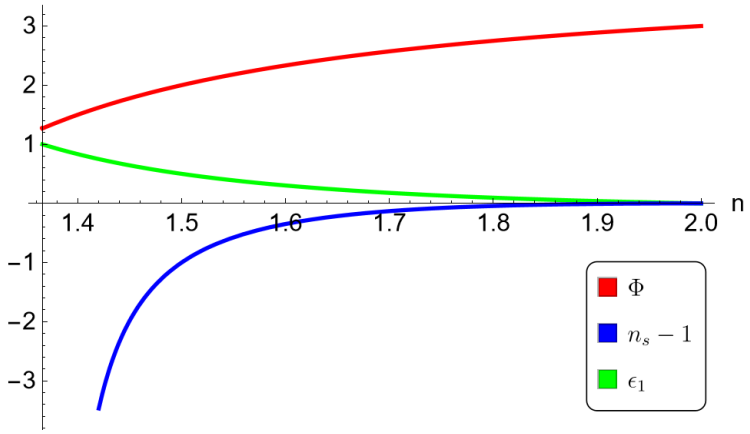

Figure 28: The curve in green represents the first SR parameter, ϵ_1 as a function of the parameter n. The plot range for n have been constrained to allow inflation to occur: $0 < \epsilon_1 < 1$. In red, the parameter Φ is represented. It is positive, so we do not have a growing solution. In blue, is the spectral index $n_s - 1$ which is red-tilted. So for the particular case studied here and with constant γ_i parameters, it is not possible to have amplification.

Second method

Let us develop the function z in Eq. (277) in terms of the SR parameters:

$$z = a\sqrt{\frac{3\mathrm{M_P^2}}{2}}\frac{\dot{F}}{\sqrt{F}\left(H+\dot{F}/2F\right)}, \tag{288}$$

The derivative of $F(R)$ w.r.t. cosmic time can be differentiated as follows:

$$\dot{F} = \dot{f_{,R}} = f_{,RR}\dot{R}.$$

Differentiating the Ricci scalar in Eq. (280) w.r.t. cosmic time and assuming non-constant SR parameters, we find:

$$\dot{R} = -6H^3\epsilon_1\epsilon_2 - 12H^3(2-\epsilon_1)\epsilon_1,$$

where we used the definition $\dot{H} = -H^2\epsilon_1$ and $\dot{\epsilon_1} = H\epsilon_1\epsilon_2$. Substituting the following results in Eq. (288), we then find:

$$z = 3\sqrt{6}\mathrm{M_P}aH^2\frac{\epsilon_1(2\epsilon_1-\epsilon_2-4)\sqrt{f_{,R}}f_{,RR}}{f_{,R}+3H^2\epsilon_1(2\epsilon_1-\epsilon_2-4)f_{,RR}}.$$

The quantities needed to verify whether the amplification is present have been found using Mathematica by making the usual substitutions:

$$\dot{R}\to HR\delta_1, \quad \dot{\delta_1}\to H\delta_1\delta_2, \quad \dot{\delta_2}\to H\delta_2\delta_3, \quad \dot{\delta_3}\to H\delta_3\delta_4,$$
$$\dot{H}\to -H^2\epsilon_1, \quad \dot{\epsilon_1}\to H\epsilon_1\epsilon_2, \quad \dot{\epsilon_2}\to H\epsilon_2\epsilon_3, \quad \dot{\epsilon_3}\to H\epsilon_3\epsilon_4.$$

It gives the results:

$$\frac{z'}{z} = \frac{a\dot{z}}{z} = aH\times\frac{\begin{array}{c}6f_{,RRR}f_{,R}^2H^2\epsilon_1(-2\epsilon_1+\epsilon_2+4)^2 - 9f_{,RR}^3H^4\epsilon_1^2(-2\epsilon_1+\epsilon_2+4)^3\\ -f_{,RR}f_{,R}^2\left(4\epsilon_1^2-2\epsilon_1(3\epsilon_2+5)+\epsilon_2(\epsilon_2+\epsilon_3+5)+4\right)\end{array}}{f_{,RR}f_{,R}(2\epsilon_1-\epsilon_2-4)\left(3f_{,RR}H^2\epsilon_1(2\epsilon_1-\epsilon_2-4)+f_{,R}\right)} \tag{289}$$

$$\begin{aligned}\frac{z''}{z} = \frac{a\dot{z}'}{z} &= (aH)^2\times\\ &-6f_{,R}^3H^2\epsilon_1(2\epsilon_1-\epsilon_2-4)\Big[6f_{,RRRR}f_{,R}H^2\epsilon_1(-2\epsilon_1+\epsilon_2+4)^2+36f_{,RRR}^2H^4\epsilon_1^2(-2\epsilon_1+\epsilon_2+4)^3\\ &-f_{,RRR}f_{,R}\left(14\epsilon_1^2-\epsilon_1(19\epsilon_2+34)+3\epsilon_2(\epsilon_2+\epsilon_3+5)+12\right)\Big]\\ &+f_{,RR}f_{,R}^3\Big[f_{,R}\Big(-12\epsilon_1^3+\epsilon_1^2(30\epsilon_2+38)-\epsilon_1(\epsilon_2(15\epsilon_2+9\epsilon_3+47)+32)+\epsilon_2\big(3\epsilon_2\epsilon_3\\ &+\epsilon_2(\epsilon_2+7)+\epsilon_3^2+7(\epsilon_3+2)\big)+8\Big)-18H^4\epsilon_1^2(-2\epsilon_1+\epsilon_2+4)^2\Big(6f_{,RRRR}H^2\epsilon_1(-2\epsilon_1+\epsilon_2+4)^2\\ &+f_{,RRR}\left(2\epsilon_1^2-\epsilon_1(5\epsilon_2+4)+\epsilon_2(\epsilon_2+\epsilon_3+4)\right)\Big)\Big]\\ &+9f_{,RR}^3f_{,R}H^4\epsilon_1^2(-2\epsilon_1+\epsilon_2+4)^2\Big[18f_{,RRR}H^4\epsilon_1^2(-2\epsilon_1+\epsilon_2+4)^3+f_{,R}\Big(26\epsilon_1^2-\epsilon_1(37\epsilon_2+62)\\ &+6\epsilon_2(\epsilon_2+\epsilon_3)+29\epsilon_2+20\Big)\Big]+3f_{,RR}^2f_{,R}^2H^2\epsilon_1\Big[f_{,R}\Big(8\epsilon_1^4-4\epsilon_1^3(6\epsilon_2+7)\\ &+2\epsilon_1^2(\epsilon_2(14\epsilon_2-\epsilon_3+26)+6)+\epsilon_1\big(32-\epsilon_2\left(7\epsilon_2^2+\epsilon_2(9\epsilon_3+31)-2\epsilon_3(\epsilon_3+6)+4\right)\big)\\ &+\epsilon_2\left(\epsilon_2^2-16\right)\epsilon_3+(\epsilon_2+4)^2\left(\epsilon_2^2-1\right)+(\epsilon_2-4)\epsilon_2\epsilon_3^2\Big)-108f_{,RRR}H^4\epsilon_1^2(-2\epsilon_1+\epsilon_2+4)^4\Big]\\ &-81f_{,RR}^5H^8\epsilon_1^4(-2\epsilon_1+\epsilon_2+4)^5-27f_{,RR}^4f_{,R}H^6\epsilon_1^3(-2\epsilon_1+\epsilon_2+4)^3\Big[6\epsilon_1^2-\epsilon_1(7\epsilon_2+6)\\ &+\epsilon_2(\epsilon_2+\epsilon_3+1)-12\Big]+f_{,RR}f_{,R}^3\epsilon_2\epsilon_3\epsilon_4\left(3f_{,RR}H^2\epsilon_1(2\epsilon_1-\epsilon_2-4)+f_{,R}\right)\end{aligned}$$
$$\overline{f_{,RR}f_{,R}^2(4-2\epsilon_1+\epsilon_2)\left(3f_{,RR}H^2\epsilon_1(2\epsilon_1-\epsilon_2-4)+f_{,R}\right)^2} \tag{290}$$

References

[1] R. L. Workman *et al.*, "Review of Particle Physics," *PTEP*, vol. 2022, p. 083C01, 2022. DOI: 10.1093/ptep/ptac097 (cit. on p. 1).

[2] B. D. Fields, K. A. Olive, T.-H. Yeh, and C. Young, "Big-Bang Nucleosynthesis after Planck," *JCAP*, vol. 03, p. 010, 2020, [Erratum: JCAP 11, E02 (2020)]. DOI: 10.1088/1475-7516/2020/03/010. arXiv: 1912.01132 [astro-ph.CO] (cit. on pp. 1, 6).

[3] G. Franciolini, "Primordial black holes: From theory to gravitational wave observations," Ph.D. dissertation, Geneva U., Dept. Theor. Phys., 2021. DOI: 10.13097/archive-ouverte/unige:156136. arXiv: 2110.06815 [astro-ph.CO] (cit. on pp. 1, 33).

[4] G. Bertone, D. Hooper, and J. Silk, "Particle dark matter: Evidence, candidates and constraints," *Phys. Rept.*, vol. 405, pp. 279–390, 2005. DOI: 10.1016/j.physrep.2004.08.031. arXiv: hep-ph/0404175 (cit. on p. 1).

[5] P. W. Graham and H. Ramani, "Constraints on Dark Matter from Dynamical Heating of Stars in Ultrafaint Dwarfs. Part 1: MACHOs and Primordial Black Holes," Nov. 2023. arXiv: 2311.07654 [hep-ph] (cit. on p. 1).

[6] B. Carr and F. Kuhnel, "Primordial black holes as dark matter candidates," *SciPost Phys. Lect. Notes*, vol. 48, p. 1, 2022. DOI: 10.21468/SciPostPhysLectNotes.48. arXiv: 2110.02821 [astro-ph.CO] (cit. on pp. 1, 33).

[7] E. W. Kolb and M. S. Turner, *The Early Universe*. 1990, vol. 69, ISBN: 978-0-201-62674-2. DOI: 10.1201/9780429492860 (cit. on p. 3).

[8] P. Peter and J.-P. Uzan, *Primordial Cosmology* (Oxford Graduate Texts). Oxford University Press, Feb. 2013, ISBN: 978-0-19-966515-0, 978-0-19-920991-0. DOI: 10.1017/CBO9780511809149 (cit. on pp. 3, 7, 14, 18).

[9] D. Baumann, "Inflation," in *Theoretical Advanced Study Institute in Elementary Particle Physics: Physics of the Large and the Small*, 2011, pp. 523–686. DOI: 10.1142/9789814327183_0010. arXiv: 0907.5424 [hep-th] (cit. on pp. 3, 6, 15).

[10] A. Caravano, "Simulating the inflationary universe: From single-field to the axion-u(1) model," Ph.D. dissertation, Munich U., Munich U., Jul. 2022. DOI: 10.5282/edoc.30905. arXiv: 2209.13616 [astro-ph.CO] (cit. on p. 3).

[11] D. Baumann, *Cosmology*. Cambridge University Press, Jul. 2022, ISBN: 978-1-108-93709-2, 978-1-108-83807-8. DOI: 10.1017/9781108937092 (cit. on pp. 5, 6, 9, 12, 14, 19, 21, 28, 30).

[12] N. Aghanim *et al.*, "Planck 2018 results. VI. Cosmological parameters," *Astron. Astrophys.*, vol. 641, A6, 2020, [Erratum: Astron.Astrophys. 652, C4 (2021)]. DOI: 10.1051/0004-6361/201833910. arXiv: 1807.06209 [astro-ph.CO] (cit. on pp. 6, 7).

[13] P. A. Zyla *et al.*, "Review of Particle Physics," *PTEP*, vol. 2020, no. 8, p. 083C01, 2020. DOI: 10.1093/ptep/ptaa104 (cit. on p. 6).

[14] A. H. Guth, "The Inflationary Universe: A Possible Solution to the Horizon and Flatness Problems," *Phys. Rev. D*, vol. 23, L.-Z. Fang and R. Ruffini, Eds., pp. 347–356, 1981. DOI: 10.1103/PhysRevD.23.347 (cit. on p. 6).

[15] M. Maggiore, *Gravitational Waves. Vol. 2: Astrophysics and Cosmology*. Oxford University Press, Mar. 2018, ISBN: 978-0-19-857089-9. DOI: 10.1093/oso/9780198570899.001.0001 (cit. on pp. 6, 7, 11).

[16] F. G. Pedro, *Quantum Cosmology: From inflation to temperature anisotropies*. 1994 (cit. on p. 6).

[17] V. Mukhanov and S. Winitzki, *Introduction to quantum effects in gravity*. Cambridge University Press, Jun. 2007, ISBN: 978-0-521-86834-1, 978-1-139-78594-5. DOI: 10.1017/CBO9780511809149 (cit. on pp. 6, 27, 31).

[18] V. Mukhanov, *Physical Foundations of Cosmology*. Oxford: Cambridge University Press, 2005, ISBN: 978-0-521-56398-7. DOI: 10.1017/CBO9780511790553 (cit. on pp. 12, 14, 19, 22, 24).

[19] J. Martin, C. Ringeval, and V. Vennin, "Encyclopædia Inflationaris," *Phys. Dark Univ.*, vol. 5-6, pp. 75–235, 2014. DOI: 10.1016/j.dark.2014.01.003. arXiv: 1303.3787 [astro-ph.CO] (cit. on pp. 13, 83).

[20] H. Motohashi, A. A. Starobinsky, and J. Yokoyama, "Inflation with a constant rate of roll," *JCAP*, vol. 09, p. 018, 2015. DOI: 10.1088/1475-7516/2015/09/018. arXiv: 1411.5021 [astro-ph.CO] (cit. on pp. 15, 16, 28).

[21] H. Motohashi and A. A. Starobinsky, "Constant-roll inflation: confrontation with recent observational data," *EPL*, vol. 117, no. 3, p. 39 001, 2017. DOI: 10.1209/0295-5075/117/39001. arXiv: 1702.05847 [astro-ph.CO] (cit. on p. 15).

[22] J. Kristiano and J. Yokoyama, "Generating large primordial fluctuations in single-field inflation for PBH formation," May 2024. arXiv: 2405.12149 [astro-ph.CO] (cit. on pp. 15, 43, 45).

[23] H. Motohashi, S. Mukohyama, and M. Oliosi, "Constant Roll and Primordial Black Holes," *JCAP*, vol. 03, p. 002, 2020. DOI: 10.1088/1475-7516/2020/03/002. arXiv: 1910.13235 [gr-qc] (cit. on pp. 16, 45, 47, 55).

[24] C. T. Byrnes, P. S. Cole, and S. P. Patil, "Steepest growth of the power spectrum and primordial black holes," *JCAP*, vol. 06, p. 028, 2019. DOI: 10.1088/1475-7516/2019/06/028. arXiv: 1811.11158 [astro-ph.CO] (cit. on p. 16).

[25] K. Dimopoulos, "Ultra slow-roll inflation demystified," *Phys. Lett. B*, vol. 775, pp. 262–265, 2017. DOI: 10.1016/j.physletb.2017.10.066. arXiv: 1707.05644 [hep-ph] (cit. on p. 16).

[26] R. K. Sachs and A. M. Wolfe, "Perturbations of a cosmological model and angular variations of the microwave background," *Astrophys. J.*, vol. 147, pp. 73–90, 1967. DOI: 10.1007/s10714-007-0448-9 (cit. on p. 18).

[27] A. Riotto, "Inflation and the theory of cosmological perturbations," *ICTP Lect. Notes Ser.*, vol. 14, G. Dvali, A. Perez-Lorenzana, G. Senjanovic, G. Thompson, and F. Vissani, Eds., pp. 317–413, 2003. arXiv: hep-ph/0210162 (cit. on pp. 19, 21, 23, 25, 26).

[28] O. Özsoy and G. Tasinato, "Inflation and primordial black holes," *Universe*, vol. 9, no. 5, p. 203, 2023. DOI: 10.3390/universe9050203. arXiv: 2301.03600 (cit. on pp. 19, 33, 35, 45).

[29] M. Maggiore, *Gravitational Waves. Vol. 1: Theory and Experiments*. Oxford University Press, 2007, ISBN: 978-0-19-171766-6, 978-0-19-852074-0. DOI: 10.1093/acprof:oso/9780198570745.001.0001 (cit. on p. 22).

[30] J.-c. Hwang, "Cosmological perturbations in generalized gravity theories: Conformal transformation," *Class. Quant. Grav.*, vol. 14, pp. 1981–1991, 1997. DOI: 10.1088/0264-9381/14/7/029. arXiv: gr-qc/9605024 (cit. on p. 26).

[31] J.-c. Hwang, "Unified analysis of cosmological perturbations in generalized gravity," *Phys. Rev. D*, vol. 53, pp. 762–765, 1996. DOI: 10.1103/PhysRevD.53.762. arXiv: gr-qc/9509044 (cit. on p. 26).

[32] A. Cerioni, "Cosmological perturbations in generalized theories of gravity," Ph.D. dissertation, Universita di Bologna, 2011 (cit. on pp. 26, 63).

[33] M. E. Peskin and D. V. Schroeder, *An Introduction to quantum field theory*. Reading, USA: Addison-Wesley, 1995, ISBN: 978-0-201-50397-5 (cit. on p. 27).

[34] E. D. Stewart and D. H. Lyth, "A More accurate analytic calculation of the spectrum of cosmological perturbations produced during inflation," *Phys. Lett. B*, vol. 302, pp. 171–175, 1993. DOI: 10.1016/0370-2693(93)90379-V. arXiv: gr-qc/9302019 (cit. on p. 30).

[35] M. Cicoli, V. A. Diaz, and F. G. Pedro, "Primordial Black Holes from String Inflation," *JCAP*, vol. 06, p. 034, 2018. DOI: 10.1088/1475-7516/2018/06/034. arXiv: 1803.02837 [hep-th] (cit. on p. 30).

[36] Y. Akrami *et al.*, "Planck 2018 results. X. Constraints on inflation," *Astron. Astrophys.*, vol. 641, A10, 2020. DOI: 10.1051/0004-6361/201833887. arXiv: 1807.06211 [astro-ph.CO] (cit. on pp. 32, 34).

[37] A. D. Linde, *Particle physics and inflationary cosmology*. 1990, vol. 5. arXiv: hep-th/0503203 (cit. on p. 32).

[38] G. F. Chapline, "Cosmological effects of primordial black holes," *Nature*, vol. 253, no. 5489, pp. 251–252, 1975. DOI: 10.1038/253251a0 (cit. on p. 33).

[39] G. Ballesteros and M. Taoso, "Primordial black hole dark matter from single field inflation," *Phys. Rev. D*, vol. 97, no. 2, p. 023 501, 2018. DOI: 10.1103/PhysRevD.97.023501. arXiv: 1709.05565 [hep-ph] (cit. on pp. 33, 41, 61).

[40] C. T. Byrnes and P. S. Cole, "Lecture notes on inflation and primordial black holes," Dec. 2021. arXiv: 2112.05716 [astro-ph.CO] (cit. on pp. 33, 36, 43).

[41] J. C. Niemeyer and K. Jedamzik, "Dynamics of primordial black hole formation," *Phys. Rev. D*, vol. 59, p. 124 013, 1999. DOI: 10.1103/PhysRevD.59.124013. arXiv: astro-ph/9901292 (cit. on p. 34).

[42] T. Nakama, J. Silk, and M. Kamionkowski, "Stochastic gravitational waves associated with the formation of primordial black holes," *Phys. Rev. D*, vol. 95, no. 4, p. 043 511, 2017. DOI: 10.1103/PhysRevD.95.043511. arXiv: 1612.06264 [astro-ph.CO] (cit. on p. 34).

[43] A. Escrivà, "PBH Formation from Spherically Symmetric Hydrodynamical Perturbations: A Review," *Universe*, vol. 8, no. 2, p. 66, 2022. DOI: 10.3390/universe8020066. arXiv: 2111.12693 [gr-qc] (cit. on pp. 34, 35).

[44] B. J. Carr, "The primordial black hole mass spectrum," *The Astrophysical Journal*, vol. 201, pp. 1–19, Oct. 1975. DOI: 10.1086/153853 (cit. on p. 35).

[45] B. J. Carr and M. J. Rees, "Can pregalactic objects generate galaxies?" *Monthly Notices of the Royal Astronomical Society*, vol. 206, no. 4, pp. 801–818, Feb. 1984, ISSN: 0035-8711. DOI: 10.1093/mnras/206.4.801. eprint: https://academic.oup.com/mnras/article-pdf/206/4/801/2902772/mnras206-0801.pdf. [Online]. Available: https://doi.org/10.1093/mnras/206.4.801 (cit. on pp. 36, 86).

[46] C. T. Byrnes, M. Hindmarsh, S. Young, and M. R. S. Hawkins, "Primordial black holes with an accurate QCD equation of state," *JCAP*, vol. 08, p. 041, 2018. DOI: 10.1088/1475-7516/2018/08/041. arXiv: 1801.06138 [astro-ph.CO] (cit. on pp. 36, 39).

[47] W. H. Press and P. Schechter, "Formation of galaxies and clusters of galaxies by selfsimilar gravitational condensation," *Astrophys. J.*, vol. 187, pp. 425–438, 1974. DOI: 10.1086/152650 (cit. on p. 37).

[48] I. Musco, "Threshold for primordial black holes: Dependence on the shape of the cosmological perturbations," *Phys. Rev. D*, vol. 100, no. 12, p. 123 524, 2019. DOI: 10.1103/PhysRevD.100.123524. arXiv: 1809.02127 [gr-qc] (cit. on p. 37).

[49] C. T. Byrnes, E. J. Copeland, and A. M. Green, "Primordial black holes as a tool for constraining non-Gaussianity," *Phys. Rev. D*, vol. 86, p. 043 512, 2012. DOI: 10.1103/PhysRevD.86.043512. arXiv: 1206.4188 [astro-ph.CO] (cit. on pp. 38, 39).

[50] B. J. Carr, K. Kohri, Y. Sendouda, and J. Yokoyama, "New cosmological constraints on primordial black holes," *Phys. Rev. D*, vol. 81, p. 104 019, 2010. DOI: 10.1103/PhysRevD.81.104019. arXiv: 0912.5297 [astro-ph.CO] (cit. on pp. 38, 39).

[51] B. Carr, F. Kuhnel, and M. Sandstad, "Primordial Black Holes as Dark Matter," *Phys. Rev. D*, vol. 94, no. 8, p. 083 504, 2016. DOI: 10.1103/PhysRevD.94.083504. arXiv: 1607.06077 [astro-ph.CO] (cit. on p. 39).

[52] B. Carr, K. Kohri, Y. Sendouda, and J. Yokoyama, "Constraints on primordial black holes," *Rept. Prog. Phys.*, vol. 84, no. 11, p. 116 902, 2021. DOI: 10.1088/1361-6633/ac1e31. arXiv: 2002.12778 [astro-ph.CO] (cit. on p. 39).

[53] A. M. Green and B. J. Kavanagh, "Primordial Black Holes as a dark matter candidate," *J. Phys. G*, vol. 48, no. 4, p. 043 001, 2021. DOI: 10.1088/1361-6471/abc534. arXiv: 2007.10722 [astro-ph.CO] (cit. on p. 40).

[54] S. W. Hawking, "Black hole explosions," *Nature*, vol. 248, pp. 30–31, 1974. DOI: 10.1038/248030a0 (cit. on p. 39).

[55] D. N. Page, "Particle Emission Rates from a Black Hole: Massless Particles from an Uncharged, Nonrotating Hole," *Phys. Rev. D*, vol. 13, pp. 198–206, 1976. DOI: 10.1103/PhysRevD.13.198 (cit. on p. 39).

[56] H. Niikura *et al.*, "Microlensing constraints on primordial black holes with Subaru/HSC Andromeda observations," *Nature Astron.*, vol. 3, no. 6, pp. 524–534, 2019. DOI: 10.1038/s41550-019-0723-1. arXiv: 1701.02151 [astro-ph.CO] (cit. on p. 40).

[57] P. S. Cole, "Small-scale probes of the early universe," Ph.D. dissertation, Sussex U., 2021 (cit. on p. 40).

[58] M. Sasaki, T. Suyama, T. Tanaka, and S. Yokoyama, "Primordial black holes - perspectives in gravitational wave astronomy," *Class. Quant. Grav.*, vol. 35, no. 6, p. 063 001, 2018. DOI: 10.1088/1361-6382/aaa7b4. arXiv: 1801.05235 [astro-ph.CO] (cit. on p. 40).

[59] K. Akiyama *et al.*, "First M87 Event Horizon Telescope Results. I. The Shadow of the Supermassive Black Hole," *Astrophys. J. Lett.*, vol. 875, p. L1, 2019. DOI: 10.3847/2041-8213/ab0ec7. arXiv: 1906.11238 [astro-ph.GA] (cit. on p. 41).

[60] K. Akiyama *et al.*, "First Sagittarius A* Event Horizon Telescope Results. I. The Shadow of the Supermassive Black Hole in the Center of the Milky Way," *Astrophys. J. Lett.*, vol. 930, no. 2, p. L12, 2022. DOI: 10.3847/2041-8213/ac6674. arXiv: 2311.08680 [astro-ph.HE] (cit. on p. 41).

[61] Y. Ali-Haïmoud and M. Kamionkowski, "Cosmic microwave background limits on accreting primordial black holes," *Phys. Rev. D*, vol. 95, no. 4, p. 043 534, 2017. DOI: 10.1103/PhysRevD.95.043534. arXiv: 1612.05644 [astro-ph.CO] (cit. on p. 41).

[62] J. Garcia-Bellido and E. Ruiz Morales, "Primordial black holes from single field models of inflation," *Phys. Dark Univ.*, vol. 18, pp. 47–54, 2017. DOI: 10.1016/j.dark.2017.09.007. arXiv: 1702.03901 [astro-ph.CO] (cit. on p. 41).

[63] E. Bagui *et al.*, "Primordial black holes and their gravitational-wave signatures," Oct. 2023. arXiv: 2310.19857 [astro-ph.CO] (cit. on p. 42).

[64] L. Chataignier, A. Y. Kamenshchik, A. Tronconi, and G. Venturi, "Reconstruction methods and the amplification of the inflationary spectrum," *Phys. Rev. D*, vol. 107, no. 8, p. 083 506, 2023. DOI: 10.1103/PhysRevD.107.083506. arXiv: 2301.04477 (cit. on pp. 42–44, 47, 53, 55–57, 66, 67).

[65] A. Y. Kamenshchik, A. Tronconi, T. Vardanyan, and G. Venturi, "Non-Canonical Inflation and Primordial Black Holes Production," *Phys. Lett. B*, vol. 791, pp. 201–205, 2019. DOI: 10.1016/j.physletb.2019.02.036. arXiv: 1812.02547 [gr-qc] (cit. on p. 45).

[66] A. Y. Kamenshchik, A. Tronconi, and G. Venturi, "DBI inflation and warped black holes," *JCAP*, vol. 01, no. 01, p. 051, 2022. DOI: 10.1088/1475-7516/2022/01/051. arXiv: 2110.08112 [gr-qc] (cit. on p. 45).

[67] A. Y. Kamenshchik, E. O. Pozdeeva, A. Tronconi, G. Venturi, and S. Y. Vernov, "Integrable cosmological models with non-minimally coupled scalar fields," *Class. Quant. Grav.*, vol. 31, p. 105 003, 2014. DOI: 10.1088/0264-9381/31/10/105003. arXiv: 1312.3540 (cit. on pp. 47, 49, 62).

[68] A. Y. Kamenshchik, A. Tronconi, and G. Venturi, "Reconstruction of scalar potentials in induced gravity and cosmology," *Phys. Lett. B*, vol. 702, pp. 191–196, 2011. DOI: 10.1016/j.physletb.2011.07.005. arXiv: 1104.2125 (cit. on pp. 47, 48).

[69] A. Y. Kamenshchik, E. O. Pozdeeva, S. Y. Vernov, A. Tronconi, and G. Venturi, "Transformations between Jordan and Einstein frames: Bounces, antigravity, and crossing singularities," *Phys. Rev. D*, vol. 94, no. 6, p. 063 510, 2016. DOI: 10.1103/PhysRevD.94.063510. arXiv: 1602.07192 [gr-qc] (cit. on p. 48).

[70] A. Y. Kamenshchik, A. Tronconi, G. Venturi, and S. Y. Vernov, "Reconstruction of scalar potentials in modified gravity models," *Phys. Rev. D*, vol. 87, no. 6, p. 063 503, 2013. DOI: 10.1103/PhysRevD.87.063503. arXiv: 1211.6272 (cit. on pp. 50, 68).

[71] E. O. Pozdeeva, M. Sami, A. V. Toporensky, and S. Y. Vernov, "Stability analysis of de Sitter solutions in models with the Gauss-Bonnet term," *Phys. Rev. D*, vol. 100, no. 8, p. 083 527, 2019. DOI: 10.1103/PhysRevD.100.083527. arXiv: 1905.05085 [gr-qc] (cit. on p. 59).

[72] M. A. Skugoreva, A. V. Toporensky, and S. Y. Vernov, "Global stability analysis for cosmological models with nonminimally coupled scalar fields," *Phys. Rev. D*, vol. 90, no. 6, p. 064 044, 2014. DOI: 10.1103/PhysRevD.90.064044. arXiv: 1404.6226 [gr-qc] (cit. on p. 59).

[73] A. Cerioni, F. Finelli, A. Tronconi, and G. Venturi, "Inflation and Reheating in Spontaneously Generated Gravity," *Phys. Rev. D*, vol. 81, p. 123 505, 2010. DOI: 10.1103/PhysRevD.81.123505. arXiv: 1005.0935 [gr-qc] (cit. on pp. 60, 63).

[74] M. Postma and M. Volponi, "Equivalence of the Einstein and Jordan frames," *Phys. Rev. D*, vol. 90, no. 10, p. 103 516, 2014. DOI: 10.1103/PhysRevD.90.103516. arXiv: 1407.6874 [astro-ph.CO] (cit. on p. 61).

[75] D. Burns, S. Karamitsos, and A. Pilaftsis, "Frame-Covariant Formulation of Inflation in Scalar-Curvature Theories," *Nucl. Phys. B*, vol. 907, pp. 785–819, 2016. DOI: 10.1016/j.nuclphysb.2016.04.036. arXiv: 1603.03730 [hep-ph] (cit. on p. 61).

[76] V. Faraoni, E. Gunzig, and P. Nardone, "Conformal transformations in classical gravitational theories and in cosmology," *Fund. Cosmic Phys.*, vol. 20, p. 121, 1999. arXiv: gr-qc/9811047 (cit. on p. 61).

[77] K. Bamba, S. Nojiri, S. D. Odintsov, and D. Sáez-Gómez, "Possible antigravity regions in $F(R)$ theory?" *Phys. Lett. B*, vol. 730, pp. 136–140, 2014. DOI: 10.1016/j.physletb.2014.01.045. arXiv: 1401.1328 [hep-th] (cit. on p. 61).

[78] C. Brans and R. H. Dicke, "Mach's principle and a relativistic theory of gravitation," *Phys. Rev.*, vol. 124, J.-P. Hsu and D. Fine, Eds., pp. 925–935, 1961. DOI: 10.1103/PhysRev.124.925 (cit. on p. 63).

[79] A. Cerioni, F. Finelli, A. Tronconi, and G. Venturi, "Inflation and Reheating in Induced Gravity," *Phys. Lett. B*, vol. 681, pp. 383–386, 2009. DOI: 10.1016/j.physletb.2009.10.066. arXiv: 0906.1902 [astro-ph.CO] (cit. on p. 65).

[80] A. Tronconi, "Asymptotically Safe Non-Minimal Inflation," *JCAP*, vol. 07, p. 015, 2017. DOI: 10.1088/1475-7516/2017/07/015. arXiv: 1704.05312 [gr-qc] (cit. on pp. 68, 69, 90, 92).

[81] A. Y. Kamenshchik, E. O. Pozdeeva, A. Tronconi, G. Venturi, and S. Y. Vernov, "Interdependence between integrable cosmological models with minimal and non-minimal coupling," *Class. Quant. Grav.*, vol. 33, no. 1, p. 015 004, 2016. DOI: 10.1088/0264-9381/33/1/015004. arXiv: 1509.00590 [gr-qc] (cit. on p. 71).

[82] A. Nishizawa and H. Motohashi, "Constraint on reheating after $f(R)$ inflation from gravitational waves," *Phys. Rev. D*, vol. 89, no. 6, p. 063 541, 2014. DOI: 10.1103/PhysRevD.89.063541. arXiv: 1401.1023 [astro-ph.CO] (cit. on p. 75).

[83] H. Motohashi and A. A. Starobinsky, "$f(R)$ constant-roll inflation," *Eur. Phys. J. C*, vol. 77, no. 8, p. 538, 2017. DOI: 10.1140/epjc/s10052-017-5109-x. arXiv: 1704.08188 [astro-ph.CO] (cit. on pp. 75, 76).

[84] T. M. C. Abbott *et al.*, "The Dark Energy Survey: Cosmology Results With ~1500 New High-redshift Type Ia Supernovae Using The Full 5-year Dataset," Jan. 2024. arXiv: 2401.02929 [astro-ph.CO] (cit. on p. 75).

[85] S. Y. Vernov, V. R. Ivanov, and E. O. Pozdeeva, "Superpotential Method for $F(R)$ Cosmological Models," *Phys. Part. Nucl.*, vol. 51, no. 4, pp. 744–749, 2020. DOI: 10.1134/S1063779620040735. arXiv: 1912.07049 [gr-qc] (cit. on pp. 76, 77, 79, 80).

[86] A. De Felice and S. Tsujikawa, "f(R) theories," *Living Rev. Rel.*, vol. 13, p. 3, 2010. DOI: 10.12942/lrr-2010-3. arXiv: 1002.4928 [gr-qc] (cit. on pp. 79, 81, 93, 94).

[87] S. Nojiri, S. D. Odintsov, and V. K. Oikonomou, "Constant-roll Inflation in $F(R)$ Gravity," *Class. Quant. Grav.*, vol. 34, no. 24, p. 245 012, 2017. DOI: 10.1088/1361-6382/aa92a4. arXiv: 1704.05945 [gr-qc] (cit. on p. 84).

[88] V. R. Ivanov, S. V. Ketov, E. O. Pozdeeva, and S. Y. Vernov, "Analytic extensions of Starobinsky model of inflation," *JCAP*, vol. 03, no. 03, p. 058, 2022. DOI: 10.1088/1475-7516/2022/03/058. arXiv: 2111.09058 [gr-qc] (cit. on p. 85).

[89] T. M. Pham, D. H. Nguyen, T. Q. Do, and W. F. Kao, "Stability investigations of de Sitter inflationary solutions in power-law extensions of the Starobinsky model," Mar. 2024. arXiv: 2403.02623 [gr-qc] (cit. on p. 85).

[90] Y. B. Zel'dovich and I. D. Novikov, "The Hypothesis of Cores Retarded during Expansion and the Hot Cosmological Model," *Soviet Astron. AJ (Engl. Transl.),*, vol. 10, p. 602, 1967 (cit. on p. 86).

UNIVERSITY OF LIEGE
Faculty of Sciences
Place du 20-Août 7, B-4000 Liège, Belgique | https://www.uliege.be